Master's thesis

NTNU
Norwegian University of Science and Technology
Faculty of Engineering
Department of Energy and Process Engineering

Cara Lynn McHardy

Linking marine plastic debris quantities to entanglement rates

Development of a life cycle impact assessment 'effect factor' based on species sensitivity

Master's thesis in Industrial Ecology
Supervisor: Francesca Verones
June 2019

Jordi Chias/naturepl.com

NTNU
Norwegian University of Science and Technology

NTNU Industrial Ecology Programme
Universiteit Leiden

Cara Lynn McHardy

Linking marine plastic debris quantities to entanglement rates

Development of a life cycle impact assessment 'effect factor' based on species sensitivity

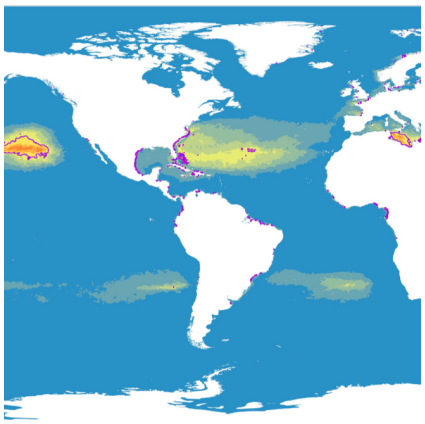

Master's thesis in Industrial Ecology
Supervisor: Francesca Verones
June 2019

Norwegian University of Science and Technology
Faculty of Engineering
Department of Energy and Process Engineering

NTNU
Norwegian University of
Science and Technology

Abstract

As production and use of plastic continues to grow exponentially, so does the share which becomes 'mismanaged waste,' ending up in the natural environment. A growing body of research has attempted to quantify the effects of anthropogenic debris on biota, especially in marine ecosystems where plastic waste has been found to accumulate in large quantities even in the most remote areas of the globe. While the necessity of preventing pollution and mitigating impacts from this harmful vector has become apparent to the larger scientific community, more responses are needed from both public and private sectors to answer this enormous challenge.

Widely used by businesses and policy-makers to quantify environmental impacts, life cycle assessment (LCA) is well-suited to link plastic production and use to its impact when it becomes debris. However, the life cycle impact assessment (LCIA) 'toolbox' currently available includes unrealistic end-of-life assumptions for plastic products. Furthermore, LCIA lacks a proper indicator metric for plastic waste and the marine ecosystems where it accumulates, limiting the appropriateness and validity of resulting LCA rankings for plastic products.

This thesis identifies marine biota entanglement in plastic waste as a first impact pathway to address in developing a methodology for mismanaged plastic waste characterization in LCIA. A compiled database of population and species-specific entanglement rates is linked to varying macroplastic densities from an existing model. Assuming a relationship between increasing plastic densities and greater rates of entanglement, the plastic density at which 50% of each modeled species is affected by debris entanglement is predicted using dose-response modeling. This leads to a species sensitivity distribution (SSD) from which "plastic debris entanglement effect factors" are derived at global, regional, and taxon scales. A global hazardous concentration (HC_{50}) of marine macroplastic debris is predicted at approximately 7.6 kg per km^2, a volume which 0.8% of world oceans are calculated to presently exceed. The associated plastic entanglement effect factor at this hazardous concentration is 6.5×10^{-2} PAF.km^2/kg, increasing to 3.9×10^{-2} PAF.km^2/kg in more pristine marine regions where few species are yet exposed to this threat above their tolerance threshold. Comparing the species sensitivity-based taxon-specific models to a previous "preliminary" effect factor approach to LCIA entanglement quantification demonstrates the improvement of the SSD methodology in characterizing the impacts of plastic waste on marine biodiversity.

Sammendrag

Etter hvert som produksjon og bruk av plast fortsetter å vokse eksponentielt, øker også andelen «feilbehandlet avfall» som ender opp i naturen. En voksende forskningsgruppe har forsøkt å kvantifisere effekten av dette plastavfallet på levende organismer, spesielt i marine økosystemer hvor det har vist seg å samles i store mengder, selv i de fjerneste områdene av kloden. Selv om nødvendigheten av å forebygge forurensning og dempe virkninger fra denne skadelige sektoren har blitt tydelig for det større vitenskapelige samfunn, er det behov for mer innsats fra både offentlig og privat sektor for å møte denne enorme utfordringen. Livssyklusanalyse (LCA) er en anerkjent vitenskapelig metode for å kvantifisere disse miljøpåvirkningene og er egnet for å knytte plastproduksjon og anvendelse til negative effekter når det blir til avfall.

Den 'verktøykasse' LCIAs for øyeblikket har tilgjengelig inneholder imidlertid urealistiske forutsetninger for plastprodukter. Videre mangler man gode målemetoder for indikatorer av plastavfall, samt for de marine økosystemene der det akkumuleres, som dermed begrenser hensiktsmessigheten og validiteten til resulterende LCA-rangeringer for plastprodukter.

Denne avhandlingen identifiserer marine biota viklet inn i plastavfall som et mulig påvirkningsområde som kan anvendes for å identifisere en ny metode for karakterisering av feilhåndtert plastavfall i LCIA. En database med statistikk over antallet individer av en art og geografisk bestemte populasjoner som vikler seg inn i plastavfall er i denne oppgaven knyttet til varierende makroplastkonsentrasjoner fra en eksisterende modell. Plasttettheten hvor 50% av artene er påvirket av plastsvinnviklinger (EC_{50}) anslått ved bruk av dose-responsmodellering, med antakelsen om et forhold mellom økningen i plastkonsentrasjoner, samt større rater av innviklinger. Dette fører til en sensitivitetsfordeling av arter som en effektfaktor for plastavfall-innviklinger avledet fra globale, regionale og artsbestemte kriterier. En globalt farlig konsentrasjon (HC_{50}) av marint makroplastisk avfall er beregnet til ca. 7,6 kg per km^2, et volum som 0,8% av verdenshavene beregnes for å nå over på nåværende tidspunkt. Den tilknyttede virkningsfaktoren ved denne farlige konsentrasjonen er 6,5 x 10-2 PAF.km^2/kg, og øker til 3,9 x 10-2 PAF.km^2/kg i marine områder med minimal tetthet av makroplastavfall. Sammenligning av sensitivitetsfordelingen av arter utviklet i denne avhandlingen med en effektfaktor utviklet i en tidligere LCA-modell demonstrerer en betydelig metodologisk forbedring i kvantifiseringen av virkningen plastavfall har på marint biologisk mangfold.

Dedicated to Jacob, with whom I discovered to the vast beauty of the open ocean:

Who, after sailing around the world in his korte broek,
braved with me the long dark Norwegian winter.

Who keeps me grounded (or at least afloat),
giving me the courage to reach for new heights.

You are the wind in my sails.

Preface

In 2014, Jacob and I spent a year sailing across the Pacific. The endless horizon over brilliant blue water, nothing to be seen but the wind, the unfathomable deep...and then, at once, a plastic bottle floats by. While I was inspired by the ancient traditions of the Pacific Island peoples, I was horrified to see moldering piles of landfilled plastic waste on tiny island atolls: cheap to import, worthless to export. The kilometers of invisible fishing nets and longlines were our nightmare on sleepless overnight sails but are more tragic for the helpless creatures in their grips. The ubiquitous plastic bag is so easily given, but never really taken away. By the time I found myself on the other side, in Indonesia, I was in full mourning for the oceans and their inhabitants. This thesis (and indeed, my entire MSc. study in Industrial Ecology) is one result of the soul-searching that followed and is hopefully only the beginning of my contribution to the search for solutions to our global plastic addiction.

Acknowledgements

This thesis would not have been possible without the support of my academic advisors at the Norwegian University of Science and Technology, Drs. Francesca Verones and John Woods. Additionally, a huge thanks and acknowledgement are due to the CML department at Leiden University, the Netherlands, who have so graciously (and without compensation) adopted me for the past year through the Erasmus+ exchange program. Dr. Peter van Bodegom took me under his wing despite an impossibly full schedule, and Drs. Martina Vijver and Thijs Bosker contributed an ecotoxicology perspective. Dr. Maarten Schraama introduced me to Dr. Ellen Cieraad, who has been an invaluable support in bringing my results together and giving perspective to the research. Maarten van't Zelvde patiently guided me throughout my ArcGIS learning and data-wrangling process, and former CML colleague Frans Rodenburg gave me a fresh tail-wind by venturing to answer my most confounding statistical questions. Finally, Astrid Carlsen at NTNU translated my abstract to Norwegian, improving my English one in the process!

Numerous marine researchers and stranding experts around the world were generous with their time in responding to my unsolicited emails and providing me with more data than I had bargained for, especially Drs. Eyüp Başkale (Pamukkale University, Turkey), Maria Corsini-Foka and Kapiris Kostas (Hellenic Centre for Marine Research, Hydrobiological Station of Rhodes, Greece), Emi Inoguchi (Everlasting Nature of Asia, Japan; IUCN/SSC Marine Turtle Specialist Group), Kazunari Kameda (Sea Turtle Association of Japan), Shaleyla Kelez (ecOceanica, Peru; IUCN/SSC Marine Turtle Specialist Group), Andrea Phillott (FLAME University & Dakshin Foundation, India), Kaj Schut (Sea Turtle Conservation Bonaire), Gabriela Velez-Rubio (KARUMBÉ, Uruguay; IUCN/SSC Marine Turtle Specialist Group), Zhong-rong XIA (Guangdong Huidong Sea Turtle National Nature Reserve Administration, China).

During my initial plastic debris impacts research, Dr. Suzanne Kühn (Wageningen Marine Research, the Netherlands) gave me valuable direction and Dr. Joseph Appiott (Secretariat of the Convention on Biological Diversity) put me in touch with his colleague Dr. Simon Harding (University of the South Pacific, Fiji) who was able to provide me with insight on their debris impacts database (CBD No.83). A special thanks goes to Dr. Andy Booth (NTNU, SINTEF) for initial inspiration and direction in my debris research, and Marcus Eriksen (The 5 Gyres Institute), for providing the underlying marine plastic debris model on which the resulting estimates are based.

I cannot forget to include my dear Mom and Dad in these acknowledgements, who taught me to never forget my roots, while at the same time giving me the wings to seek the world (not to mention their tireless editorial support with my manuscripts!) – I love you both!

Finally, a special thank you is owed to the citizens of Norway, who welcome foreigners like me to study without fees in their prestigious and well-funded universities. In the face of rising educational costs leading to uneven access in many countries (including my own), their trust in universal education and its ability to transform global society is commendable. Tusen takk!

Table of Contents

List of Figures

List of Tables

List of Abbreviations

AICC	Akaike information criterion corrected for sample size
EC	Effect concentration/density at which a cut-off percentage of individuals are observed to be affected by a stressor
EC_{50}	Median effect concentration/density, at which 50% of a population is affected by a stressor
EF	(Average) effect factor
EF_{50}	Median linear effect factor
FF	Fate factor
GIS	Geographic information systems (e.g. ArcGIS program by ESRI)
HC_{50}	Hazardous concentration/density at which 50% of representative species are exposed to a stressor above their EC_{50} level
IHO	International Hydrographic Organization
IUCN	International Union for Conservation of Nature and Natural Resources
LCA	Life cycle assessment
LCIA	Life cycle impact assessment (phase of LCA)
MLE	Maximum likelihood estimation
NOAA	U.S. National Oceanic and Atmospheric Administration
PAF	Potentially affected fraction of species
RMU	Regional management unit (for sea turtles)
SSD	Species sensitivity distribution
SWOT	The State of the World's Sea Turtles Online Database

1 Introduction

Plastic, in its wide variety of forms and uses, has become a ubiquitous and seemingly indispensable part of human life around the globe. Due to non-biodegradability and a century of improper disposal, this material has also become a pervasive form of pollution on our planet (Geyer et al. 2017).

While harmful consequences of plastic debris in the marine environment are often implicitly assumed, quantification of this harm is important in order to understand the true magnitude of this problem. The effects of plastic pollution have now been studied for a wide range of marine species (e.g. Browne et al. 2015; Kühn et al. 2015; Li et al. 2016; Ryan 2018; Secretariat of the Convention on Biological Diversity 2016; Werner et al. 2016). Although many gaps remain in our understanding of the fate and effects of plastics in the environment, there is international scientific consensus that this material must be regulated as a persistent marine pollutant (Basel Convention 2018; Rochman et al. 2016).

Meanwhile, production and use of plastic continue to grow at an exponential rate around 2.5 times as fast as global economic growth, with half of the global production weight, 3900 metric tonnes, occurring in the last 13 years (Geyer et al. 2017). Ease of manufacture, economy, hygienic properties, and light weight are some of the reasons often cited for this still-growing plastic addiction (Allen et al. 2017). While much research in recent years has focused on marine plastic debris, the majority of this waste originates from land-based sources (Worm et al. 2017), making it imperative for policy-makers to address these land-based "leakages" in addition to the most insidious marine-based sources such as "ghost gear" from fishing activities (Haward 2018).

Life cycle assessment (LCA), a method commonly used by decision-makers to quantify the environmental impacts of products, does not (yet) include any quantification of improper disposal of plastic waste, nor a methodology to assess its environmental impact (Woods et al. 2016). This has led to speculation that LCA results have actually encouraged an increase in inefficient plastic use due to a bias towards measuring greenhouse gas emissions during industrial production and transport, and unrealistic representation of end-of-life processes and impacts (Schweitzer et al. 2018).

This thesis identifies marine biota entanglement in plastic debris as a first impact pathway to address in the methodological development of "effect factors" (EF) characterizing biodiversity loss resulting from improper disposal of plastic waste. Firstly, an effects database is compiled with records of marine species entanglement rates around the world. Restrictions on geography, number of species and other factors which can be modeled due to data availability are analyzed. Assuming a relationship between increasing plastic density and greater rates of entanglement, the plastic density at which 50% of each modeled species is affected by debris entanglement is predicted using dose-response modeling. This leads to a species sensitivity distribution from which "plastic debris entanglement effect factors" are derived at global, regional, and taxon scales. A comparison of these models to a previous "preliminary" effect factor approach to entanglement quantification in the life cycle impact assessment (LCIA) phase of LCA demonstrates the improvement of the species-sensitivity methodology in characterizing plastic waste impacts on marine biodiversity.

2 Background

2.1 Plastic waste in the marine environment

The growth in use of plastic products has occurred simultaneously with globalization of industrial supply chains, exponentially accelerating in the last two decades with no end in sight (Geyer et al. 2017). Plastic waste is also extensively transported internationally, with many western countries sending their plastic waste for recycling in Asian nations which, after years of accepting the environmental burden of this low-quality waste, are now increasingly refusing or returning these shipments (Brooks et al. 2018; Reality Check team 2019; Waste Management Review 2018). Despite this increasing awareness of the hazards of plastic pollution in the environment, the scale of mismanaged plastic waste globally continues to grow. Plastic waste emissions to the environment reached up to 99 million metric tonnes in 2015 and could triple by 2060, with African and Asian nations bearing a disproportionate responsibility for this discharge (Lebreton & Andrady 2019). Currently, nearly half of all plastic debris in the environment is believed to originate from mismanaged wastes, with total yearly environmental plastic emissions of more than 8 million metric tonnes worldwide (Figure 1) (UN Environment 2018). This points to a system in crisis, with ever-increasing plastic waste and large amounts continuing to leak into the environment, coupled with the growing realization that only a small portion of it is economically viable to recycle. The bulk of this waste ends up in incinerators or landfills, often with marginal pollution controls.

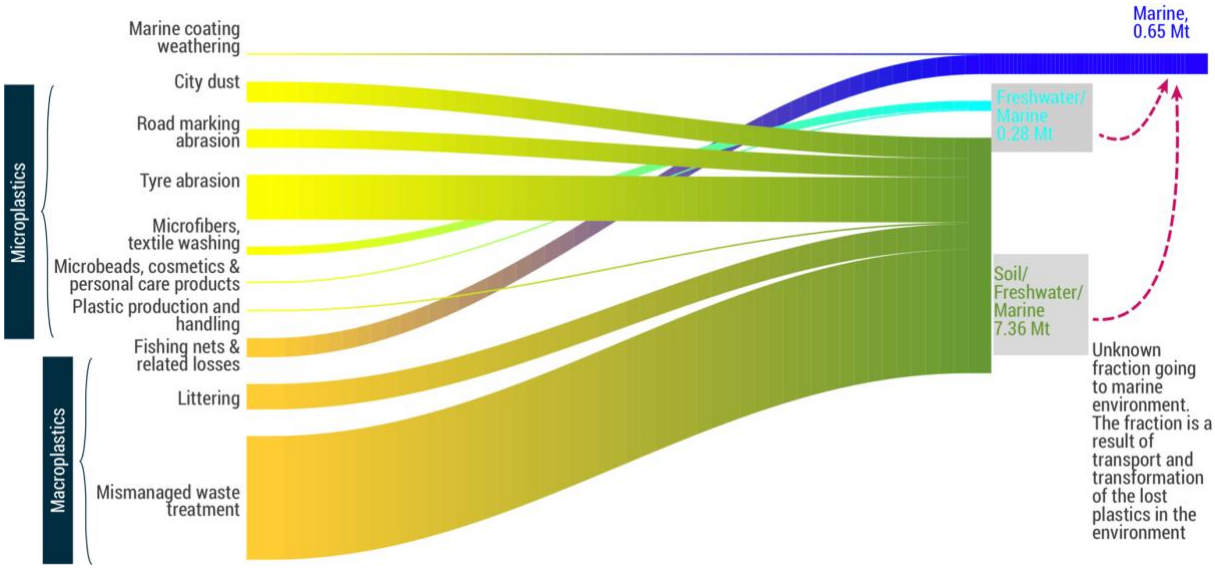

Figure 1: Sources of micro- and macroplastic debris and pathways to terrestrial, freshwater and marine ecosystems (UN Environment 2018).

Additionally, the last several decades have seen a rapid increase in industrial-style fishing effort, including expanding total fishing grounds and a transition to durable, buoyant plastic fishing gear. With this fishing intensification has come an increasing burden of abandoned, loss, or otherwise discarded fishing gear, spreading malignantly in both coastal and international waters where maritime pollution enforcement is markedly limited (Macfadyen et al. 2009). While estimates of total global and regional losses of fishing gear are generally lacking, at-sea and coastal observations as well as estimates

from some fisheries document a large and increasing environmental load (UN Environment 2018). Fishing gear losses are especially significant as they are emitted directly to the marine environment where they can continue to trap biota for many years in a cycle of "ghost fishing:" alternately sinking and rising in the water column with entrapment and subsequent decomposition of biota (FAO 2016).

2.2 Life cycle impact assessment

Life cycle assessment, an analytical tool for "hotspot analysis" of environmental and human-health impacts of products and processes, is often applied to provide the scientific basis for ecologically-responsible decision-making in both private and public sectors (Zampori et al. 2016). LCA analysis is by definition holistic, including resource extraction, manufacturing, distribution, use and disposal phases in the calculating of impacts (Curran 2013).

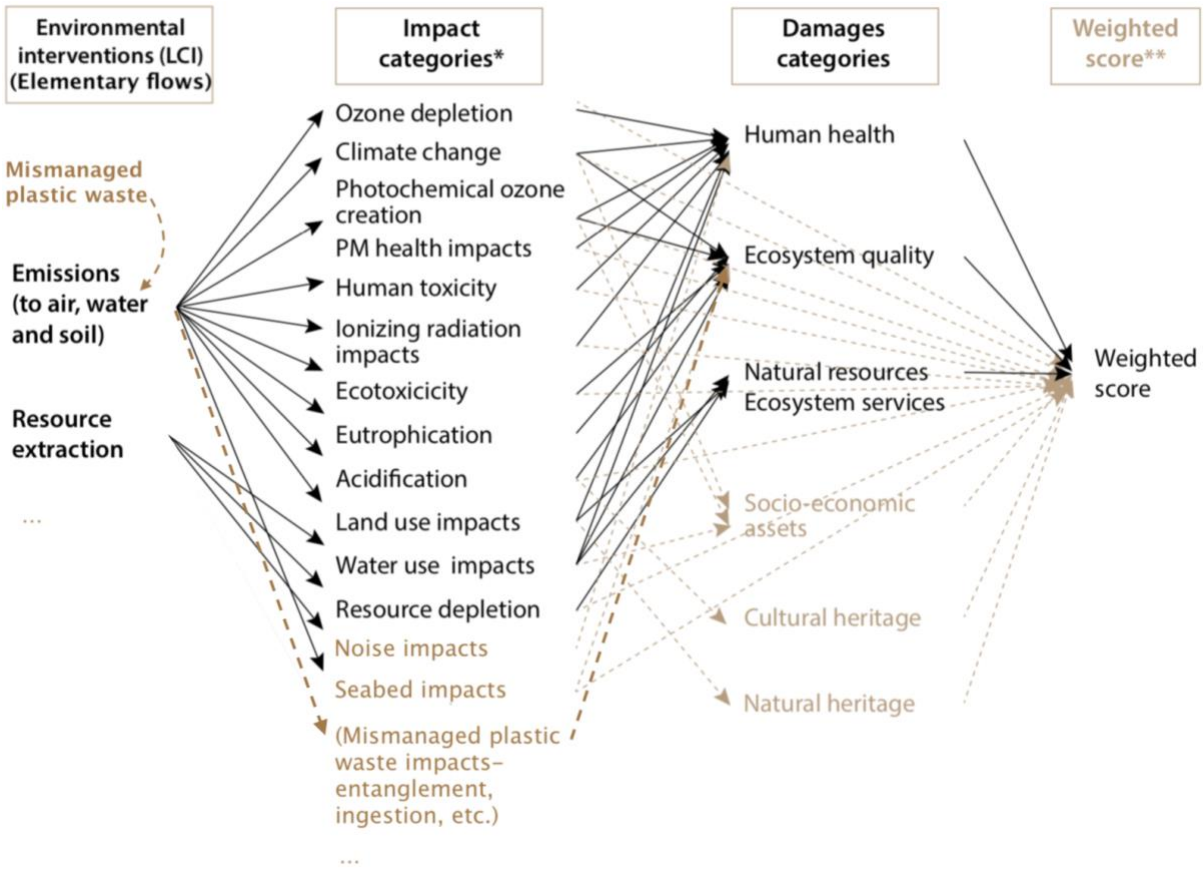

Figure 2: Current LCIA framework with added mismanaged plastic waste impact characterization. Brown text and dotted lines indicate non-operational categories; suggested mismanaged plastic waste impact category in parentheses. *Non-exhaustive list, subject to development. **Weighting (and normalization) are optional steps. Adapted from (UNEP/SETAC Life Cycle Initiative 2016).

As illustrated in figure 2, the impact assessment (LCIA) phase of LCA relates industrial processes (both consumptive and emissive) to one or more relevant environmental effects using "impact categories" (e.g. climate change, resource depletion, ecotoxicity). These harms "per functional unit of production" can be reported per impact category, and/or summed in "damage categories," (e.g. human health, ecosystem quality, natural resources/ecosystem services). For very general comparisons, a weighted/normalized

final "score" can also be presented, although this involves a value judgement and is not compliant with International Organization for Standardization norms (ISO14044 2006; Rosenbaum et al. 2017; UNEP/SETAC Life Cycle Initiative 2016).

Characterization of impacts in LCIA generally includes both "fate" and "effect" factors, where fate corresponds to environmental residence time, and effect is the consequent ecological impact (Hauschild & Huijbregts 2015b). For each measured stressor, the sum of all associated fate factors (FF) multiplied by all effect factors (EF) equals the characterization factor (CF) for the stressor in region i (equ 1) (Hauschild & Huijbregts 2015a).

$$\mathrm{CF}_i = \sum_i \mathrm{FF}_i * \mathrm{EF}_i \quad (1)$$

In LCIA effect factor calculation, it is recommended practice to use species sensitivity distributions (SSDs) derived from dose-response modeling in measuring the ecotoxicity of pollutants. Dose-response modeling is often used in ecological risk assessment and to estimate the relationship between level of exposure to a stressor (the 'dose') and severity of effects experienced by a particular species (van Leeuwen 2007). In dose-response modeling, the effect concentration/density (EC) of a stressor is the concentration or density at which a cut-off percentage of individuals are observed to be affected. In LCIA, the median effect concentration/density (EC_{50}) is considered a valid ecological endpoint for measuring the acute toxicity of a substance for a species (Hauschild & Huijbregts 2015b; McKone et al. 2006; Traas & van Leeuwen 2007).

As outlined by Posthuma et al. (2002), an SSD is a cumulative distribution function ranking an ecologically representative assemblage of species by ascending stressor levels related to a chosen constant EC value. The SSD shows the relationship between the concentration/density of the stressor and the potentially affected fraction of species (PAF) at the chosen EC value, serving as an environmental quality criterion targeted for preventing or reducing harm beyond a perceived tipping point for the ecosystem (Posthuma et al. 2002). In LCIA comparative analyses, it is appropriate to compare HC_{50} values, the hazardous concentration/density at which 50% of representative species are exposed to a stressor above their EC_{50} – median effect level (Hauschild & Huijbregts 2015a; Henderson et al. 2011; Rosenbaum 2015).

In LCIA stressor characterization, the species-sensitivity derived model function describing the PAF is then used to calculate average EFs representing the average gap between the current environmental status and the ideal "zero effect" state per unit of stressor emission (Huijbregts et al. 2011). Linear EFs are used for generalized characterizations where only one "constant effect" is modeled and compared, or when information on background pollutant concentrations is lacking (Hauschild 2018).

2.2.1 LCIA and the quantification of plastic waste impacts

The most widespread and visible impacts of macroplastic debris are considered to be ingestion and entanglement of biota, while other environmental impacts of plastic debris including smothering of benthic environments, leaching of toxic chemicals, and transport of invasive species and diseases are also insidious but more difficult to quantify (Gregory 2009). Impacts to humans include the economic costs of litter cleanup, loss of aesthetic value and loss of ecosystem services through damage or destruction of subsistence fisheries (Gregory 2009), as well as potential human health impacts from chemicals (European Commission 2018).

Woods et al. (2019) proposed characterizing in the context of LCIA the damage to marine ecosystems ultimately caused by the release of plastic waste into the environment (Figure 3), including entanglement, ingestion, non-native species introduction via rafting, and habitat alteration/destruction. Of four indicated impact pathways, they developed a preliminary effect factor methodology for characterizing one of these – entanglement of marine organisms resulting in marine biodiversity loss (Woods et al. 2019). By their own evaluation, the resulting model estimates for total PAF do not align well with their modeled densities of marine macroplastics. They suggest that in order to more accurately link varying plastic densities to the scaling of associated effects, SSD information derived from population or species-level entanglement rates should be coupled with plastic densities found within the geographical ranges of species and regional population groups, if data is available. More discussion and comparisons to the Woods et al. study can be found in results section 4.7.

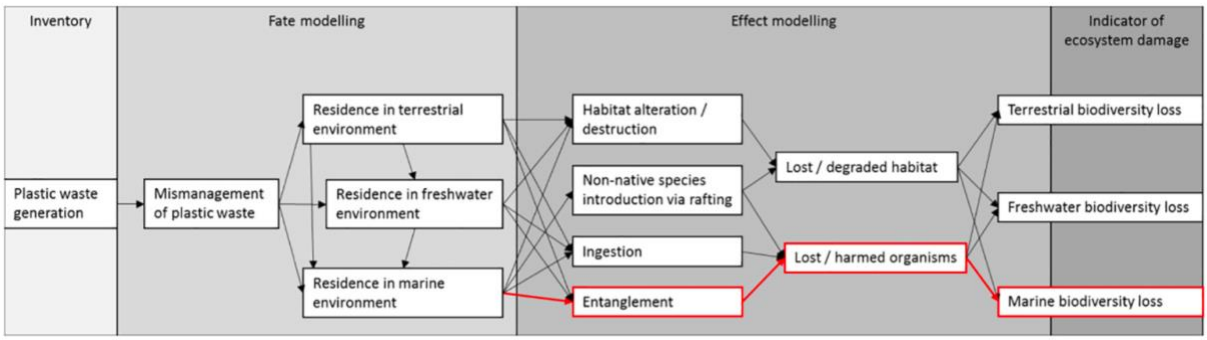

Figure 3: LCIA impact pathways to ecosystem damage caused by mismanaged plastic waste: Proposed entanglement effect pathway to marine biodiversity loss outlined in red (Woods et al. 2019)

3 Materials and Methods

3.1 Methodology overview

The subsequent sections describe the data, calculations, and methodological decisions made in the process of creating an effect factor characterizing mismanaged plastic waste for use in the LCIA framework. An overview of the steps taken in this EF model development are detailed in the following flowchart (Figure 4).

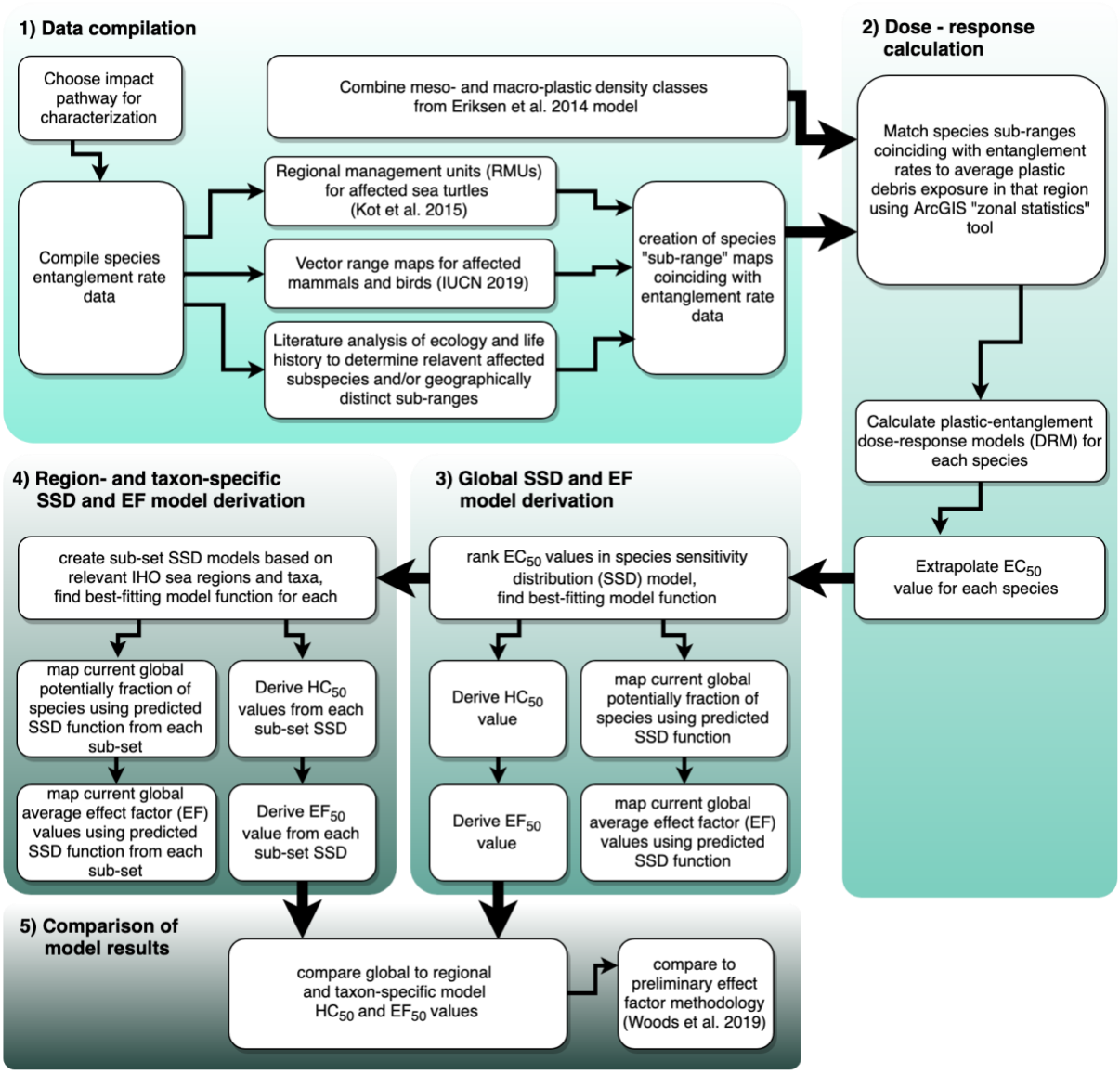

Figure 4: Flowchart of mismanaged plastic waste effect factor model creation process

3.2 Data compilation

3.2.1 Choice of impact pathway

In a preliminary project report providing background for this thesis, a database was compiled of known biota interactions with plastic debris in all the world's ecosystems. The database includes observations of plastic debris effects (including entanglement and ingestion) on 660 marine/estuarine species, 74 freshwater species and 78 terrestrial species (Figure 5) (McHardy 2018). Of these, 705 species across all ecosystems were reported as entangled in plastic debris, representing 82% of all reported plastic debris impacts to biota and 80% of reported impacts to marine species (Figure 6). This includes 36% of all seabird species, 70% of all marine mammal species, and all sea turtle species.

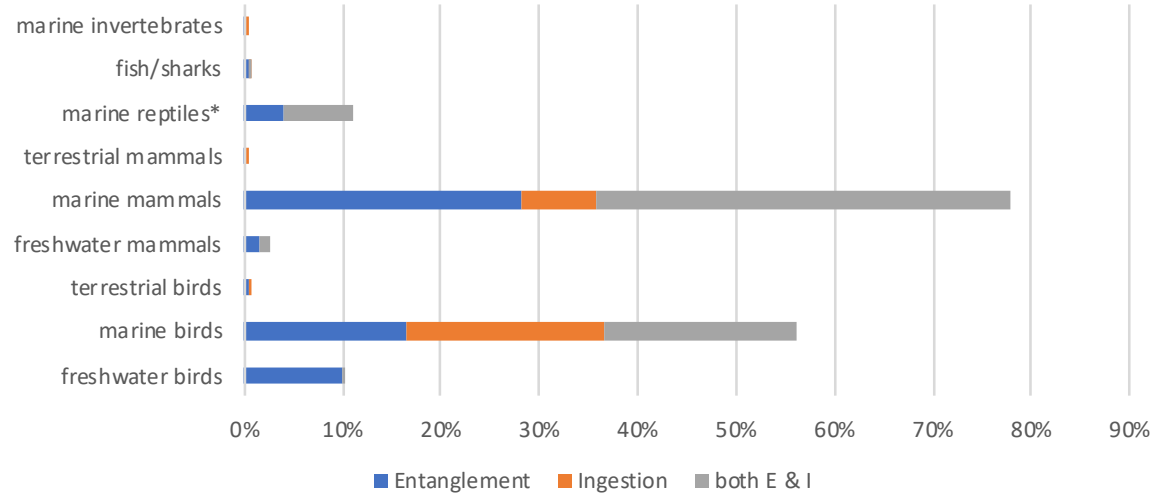

Figure 5: Percentage of all species known to be affected by entanglement or ingestion of plastic debris.*All 7 marine turtle species are affected by entanglement & ingestion (McHardy 2018).

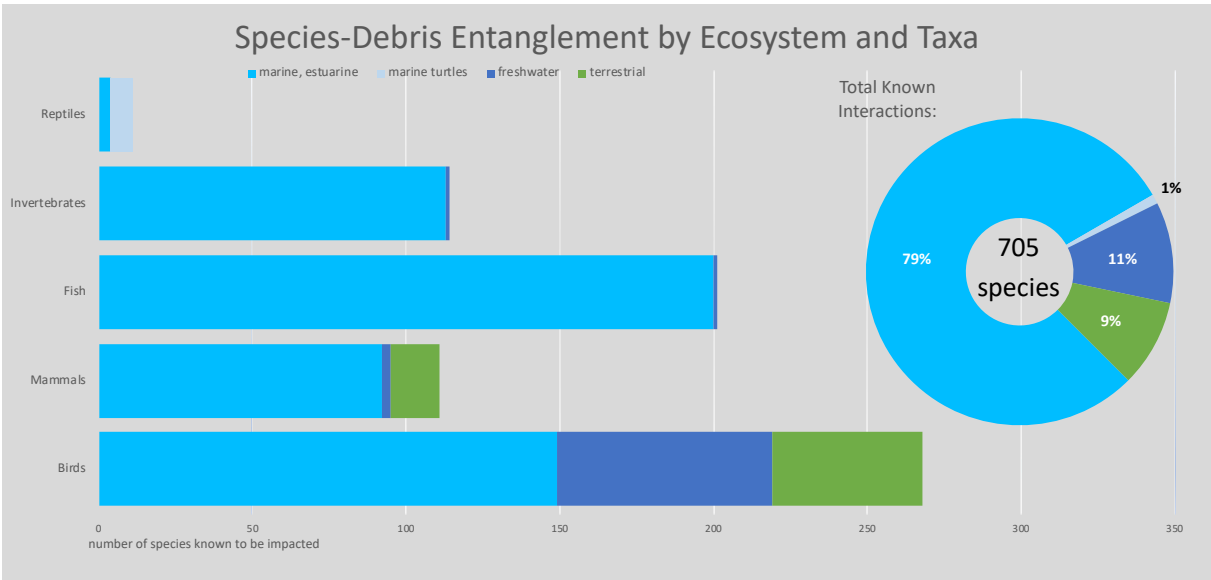

Figure 6: Entanglement occurrence by ecosystem and taxa. Data from: (McHardy 2018)

As nearly all (97%) of the reports catalogued in the McHardy (2018) database did not specify the final result of the encounter (e.g. injury, death, recovery), "affected" by plastic debris simply denotes the interaction, with no implied result. However, the full impact of even a short-term encounter with debris can have longer-term effects, ranging from slight injury to severe, long-term disability or death. In order to visualize the "adverse outcome pathways" (Kramer et al. 2011) initiated by biota encounters with plastic waste, the author compiled and detailed all interconnecting pathways of known impacts by increasing severity for both biota entanglement and ingestion of plastic waste (McHardy 2018). The potential pathways of impact for plastic debris entanglement with biota begin with the event initiating entanglement, then the entanglement itself, followed by bodily harm, restricted movement, sub-lethal injuries, lethal results, reproductive effects and finally population-level effects, as diagramed in Figure 7.

Based on the database and biological effects detailed above, "marine biota entanglement" was identified as the most appropriate and feasible first impact pathway to address in the methodological development of effect factors characterizing biodiversity loss resulting from improper disposal of plastic waste. Although hundreds of marine species have been recorded as becoming entangled in plastic debris, most studies only identify entanglement observations, without attempting to quantify the rate at which this occurs for the studied population, or the end result for the individual (McHardy 2018). However, assuming a relationship between increasing plastic densities and greater rates of entanglement, dose-response models can be formulated for species when such rates and plastic densities are available. Predictions of the plastic density at which 50% of each species are affected by debris entanglement (EC_{50}) can then be ranked in a species sensitivity distribution from which a "plastic debris entanglement effect factor" can be derived.

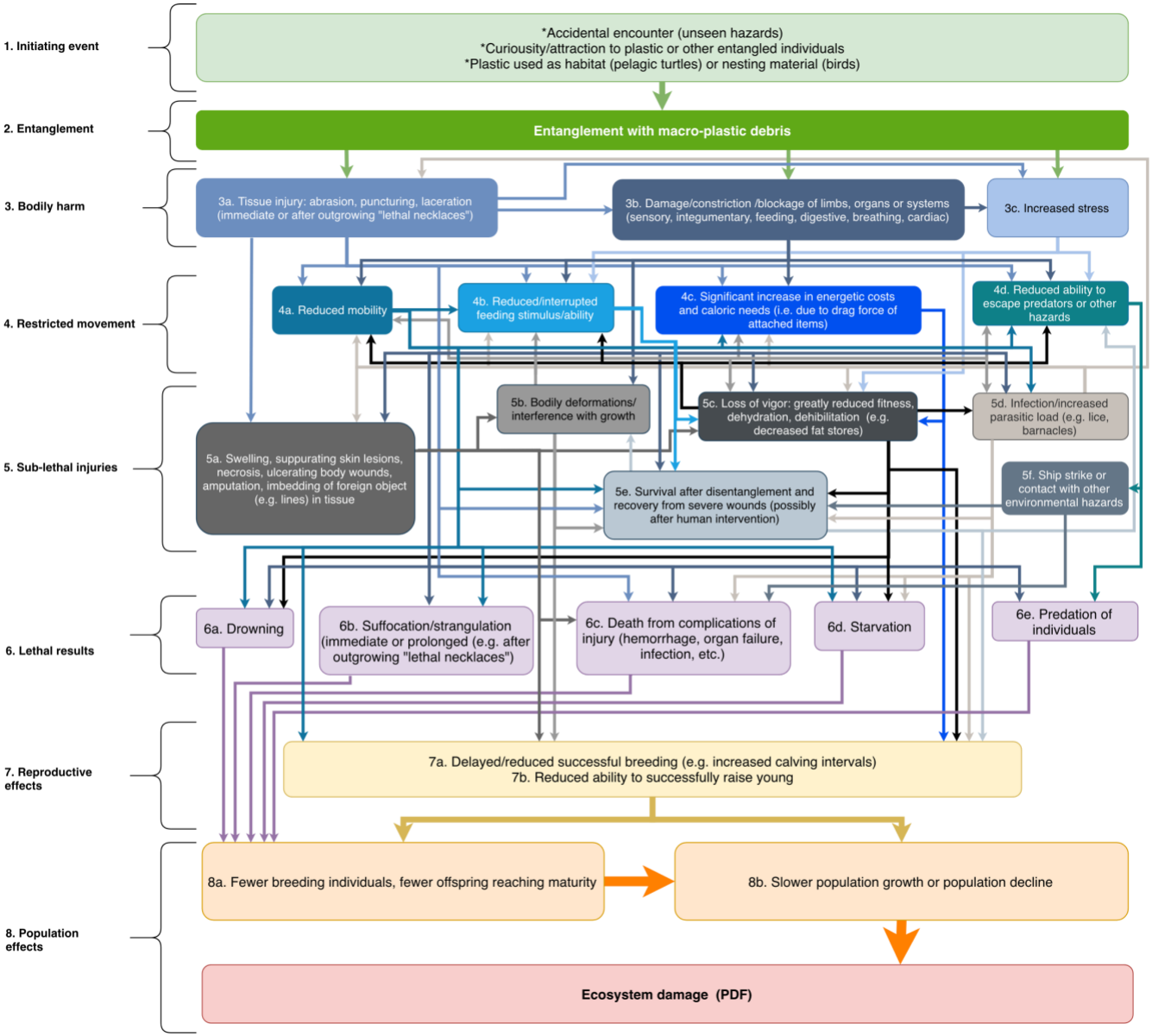

Figure 7: Pathways of impact caused by biota entanglement in macroplastic debris. Successive stages (1-8) are color-coded, with arrows between stages matching source stage color) (source: McHardy 2018)

3.2.2 Compiling entanglement rates by species and region

Debris entanglement reports were only included in this study if data quantifying *rates* of entanglement was available. In order to best correspond temporally with modeled plastic debris densities, compiled data was limited to observations including the years 2007 to 2015. Much of the modeled data was collected in a generic plastic debris effects database assembled by the author in an earlier project report (McHardy 2018), which was complimented with additional data collected in an updated document search ending 31 March 2019. Academic research was sourced from Scholar.google.com and Scopus.com databases, while "grey literature" was sourced from a Google.com search as well as data requests sent to relevant researchers and stranding networks worldwide. Search terms were:

> *TITLE-ABS-KEY (plastic OR "macroplastic" OR "debris" OR "plastic pollution" OR "plastic waste" OR "foreign object" OR "foreign body" OR litter OR anthropogenic OR "fish* gear" OR "fish* net" "derelict fish*" OR "discard* fish*") AND TITLE-ABS-KEY(effect OR entangle* OR harm OR hazard OR interact* OR impact OR mortality OR strand* OR trauma)*

While most population entanglement rates were taken directly from academic studies quantifying species interactions with debris, several rates were derived directly from stranding databases, their annual reports, or email interactions with researchers. Although stranding data is known to grossly underestimate total at-sea mortality of species, it is in many cases the best available proxy for causes and rates of mortality in the overall population (Peltier et al. 2012; Peltier & Ridoux 2015; Santos et al. 2018; Young et al. 2019). In all cases, entanglement rates were defined as the number of entangled individuals out of the total population observed.

While many entanglement rates were detailed in the database compiled by the researcher in a previous report (McHardy 2018), a focus on marine entanglement and detailed reading of the reports underlying these rates yielded more usable data for the current model. Figures from a technical report commissioned by the European Commission's Joint Research Centre for the Marine Strategy Framework Directive (Werner et al. 2016) as well as a 2016 review of "*Sources, occurrence, and effects of plastic waste in the marine environment"* by Li et al. (2016) were included in the author's original database. Additional entanglement rates later added to the database include:

- 2007 to 2009 stranding data analyzed by Adimey et al. (2014) defining entanglement rates for manatees (*Trichechus manatus*), bottlenose dolphins (*Tursiops truncatus*), loggerhead sea turtles (*Caretta caretta*) and green sea turtles (*Chelonia mydas*) in Florida, USA.
- Additional entanglement rates for non-breeding Northern gannets (*Morus bassanus*) compiled by Rodríguez et al. (2013).
- Additional details on Antarctic fur seal (*Arctocephalus gazella*) entanglement rates in Waluda and Staniland (2013).
- Rates of entanglement for the seven sea turtle species assembled from a stranding database compiled by the U.S. National Oceanic and Atmospheric Administration Southeast Fisheries Science Center Sea Turtle Stranding and Salvage Network (NOAA STSSN 2014), the Australian Northern Territory StrandNet report (Mackarous & Griffiths 2016) a European Commission feasibility study for the implementation of a marine debris entanglement

indicator (Claro et al. 2018) and personal communications with marine turtle researchers (Başkale et al. 2018; Kameda et al. 2013).

For threatened (or formerly threatened) species such as the North Atlantic right whale (*Eubalaena glacialis*), American manatee (*T. manatus*), several eared (*Otariidae*) seal species and all marine turtle species, dedicated organizations and/or researchers are engaged in long-term population monitoring with at-sea observers as well as stranding and rehabilitation networks, and often have detailed entanglement records (Adimey et al. 2014; Duncan et al. 2017; Knowlton et al. 2012; Lawson et al. 2015; Pettis et al. 2018; Raum-Suryan et al. 2009; Waluda & Staniland 2013). For most bird, grey seal (*Halichoerus grypus*) and other cetacean species entanglement rates, data has mainly been collected through beach (stranding) observations (Adimey et al. 2014; Dau et al. 2009; Rodríguez et al. 2013; Schulz et al. - in publication, in Werner et al. 2016). For breeding colonies of northern gannets on Helgoland island, Germany, more comprehensive entanglement counts could be conducted for birds entrapped in plastic debris used as nesting materials (Adimey et al. 2014; Dau et al. 2009; Rodríguez et al. 2013; Schulz et al. - in publication, in Werner et al. 2016). Also uniquely, entanglement rates for three eared seal species (*A. gazella, A. pusillus and Eumetopias jubatus*) are based on surveys of entire regional populations, as researchers regularly observed rookeries and counted all individuals as well as their entanglement status (Lawson et al. 2015; Raum-Suryan et al. 2009; Waluda & Staniland 2013). This was possible as these species are non-migratory and spend a fair amount of time on land, but for many other marine species such complete regional population surveys are not feasible due to large, migratory ranges and cryptic life histories. The full list of entanglement data used in the model can be found in Appendix 1.

3.2.3 Model of marine plastic debris density

Spatial distributions and volumes of plastic debris in open oceans were estimated by Eriksen et al. (2014) using an oceanographic model of floating debris-dispersal calibrated by sample and visual survey data gathered during 24 expeditions (2007-2013) across the five subtropical gyres, Mediterranean Sea, Bay of Bengal and coastal Australia. The model categorizes floating plastic counts and weights for four size classes: two microplastic sizes (0.33-1.00mm, 1.01-4.75 mm), mesoplastic (4.76–200 mm), and macroplastic (>200mm) (Eriksen et al. 2014). For the purposes of this thesis, their geospatial models characterizing the weights of the two larger categories – meso- and macroplastic, were merged and their combined weight (g/km^2) was used to characterize entanglement-hazard plastic densities in world oceans (Figure 8). This size choice is due to the fact that nearly all documented marine debris entanglement encounters are with megafauna, therefore entanglement only happens with meso- and macro-plastic (e.g. Gall & Thompson 2015; Kühn et al. 2015; Ryan 2018; Worm et al. 2017). Hereafter, these combined plastic categories (>4.75 mm) are referred to as "macroplastic."

3.2.4 Regional specification of entanglement rates

While the compiled entanglement rates each correspond to a specific regional species population, some rates were derived from samples collected on one beach, whereas others were integrated from observations over a larger area (i.e. the entire U.S.A. east coast). In order to connect these rates to likely regional populations, vector range maps published by the International Union for Conservation of Nature and Natural Resources' (IUCN) *Red-list of Threatened Species* were used to delineate marine species' ranges (IUCN 2019).

To quantify the likely smaller "home-ranges" of sampled populations affected by entanglement, an in-depth analysis of the available literature took into account each species' geographic range, migratory patterns, ecology and life history. With the exception of the highly-migratory North Atlantic right whale (*Eubalaena glacialis*), species' full global ranges could be subdivided into smaller regions. The range of a recognized subspecies defined these sub-ranges for five species: the Australian fur seal (*A. p. doriferus*) (Hofmeyr 2015; Kirkwood et al. 2010), North Atlantic minke whale (*Balaenoptera acutorostrata acutorostrata*) (Cooke 2018a; Quintela et al. 2014), Florida manatee (*T. m. latirostris*) (Deutsch et al. 2003; Deutsch et al. 2008), Loughlin's Steller sea lion (*E j. monteriensis*) (Gelatt & Sweeney 2016a, 2016b) and California brown pelican (*Pelecanus occidentalis californicus*) (BirdLife International 2018d; Elliott 2018). For marine turtle species, sub-ranges were defined by Regional Management Units (RMUs) (Wallace et al. 2010) from *The State of the World's Sea Turtles Online Database* (Kot et al. 2015). Although marine turtles species are highly migratory with ranges spanning most oceans, RMUs combine nesting sites, population abundances and trends, population genetics, and satellite telemetry to delineate turtles into likely population segments with specific sub-ranges (Wallace et al. 2010).

For most species, the smallest identifiable sub-ranges still required grouping all known entanglement rates in one region. In these cases, the total observed number of entangled versus unentangled individuals from these studies was summed to calculate an overall regional entanglement rate. An example of this aggregation can be seen for the Northern gannet (*Morus bassanus*), where observations from across their Northeast Atlantic and Mediterranean wintering areas were combined to one overall entanglement rate as they represent a non-distinct population (BirdLife International 2018c; Fort et al. 2012). Exceptionally, separate entanglement rates were reported for breeding versus non-breeding Northern gannets in this Northeastern Atlantic population (Rodríguez et al. 2013; Schulz et al. - in publication; Werner et al. 2016). It was decided to treat this breeding population as a separate "species-exposure group" rather than averaging these rates due to geographic similarity, as although the same individuals may belong to both breeding and non-breeding groups, their range and behavior while nesting and breeding is distinctively different. A smaller foraging range (<450km) and the tendency to incorporate debris into nests, are among the behaviors exposing the breeding, nesting and fledgling birds to plastic debris in an entirely other manner than during their wintering phase (BirdLife International 2018c; Dewey 2009; Mowbray 2002).

Rationales, citations and maps for sub-ranges associated with entanglement rates, as well as the IUCN Red List status of each cited species and subspecies can be found in Appendix 2.

3.3 Dose-response model calculation

3.3.1 Matching entanglement rates to plastic debris exposure

Species ranges divided into the smallest possible population-specific sub-ranges were used for normalization of the detailed (to 0.2 decimal degrees) plastic density data from the Eriksen et al. (2014) model to the less spatially-specific available entanglement rates. The "spatial analyst: zonal statistics" tool in ArcGIS (ESRI 2017) was used to compute the mean weight of plastics in these species-specific regions.

3.3.2 Dose response modeling

The regional average macroplastic debris densities (effect concentrations/densities) and their related entanglement rates were used to calculate linear dose-response models of this relationship for each species-exposure group, assuming a zero percent entanglement rate in the absence of plastic debris. For those species with derived entanglement rates for several regions, the model was weighted by number of observations per entanglement rate to account for the strength of the data supporting the rate, and Akaike information criterion corrected for sample size (AICC) values for various curve types were compared using maximum likelihood estimation (MLE) to find the best fit. From these models, an EC_{50} value for each species could be calculated. For brevity, only the most complex dose-response model (for the loggerhead sea turtle) is exhibited in the results, while dose-response models derived for all 20 species are displayed in Appendix 3.

3.4 Global species sensitivity distribution and effect factor model derivation

3.4.1 Species sensitivity distribution modeling

EC_{50} values for each of the species-exposure groups were extrapolated from their respective dose-response models and used to fit a species sensitivity distribution model curve by MLE using the "ssdtools" package in R-studio (Thorley 2018).

The best-fitting log-logistic cumulative distribution function predicts a PAF value for sensitivity of all modeled marine species to plastic at location i, where constant α is the curve's scale, β is its shape, and P_i is the density of marine macroplastic debris (g/km^2) at location i (eq 2).

$$\mathrm{PAF}_i = \frac{1}{(1+(\mathrm{P}_i/\alpha)^{-\beta}} \quad (2)$$

Based on this global SSD model, predicted PAF values corresponding to each plastic density (g/km^2) in the macroplastic debris model (approximately 0.2 decimal degrees grid-cell resolution) were calculated and mapped in ArcGIS (ESRI 2017).

3.4.2 Effect factor model calculation

For this study, an average effect factor model (PAF.km^2/g) was calculated where the EF at location i is the ratio of the PAF in location i to the plastic density (P; g/km^2) in that location (eq 3).

$$\mathrm{EF}_i = \frac{\mathrm{PAF}_i}{\mathrm{P}_i} \quad (3)$$

Predicted EF values (PAF.km^2/g) corresponding to each PAF value in the global SSD model were calculated and mapped in ArcGIS (ESRI 2017).

3.5 Model comparisons

3.5.1 Regional and taxon-specific model comparison

As recommended in Woods et al. (2018), it is important to compare environmental impact indicators at varying scales, taxonomic coverages, and relative to absolute loss measures before deciding on a final form of effects characterization. In order to gauge the sensitivity of the global models to difference in spatial scale or taxonomic group,

relevant sub-sets of the original SSD data were used to formulate new models at these scopes. Taxon-specific models were created for mammals, birds, and turtles, while eight International Hydrographic Organization (IHO) sea regions where at least six of the originally modelled species occur were found to be relevant: the Caribbean Sea, Indian Ocean, North Atlantic Ocean, South Atlantic Ocean, North Pacific Ocean, South Pacific Ocean, North Sea/Norwegian Sea and Mediterranean Sea. The North Sea and Norwegian Sea were combined into one model as all eight relevant modelled species occur in both regions.

The spread of all resulting predicted SSD and EF model functions were compared to the global model to determine if and under which circumstances these more specific models would be preferred over a global average approach. Regional and taxon-specific model results, including HC_{50} values, were compared to determine which taxa and regional subset of species have greater sensitivity to entanglement in plastic debris. A linear EF value at which 50% of species are affected (EF_{50}) was also used to analyze model differences, where the denominator is the median hazardous plastic density (P_{HC50}; g/km^2) for model *j* (eq 4).

$$\mathrm{EF}_{50_j} = \frac{0.5}{\mathrm{P}_{HC50_j}} \tag{4}$$

3.5.2 Comparison to a preliminary methodology

Prior to the study presented here, an LCIA approach to quantifying plastic debris entanglement impacts on marine species was tested by Woods et al. (2019). They quantified PAF as the percent of all known marine species in taxon *t* present in a grid cell *i* which have ever been observed entangled in plastic waste, effectively setting the density at which entanglement will occur at 0.28 g/km^2 (the lowest modeled marine macroplastic density). Each modeled taxon's current exposure to plastic was introduced in the effect factor equation, wherein the PAF was divided by the median plastic density present in grid-cell *i*, P_i (eq 5, from (Woods et al. 2019).

$$\mathrm{EF}_{t,i} = \frac{\frac{species\_affected_{t,i}}{total\_species_{t,i}}}{\mathrm{P}_i} = \frac{\mathrm{PAF}_{t,i}}{\mathrm{P}_i} \tag{5}$$

While their method yielded spatially- and taxon-specific models quantifying an effect factor for plastic debris entanglement, they concluded that their parameters were too broad for a realistic spatially-explicit effect factor. As their recommendations for further model development included linking species- and population-specific entanglement rates to plastic debris exposure, it is appropriate to compare the data sources, methods and results of the current study to their original approach. While they did not quantify HC_{50} or EC_{50} values in their results, the spectrum of PAF and EF values mapped in three of their five spatially-specific taxon models were comparable to the three taxa presented in the current study. The magnitude and geographical location of modeled PAF and EF "hotspots" and implications of this are evaluated.

4 Results

4.1 Species entanglement rates and plastic debris exposure

Entanglement rates and associated mean plastic densities used in the study are shown in Table 1, while a detailed list including underlying sources is found in Appendix 1. In all, entanglement rates observed between 2007 and 2015 were modeled for 20 species-exposure groups, including eight mammal species, seven turtle species and five bird exposure-groups. Included were all marine turtle species (Rasmussen et al. 2011), 6% of all marine mammal species (Committee on Taxonomy 2018) and 1.2% of all marine bird species (Gill & Donsker (Eds) 2018). Most compiled observations occurred on both the east (13) and west (11) coasts of the North Atlantic, Mediterranean Sea (10), Australian Indian Ocean (6), and North Sea (5), while three observations each were reported from the South Atlantic and North Pacific.

After combining the two largest plastic debris classes from the Eriksen et al. (2014) model, the estimated dispersion of all macroplastic (>4.75 mm) densities over world oceans was visualized (Figure 8). In this model, marine macroplastic densities are predicted to vary from 0.28 g/km^2 to approximately 3.9 x 10^5 g/km^2 (390 kg/km^2).

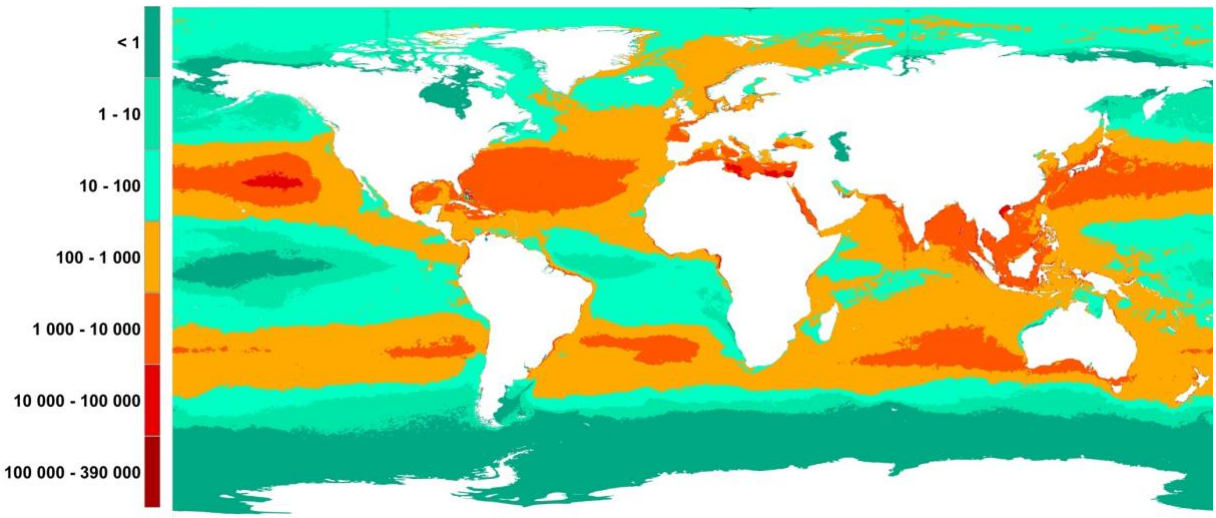

Figure 8: Global marine macroplastic debris density (g/km^2): combination of meso- and macro-plastic models by Eriksen et al. (2014).

The sub-ranges of the sampled species populations were associated with the mean plastic densities within the same region (see Methods 3.2.3 – 3.2.4). For most species, only one regional entanglement rate could be compiled. In the cases of the Antarctic fur seal (*A. gazella*), hawksbill sea turtle (*Eretmochelys imbricata*), Kemp's ridley sea turtle (*Lepidochelys kempii*), leatherback sea turtle (*Dermochelys coriacea*), loggerhead and non-breeding northern gannet, several entanglement rates associated with populations having non-distinct sub-ranges were averaged and each matched to one regional mean plastic debris density. Rates for more than one distinct population could only be quantified for loggerhead, green and hawksbill sea turtles. Of these three species, the

loggerhead stands out as having entanglement rates defined for six[1] distinct populations, while two regional rates were derived for the hawksbill and three for green sea turtles.

Table 1: Species entanglement rates and associated mean plastic densities (g/km^2). Blue: marine birds, violet: marine mammals, green: marine turtles. Range delineation used to calculate mean plastic density in region of exposure per species population, total observed individuals from the population and percent of that population sample which were entangled.

Common name	Scientific name	range delineated for plastic densities	Mean plastic density (g/km^2)	Total observed	Percent affected
Northern gannet (breeding)	*Morus bassanus*	Helgoland Isl. breeding range: 450km radius	915.84	1340	3.1%
Northern gannet (non-breeding)	*Morus bassanus*	E Atlantic/Medit. wintering areas (non-breeding grounds)	580.39	3672	0.93%
Common Guillemot/ Common Murre	*Uria aalge*	IUCN sub-range Atlantic split with IHO quadrant E. Atlantic	343.61	6261	1.1%
Northern Fulmar	*Fulmarus glacialis*	IUCN sub-range Atlantic	186.71	67	1.8%
Brown Pelican	*Pelecanus occidentalis*	IUCN sub-range N. Pacific	390.93	557	63%
Antarctic fur seal	*Arctocephalus gazella*	IUCN range subsection: intersection with IHO Atlantic + Southern Ocean (Atlantic quadrant) sea regions	0.32	No data	0.04%
Afro-Australian Fur Seal	*Arctocephalus pusillus*	Sub-range Australia	2859.99	60000	0.13%
Common bottlenose dolphin	*Tursiops truncatus*	Intersection: IHO North Atlantic & IUCN range	1264.42	2413	5.5%
Common minke whale	*Balaenoptera acutorostrata*	IUCN range	1048.78	11	9.1%
Florida manatee	*Trichechus manatus*	IUCN range in Florida	3931.27	4962	7.7%
Grey seal	*Halichoerus grypus*	IUCN range intersection with IHO subregions around Cornwall: Celtic Sea & English Channel	1398.01	58	4.3%
North Atlantic right whale	*Eubalaena glacialis*	IUCN range	668.2	61	84%
Steller sea lion	*Eumetopias jubatus*	IUCN sub-range: E Pacific subspecies	98.3	73077	0.26%
Green Sea Turtle	*Chelonia mydas*	Average of RMU 39 & RMU 40 (undefined populations)	312.28	28	46%
		RMU 48	6385.61	14	21%
		RMU 50	2584.55	2328	4.9%
Hawksbill Sea Turtle	*Eretmochelys imbricata*	RMU 14+RMU 12 (non-overlapping)	811.62	23	65%
		RMU 10	2372.16	385	8.6%
Leatherback Sea Turtle	*Dermochelys coriacea*	RMU 51	1426.54	2281	7.1%
Olive Ridley Sea Turtle	*Lepidochelys olivacea*	RMU 03	712.66	31	84%
Flatback Sea Turtle	*Natator depressus*	RMU 59 & RMU 60 (population weighted)	165.7	10	40%
Kemp's Ridley Sea Turtle	*Lepidochelys kempii*	RMU 58	2289.24	2497	3.8%
Loggerhead Sea Turtle	*Caretta caretta*	RMU 25	1902.88	1411	3.1%
		RMU 25 & RMU 23[1]	1781.85	47	38%
		RMU 25 & RMU 26[1]	2052.11	2080	8.2%
		RMU 26	4248.78	134	20%
		RMU 29	755.32	3	33%
		RMU 31	1689.67	535	0.19%

[1] Two of these regional population distinctions are based on observations in an area where two RMUs are overlapping (RMU 23 overlaps with RMU 25 in the Canary Islands, Spain; RMU 25 overlaps with RMU 26 in the Northeast Atlantic and Western Mediterranean Sea. In these cases, the population-weighted average of plastic densities in these regions is calculated.

4.2 Global model coverage

Taking all studied species' ranges into account, the overall area where the model contains at least one species spans much of the world's marine regions (Figure 9). With the exception of the brown pelican (*P. occidentalis*), all modeled bird species occur only in the northern hemisphere, while the Antarctic fur seal and common minke whale (*B. acutorostrata*) are the only represented species occurring in the Southern Ocean. Nearly all (16) of the 20 included species occur in the North Atlantic, while 11 of the species occur in either the North or South Pacific, ten of the species occur in either the South Atlantic or Indian Ocean, nine in the Caribbean, and eight in the North and Norwegian Seas.

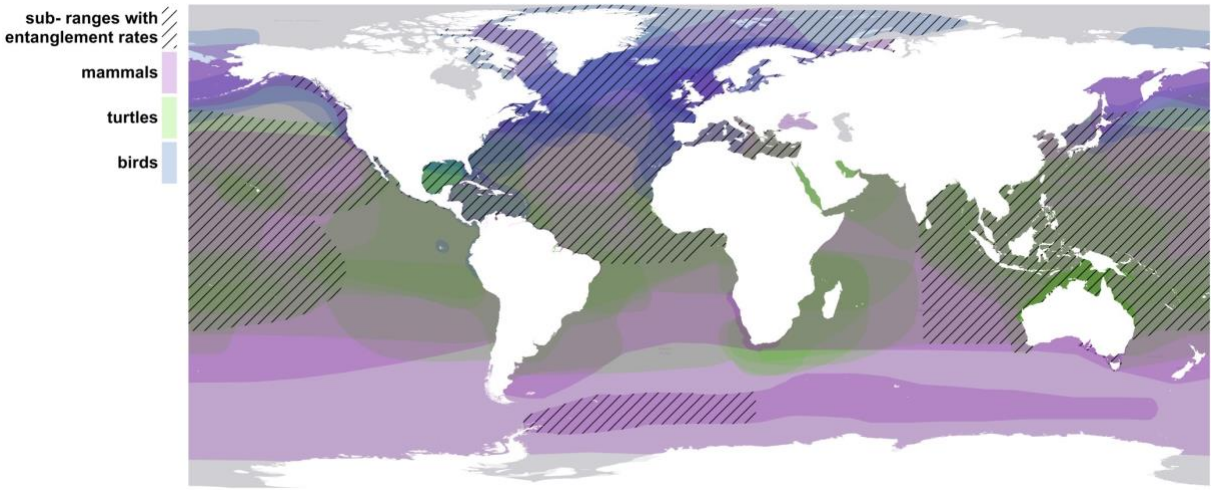

Figure 9: Total model coverage: overlay of all species ranges used in modeling. Full species' ranges shaded by taxon (purple – marine mammals, green – marine turtles, blue – marine birds); species sub-ranges with entanglement rates (hatched lines).

4.3 Dose-response models

Based on each best-fitting observation-weighted linear dose-response model, a predicted plastic density at a projected 50% entanglement rate determined a likely EC_{50} value for each of the species and the two northern gannet exposure groups. For loggerhead sea turtle entanglement, a quasi-binomial generalized linear model with logistic link function was determined to be best fitting due to over-dispersion in the data, and the EC_{50} value was calculated to be 6.0 x 10^3 g/km^2 (Figure 10). A model of this level of complexity was not appropriate for any other species due to lack of sufficient regional entanglement data points. As can be seen in the model, the data points based on smaller sample sizes tend to exhibit higher entanglement rates, likely due to greater observation bias in these studies. The predicted curve was weighted by sample size to compensate for this bias in the model. Dose-response models and EC_{50} values for each of the 20 modeled species-exposure groups are detailed in Appendix 3.

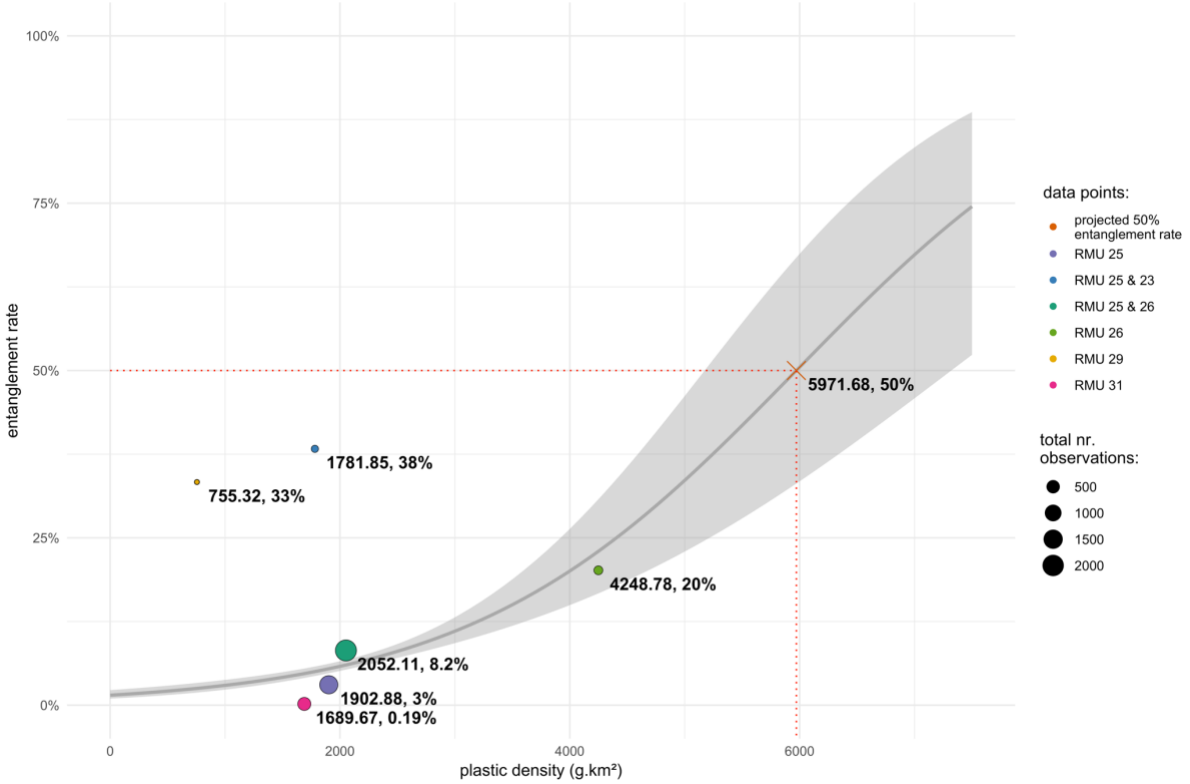

Figure 10: Loggerhead sea turtle (*Caretta Caretta*) dose-response model: binomial generalized linear model with logistic link function, weighted by number of observations.

4.4 Global marine species sensitivity distribution

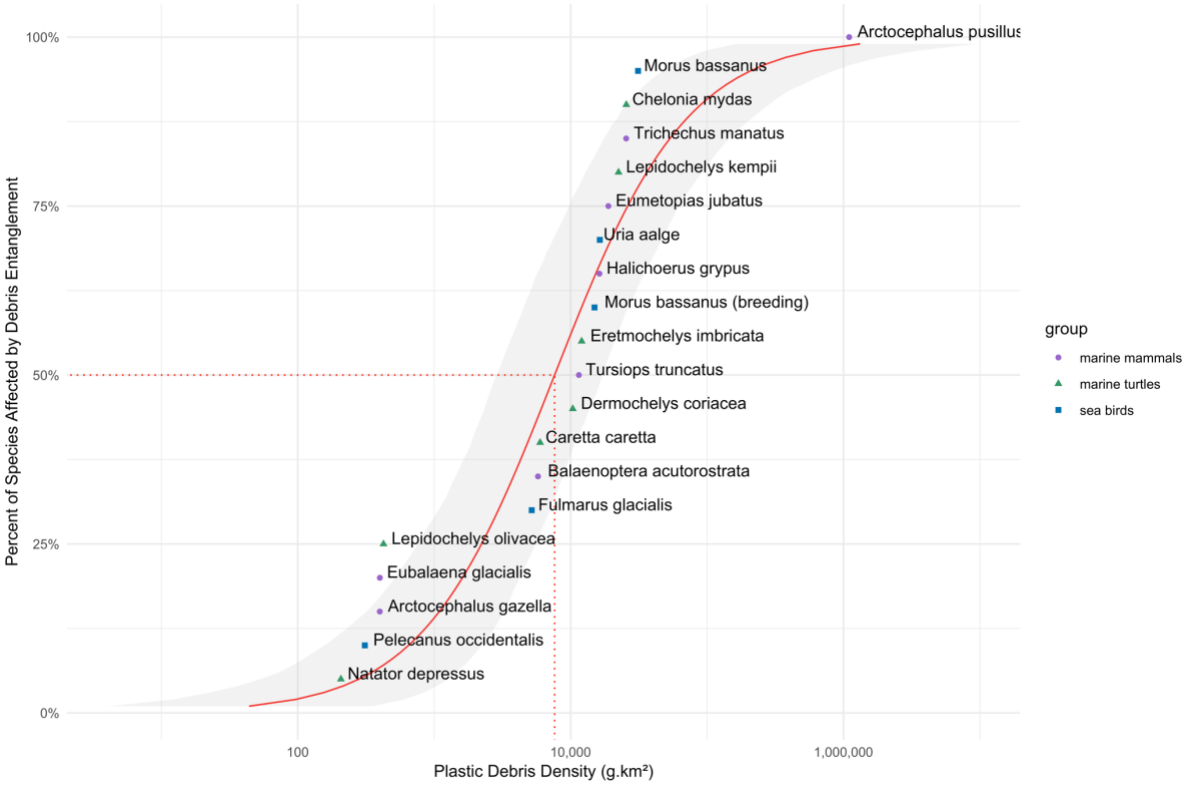

Figure 11: Global marine species sensitivity to macroplastic debris entanglement (fitted to log-logistic cumulative distribution). The modeled estimate of marine plastic debris density affecting 50% of species above their median effect level is 7.6 x 10^3 g/km^2 (HC_{50}).

The 20 ranked species-exposure group EC_{50} values calculated in section 4.3 were ranked and plotted in a global species sensitivity distribution, and the best-fitting log-logistic model curve was determined using MLE and comparing the AICC statistic (Figure 11). No obvious taxonomically-related pattern in sensitivity is discernable from the SSD ranking. The species in the distribution most sensitive to plastic debris entanglement is the flatback sea turtle (*Natator depressus*) with an EC_{50} value of 2.0 x 10^2 g/km^2 plastic density, while the least sensitive of the group is the Afro-Australian Fur Seal (1.1 x 10^6 g/km^2). Based on the 20-species SSD model, the HC_{50} value, at which 50% of representative species are exposed to macroplastic debris above their median effect level, was calculated at 7.6 x 10^3 g/km^2. The species with sensitivity closest to this median is the loggerhead sea turtle (6.0 x 10^3 g/km^2), followed by the common minke whale (5.8 x 10^3 g/km^2). EC_{50} species sensitivity values fell within 5 orders of magnitude, with all but the Afro-Australian fur seal falling within 3 orders of magnitude (EC_{50} at at 2.0 x 10^2 to 3.1 x 10^4 g/km^2). A 19-species model was fitted without this outlier, and the resulting HC_{50} value was 7.0 x 10^3 g/km^2, within the confidence range of the original model. It was decided to leave the Afro-Australian fur seal data point in as the underlying data is based on peer-reviewed literature and was not the only species with a data collection method based on observations of the entire local population (see 4.1, paragraph 3).

Based on this global, 20-species SSD model, predicted potentially affected fraction of species values were calculated for each grid-cell in the macroplastic debris model (approximately 0.2 decimal degree resolution) and mapped in ArcGIS (ESRI 2017)

(Figure 12). As expected, the model shows larger PAF values in regions where plastic densities are higher, including in the five oceanic gyres, plastic pollution-hotspot coastal regions, and enclosed seas such as the Mediterranean. Nearly 4.1 million km^2, or 0.8% of the world's marine areas, are predicted to have plastic densities above the HC_{50} value, where 50% of species are vulnerable to entanglement rates above their median effect level. These hotspots above 50% PAF are especially concerning as many of them are located in areas of high biodiversity which are also at high risk from multiple other hazardous vectors including climate change, sea level rise, ocean acidification, and overexploitation of fisheries (United Nations (Ed.) 2017).

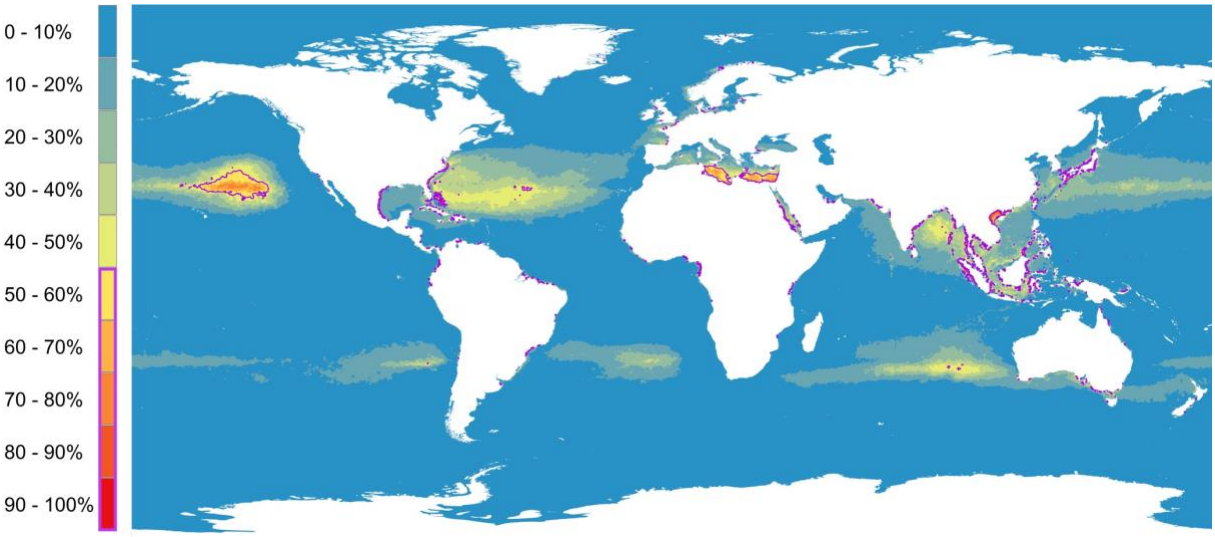

Figure 12: Global spatially-explicit potentially affected fraction of species (PAF): based on global species sensitivity distribution and corresponding plastic density per grid-cell (eq 2). Purple-outlined areas where PAF is above 50% (HC_{50})

4.5 Global effect factor model

Using values calculated in the global PAF model (section 4.4), an average EF model (PAF.km^2/g) was derived, covering each mapped grid cell at the same resolution. This was also mapped in ArcGIS (ESRI 2017) (Figure 13). At first glance it looks like the inverse of the PAF map, with higher EF values in regions with lower plastic densities. However, as the y-values in this model equal the slope of the PAF model at the related plastic densities, this represents the *average effect* on species that would be caused by each additional unit of plastic debris in these regions. EF values are higher at lower plastic densities where fewer species are initially affected, and lower at higher plastic densities where more species are already affected. The median linear effect factor (EF_{50}), at which 50% of species are affected by entanglement, is 6.5 x 10^{-5} PAF.km^2/g in the global, 20-species model. All areas with a PAF below 50% have an EF value above this median, to a maximum of 3.9 x 10^{-4} PAF.km^2/g in areas with minimum plastic debris densities (0.28 g/km^2).

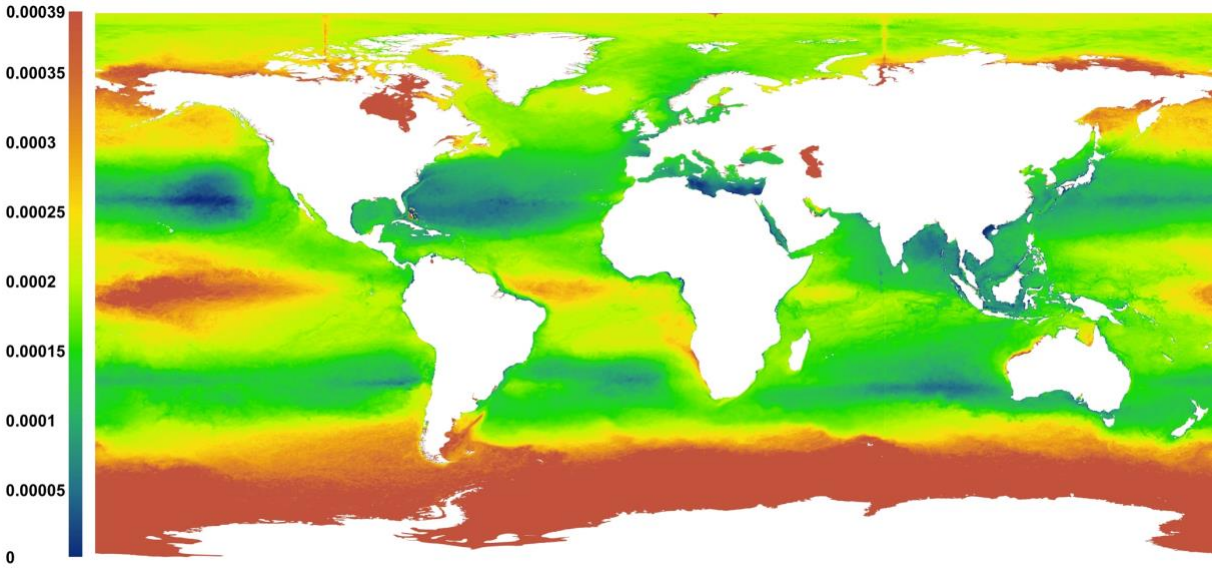

Figure 13: Global spatially-explicit effect factor (PAF.km^2/g): Average effect factor based on global species sensitivity distribution and corresponding plastic density per grid-cell (eq 3). Darkest blue areas show below-median EF (corresponding to HC_{50} and higher PAF-levels), while warmer colors show increasing EF (lower current PAF-levels and plastic densities).

4.6 Regional and taxon-specific model comparison

In order to test the sensitivity of the EF model to changes in scope of the species sensitivity distribution, several regional and taxon-specific subsets of the SSD model were formulated and the resulting values for HC_{50}, average EF and EF_{50} and were compared.

All HC_{50} plastic densities were found to occur within two orders of magnitude for all models, although the best-fitting model function varied between log-normal, log-logistic, log-gumbel, gamma, and Weibull curves (Figure 14). Overall, the South Pacific Ocean model has the overall lowest associated HC_{50} plastic density (3.0×10^3 g/km^2) while the Mediterranean Sea model has the highest HC_{50} (1.1×10^4 g/km^2). Of the taxon models, the turtles-specific model has the lowest HC_{50} plastic density (6.3×10^3 g/km^2) of the taxon models, while bird- and mammal-specific models have similar HC_{50} plastic densities at 9.0×10^3 g/km^2 and 9.9×10^3 g/km^2, respectively.

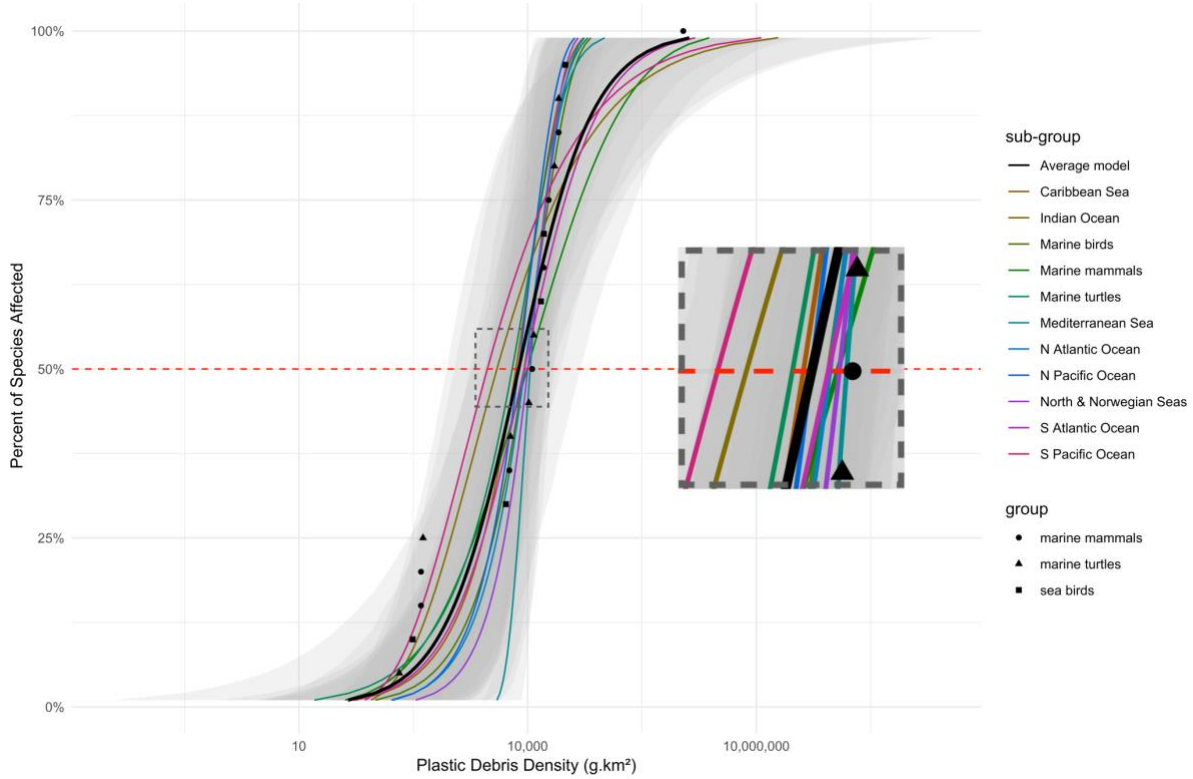

Figure 14: Species sensitivity distribution comparison of global model to regional and taxon-specific models. Inset shows close-up of HC_{50} of all models.

The ranking order of EF_{50} values is the opposite of HC_{50} values, with highest EF_{50} values occur for models with the lowest HC_{50} plastic densities (Figure 15 and Appendix 6). At plastic densities lower than 10^4 g/km^2, models are widely divergent, several of the models exhibiting an EF which increases and peaks before beginning to decrease, while other model curves have a continuous negative slope. This suggests that while the taxon- and spatially-specific models may be relevant for lower plastic densities, this distinction will become less relevant in debris-hotspot regions. Roughly 2.6 million km^2, or 0.5% of the world's marine areas, currently contain macroplastic densities above this 10^4 g/km^2 threshold.

All compared regional and taxon-specific SSD and EF models, as well as associated maps of spatially-specific PAF and average EF values, can be found in appendix 4 (regional models) and appendix 5 (taxon-specific models). A full comparison of model parameters, HC_{50} plastic densities and EF_{50} values can be found in Appendix 6.

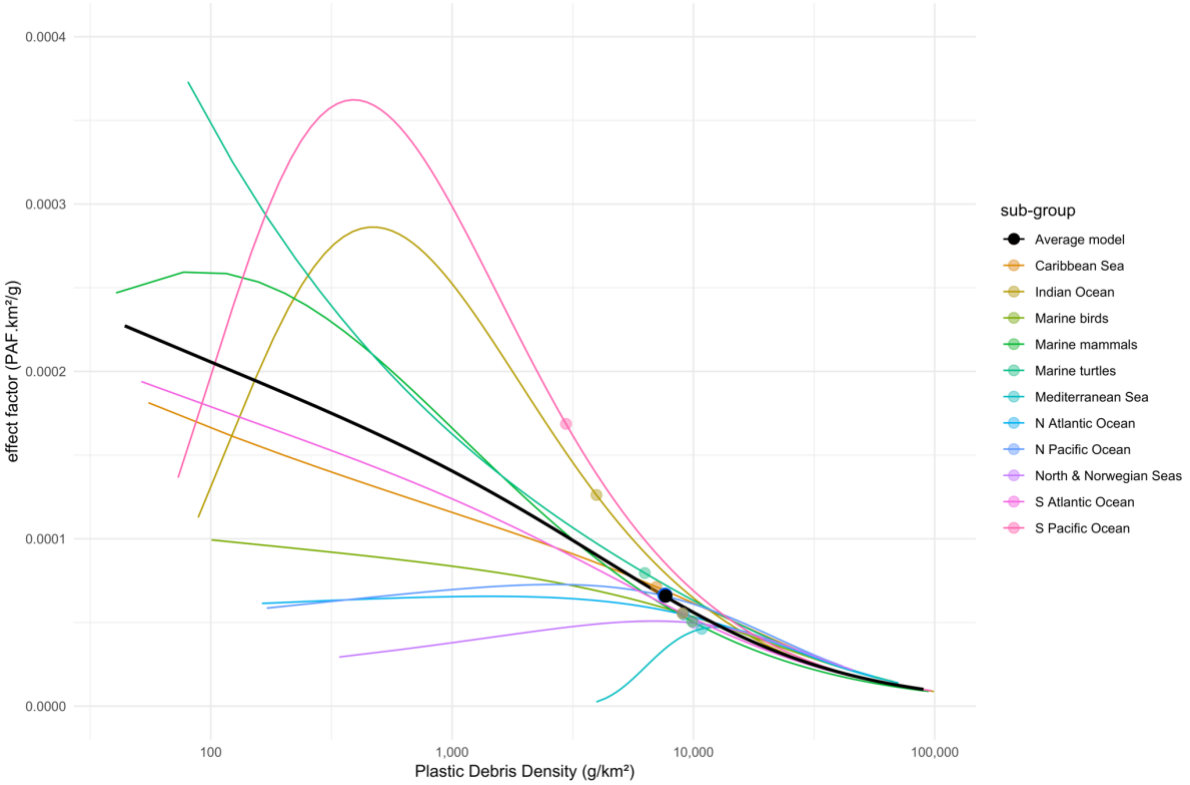

Figure 15: Effect factor model comparison of average model to region and taxon-specific models. Points show effect factor at 50% PAF for each model.

4.7 Comparison to Woods et al. (2019) preliminary model

The effect factor approach presented here was inspired by the methodology of Woods et al. (2019) in their quantification of macroplastic entanglement impact on marine species. While the same marine macroplastic density data was used (Eriksen et al. 2014) and both methods generate spatially-differentiated models, major differences include the choice of included species and the addition of species sensitivity distribution modeling in the new approach. Due to this methodological difference, their resulting models are taxon-specific, while the new method includes a general global average model (Figure 11, Figure 12 and Figure 13) as well as regional and taxon-specific models.

Woods et al. found that their models show the highest PAF in some areas with the lowest modeled macroplastic densities, which is unrealistic and likely due to regional variance in species richness rather than a necessarily greater risk in these regions. In contrast, the highest PAFs in the new model occur in regions with highest macroplastic densities, a more likely pattern. These significant disparities between our results can be explained by different source data choices as well as significant methodological distinctions between their approach and the new approach introduced here.

While Woods et al. quantified entangled species listed in Kühn et al. (2015), the new method utilizes 10 separate sources – a mix of stranding data reports, academic literature and personal communication with marine researchers – to quantify rates of entanglement. This allowed for modeling of dose-response relationships between plastic densities and entanglement rates. Additionally, while Woods et al. used OBIS occurrence data (OBIS 2018) and both BirdLife International and IUCN range maps (BirdLife International 2018a; IUCN 2018) in two separate approaches to quantify PAF and EF values, the new model discerns ranges of species and sub-ranges of local entangled populations using IUCN (2019) range polygons, subsections of the same, and Regional Management Units (RMUs) (Wallace et al. 2010) from *The State of the World's Sea Turtles Online Database (SWOT)* (Kot et al. 2015).

The Woods et al. models included the entire marine taxa for Actinopterygii, Chondrichthyes, Aves, Mammalia and Reptilia, and the last three of these can be compared with the new marine mammal, bird and turtle-specific models introduced here. They concluded that while the OBIS dataset included more total species for Actinopterygii and Chondrichthyes, the IUCN/BirdLife-based modeling approach has lower uncertainty. This is due to the fact that the OBIS one-dimensional observation-based point-series required conversion to two-dimensional species ranges split by marine ecoregion boundaries (Spalding et al. 2007), whereas vectorized species ranges from IUCN and BirdLife are expert-curated and could be used without modification (Woods et al. 2019). Accordingly, while both the OBIS-based and IUCN/BirdLife-based models show increased PAF intensity corresponding to where species richness is greatest, the IUCN/BirdLife-based models show more ecologically-realistic patterns. A side-by-side PAF and EF spatial model comparison of the Woods et al. IUCN/BirdLife-based model maps and the present SSD-based modeling approach is shown in Tables 2-4 below. In Table 2, it can be seen that for Aves, the Woods et al. model shows greatest PAF in North Atlantic and Arctic regions, followed by regions below the Tropic of Capricorn (23.5°S). Conversely, the new bird SSD-based model shows relatively small regions of PAF above 50%, corresponding with highest macroplastic density gyre and coastal regions.

Table 2: Comparison of SSD-based bird species models to Woods et al. (2019) BirdLife range-based Aves model

Birds:	**SSD-based models:** (5 marine bird species)	**Woods et al. BirdLife Aves models:** (642 marine bird species)
PAF (0-100%)	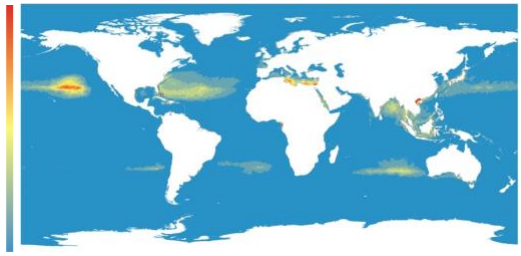	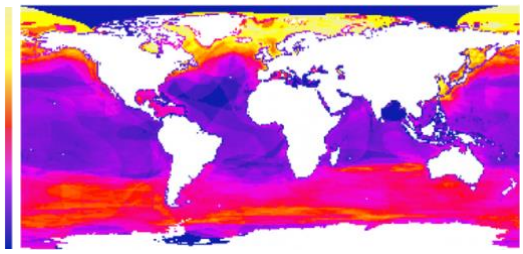
EF (PAF.km^2/g)	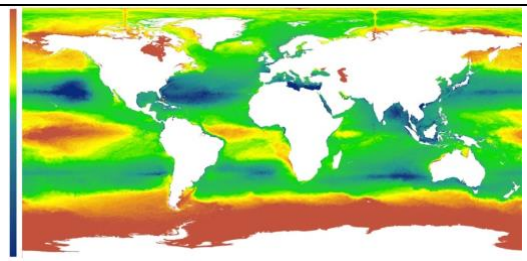	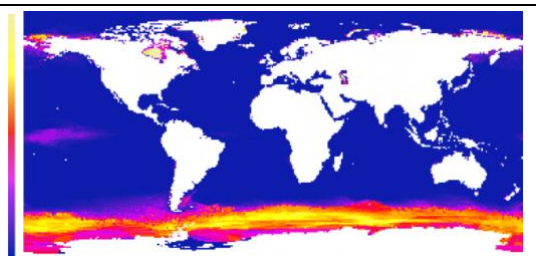
Maximum EF (PAF.km^2/g)	*1.4 x 10^{-4}*	*3.54*

Table 3: Comparison of SSD-based mammal species models to Woods et al. 2019 IUCN range-based Mammalia models

Mammals	**SSD-based models:** (8 marine mammal entanglement rates)	**Woods et al. IUCN Mammalia models:** (129 marine mammal entanglement observations)
PAF (0-100%)	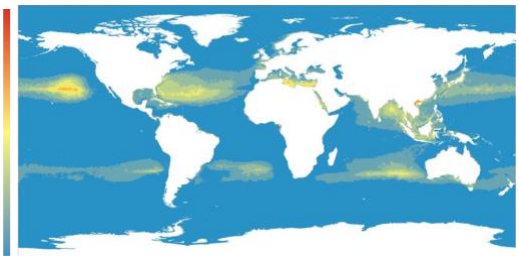	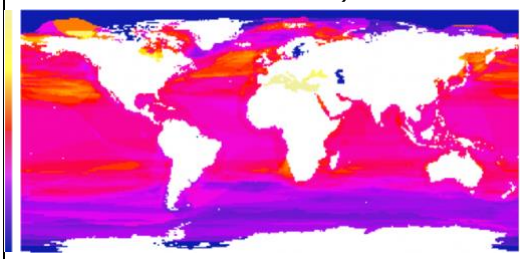
EF (PAF.km^2/g)	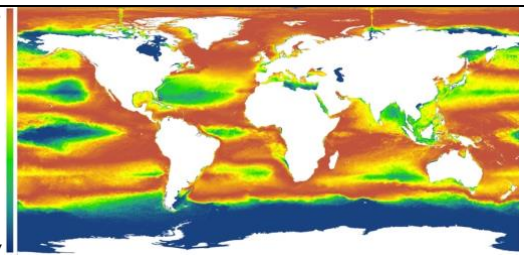	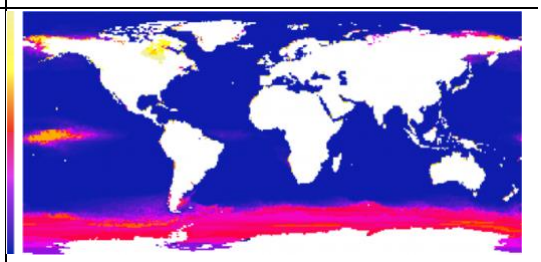
Maximum EF (PAF.km^2/g)	*2.6 x 10^{-4}*	*3.54*

For Mammalia (

Table 3), the Woods et al. model shows a high PAF in the North Pacific, South Pacific, South Atlantic and South Indian Ocean gyres, as well as north of the North Atlantic gyre.

The mammal SSD-based model shows similar impacts, but again matches patterns of higher plastic concentrations in the oceanic gyres and pollution-hotspot coastal regions.

In Table 4 we see that the Woods et al. Reptilia model shows the highest sensitivity of all their models, with a rather uniform pattern of high PAF throughout all oceans where reptiles are found as well as PAF hotspots in coastal regions. The new turtle SSD-based model also shows turtles to have the highest overall sensitivity of the three taxa we modelled, but yet again this matches the pattern of highest PAF in regions of greatest macroplastic densities.

Table 4: Comparison of SSD-based marine turtle species models to Woods et al. 2019 IUCN range-based Reptilia models

Reptiles:	**SSD-based models:** (7 marine turtle entanglement rates)	**Woods et al. IUCN Reptilia models:** (129 marine turtle entanglement observations)
high **PAF** (0-100%) *low*	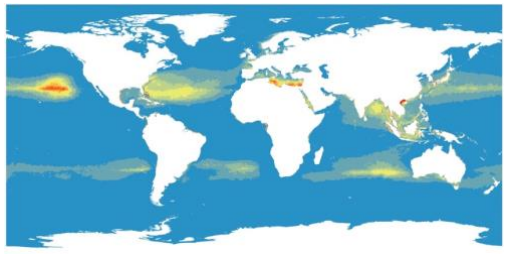	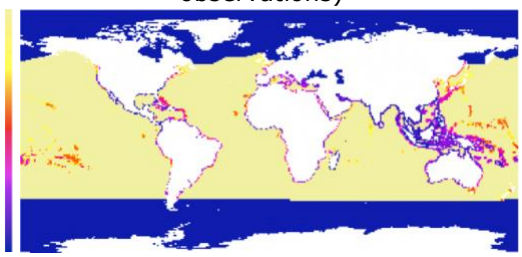
high **EF** (PAF.km^2/g) *low*	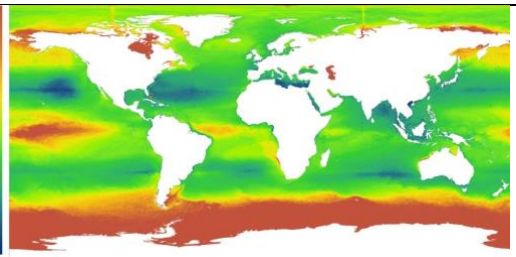	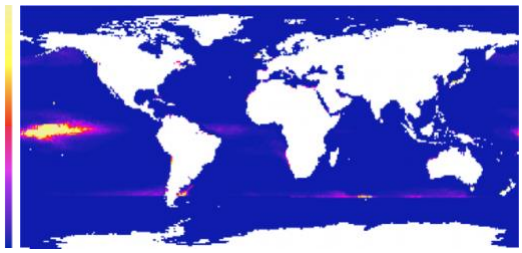
Maximum EF (PAF.km^2/g)	*3.7 x 10^{-4}*	*3.54*

In calculating average effect factors, the same methodology was used in the new models as in the Woods et al. research, aiming to model the average distance between current and ideal (zero-pollution) environmental conditions. Due to differences in the underlying PAF models, however, the resulting EF values in the new SSD methodology are four orders of magnitude smaller than in the Woods et al. model (*Maximum EF*, Tables 2-4). For all five of the Woods et al. OBIS-based taxa models, EFs (projecting where additional plastic pollution will likely cause the most harm) show highest intensity in the Southern Ocean, equatorial Pacific and some Arctic regions. This is also generally true for their five IUCN/BirdLife-based models, except that Actinopterygii, Chondrichthyes, and Reptilia have low intensity 'gaps' in a few southern areas (likely an artifact of limits in range map coverage), and Actinopterygii shows no recognizable EF intensity anywhere. The new SSD methodology EF models for birds and turtles similarly display high values in Arctic, Equatorial Pacific, and Southern Ocean regions where plastic densities are currently low, while the mammals-only EF model conversely shows low intensity in regions with both low and high plastic densities due to the initially positive slope of the predicted EF model curve, predicting few additional effects at both extremely low and extremely high pollution levels.

5 Discussion

5.1 Novelty of the methodology

To the author's knowledge, this is the first methodology scaling species sensitivity to marine macroplastic densities, thereby quantifying plastic debris-correlated potentially affected fraction of species and effect factors. Species sensitivity distributions are widely used in ecotoxicology and environmental risk assessment, and have been successfully applied in the development of various ecosystem quality indicators in LCIA, increasing the ecological realism of the methodology (Curran et al. 2011; Woods et al. 2018).

The general low availability of entanglement rate data means the new SSD-based EF-modeling approach can only yet represent a selection of birds, mammals, and all marine turtles, whereas the precursor Woods et al. (2019) method was able to display an effect factor model each for the entirety of five major taxonomic groups. However, the PAFs resulting from the Woods et al. methodology were (according to their own analysis) not realistic, calling into question the usefulness of the method. One of their recommendations to make their method more operational was to add SSD-based models based on species- or population-specific entanglement rates, which has been done in the new methodology presented here.

A strength of the SSD methodology for quantifying the impacts of mismanaged plastic waste is that it can be scaled by region and taxon as needed to suit analysis. Temporal scaling may also become an option as dynamic models of marine plastic debris become available (van Sebille et al. 2012). As shown in the results, while median species sensitivity to plastic debris entanglement in some regions was close to the global average model, in other regions such as the South Pacific Ocean, median sensitivity was nearly double the average, whereas in the North and Norwegian Seas as well as the Mediterranean Sea, this value was more than two-thirds lower. However, these differences may change in significance if more species' and populations' sensitivities to debris entanglement are compiled to augment the model.

5.2 Implementation in LCA

Not all macroplastic debris is equally likely to entangle marine species, and this is important in determining for which types of LCA analysis the modeled effect factor could be an appropriate addition. A survey of marine experts established that fishing-related items (buoys and rope, monofilament, nets) are considered to be the most likely debris to entangle marine biota, followed by plastic bags, balloons and packaging (Wilcox et al. 2016). In the current study, 63% of debris cited in population entanglement rates are fishing-related, agreeing roughly with the overall percentages in our generic debris effects database (Figure 16) (McHardy 2018). Derelict fishing gear was also found to comprise 70.4% of macroplastic (>200mm) debris items (by weight) seen in the visual survey transects recorded by Eriksen and colleagues (2014) while compiling their marine plastic debris model used in our parameters (Table 5).

This data points to fishing gear and fishery products as obvious candidates for using an entanglement-related EF in characterizing impacts as a part of their LCA evaluation. Both commercial and recreational fishing industries can be included as well as their

related equipment and products. Additionally, packaging products such as plastic bags, films, ring-like objects (wrapping bands, six-pack rings, etc.), balloons, strings/lines, and landscape netting are appropriate to consider for entanglement effects in LCA. Adding an appropriate 'fate factor' for these varying products can account for their rate of occurrence in marine ecosystems.

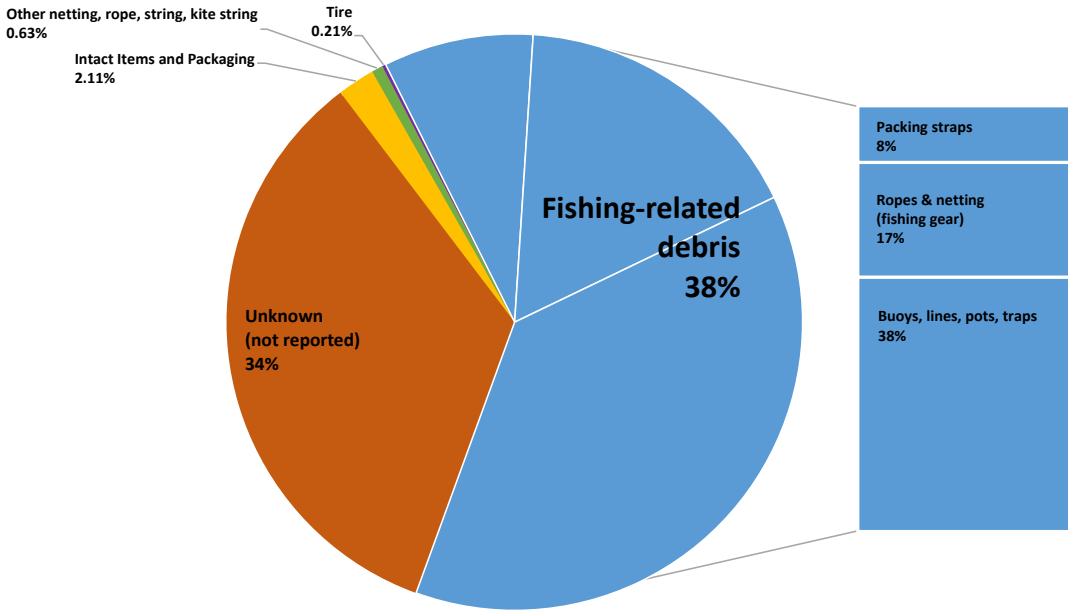

Figure 16: Debris types reported in population entanglement rates

Table 5: Percent distributions of macroplastic (>200mm) items by type (Eriksen et al. 2014). Count data collected in visual survey transects conducted in the North Pacific, South Pacific, South Atlantic, Indian Ocean, and Mediterranean Sea. Weights averaged from coastal debris surveys conducted on several continents and used in calculating a global spatial model of marine macroplastic density used in our research.

Category	Subcategory	Items	% Count	% Weight
Plastic Fishing Gear:	Buoy	319	7.4	58.3
	Line	369	8.6	11.1
	Net	102	2.4	0.9
	Other fishing gear	70	1.6	0.1
Other Plastics:	Bucket	180	4.2	15
	Bottle	791	18.4	4.9
	Foamed polystyrene	1116	26	8
	Plastic bag/film	420	9.8	0.8
	Misc. plastics	924	21.5	0.8
Total		4291	99.9	99.9

5.3 Model uncertainty

The methodology demonstrated here consists of several steps, and uncertainties can be found in each phase of the process. As the data utilized in creating this model came from diverse sources, uncertainty arises from decisions over the temporal scope of data (i.e. how contemporaneous the entanglement data is with the modeled macroplastic densities) as well as which sources were considered admissible. Sampling approaches and reporting consistency among stranding data collectors around the world is widely

varied, based on differing program objectives and effort over time, adding to the uncertainty of data comparison at regional or global scales (Claro et al. 2019). In matching the entanglement rates to the plastic density model, decisions were made as to species ranges and sub-ranges to use for calculating associated average plastic densities. For marine turtles, vectorized maps were available of population-specific RMUs, identified based on extensive studies of nesting sites, populations (genetics, abundance and trends), and tracking data. For other species, however, home ranges of specific populations have not been as explicitly quantified, so range delineation descriptions for subspecies or sub-populations were used to crop range polygons provided by IUCN, adding a level of uncertainty.

In dose-response modeling, the choice was made to use linear, origin-intercept models of species responses in order to incorporate species with only one or few available entanglement rates into the SSD, adding considerable uncertainty to the resulting EC_{50} values used in the ranking model. In some dose-response models, contradictory stranding data appears to show higher entanglement at lower plastic densities (e.g. loggerhead). This is likely due to a combination of biased stranding data and inaccurate estimation of true debris exposure. Bias inherent in small sample sizes was addressed by using the total number of observations as a weighting factor in the model. Nearly all the ranked SSD models had 95% confidence limits separated by one order of magnitude, with the 19 species model (minus *A. pusillus*), North Pacific, and North Atlantic models having the narrowest confidence intervals. The widest confidence intervals belong to the mammals-only model, followed by the South Atlantic model.

5.4 Data availability and biases

While most current reports of entanglement are simply qualitative in nature, an effort was made to catalog *rates of entanglement* based on percentages of defined population segments observed entangled in plastic debris. In most debris studies where rates are defined, these populations are approximated by stranding statistics, and the percent of stranded individuals found to be entangled in plastic debris quantify regional population entanglement rates. Using stranding statistics to define overall entanglement rates is known to often grossly underestimate true rates of occurrence as many affected individuals will never make it to shore (Monteiro et al. 2016), and observation rates vary over geographic and temporal time scales. This bias is less of an issue for species where more direct forms of observation are possible: nest entanglement rates have been observed for whole colonies of birds, and drone-assisted surveys have counted entire seal breeding colonies, identifying entanglement rates fairly accurately (Claro et al. 2019; Ryan 2018).

Despite the severe shortcomings of stranding data as a measure of entanglement rates, these statistics remain by far the most comprehensive spatial and temporal record of plastic debris impacts on marine species. It may be warranted, however, to adjust certain reported entanglement rates by an "observation factor," correcting for the known underestimate that stranding statistics represent, when modeling these in an EF approach. This observation factor could be adjusted to account for coastal geography and local currents, or based on local "drifter" experiments, in which simulated or actual carcasses are monitored to see the rate at which they are deposited on observed coastlines (Koch et al. 2013; Peltier et al. 2012; Santos et al. 2018; Young et al. 2019).

Another confounding issue with stranding data is that it is often impossible to unequivocally distinguish debris-entanglement as the cause of injuries and deaths where

debris is no longer present: some entanglements do not leave noticeable marks, and causes of old injuries cannot always be determined (Mackarous & Griffiths 2016; NOAA STSSN 2014; Vélez-Rubio et al. 2013). Furthermore, it is not always possible for observers to distinguish between fishing gear entanglements resulting from active gear – which is not considered debris – versus abandoned, lost or otherwise discarded fishing gear – which is considered debris (Claro et al. 2019). A study on turtle bycatch on the Brazilian coast found that only 30% of by-caught turtles killed in the pelagic long-line fisheries were later observed on the adjacent coast, and of those found, none had external evidence of fisheries interaction (Monteiro et al. 2016). This illustrates how both identification of debris-caused injuries and lethality in general are difficult to isolate, even for experienced researchers.

Life-threatening impacts are to be expected to occur in many entanglement cases; fishing line and rope entanglement, for example, is expected to be lethal for 25–50% of affected birds (Wilcox et al. 2016). However, as illustrated above, lethal impacts and harm at the *ecological* level can be hard to definitively prove using the opportunistic sampling techniques that are commonly practiced (Rochman et al. 2016). Most entanglement rate reports referenced in this study (87.8%) did not clearly reference the severity or final outcome of entanglements. Of those which did reference an outcome, direct harm or death was the most likely outcome (8.7%), followed by indirect harm or death (2.6%). In ecological risk assessment, modeling methods such as "adverse outcome pathways" are used to bridge the gap between lower-order (sub-organismal, organismal) and higher-order (population and ecosystem level) effects (Kramer et al. 2011). If such methodology is used to infer lethal impacts from entanglement, the resulting effect factor metric for use in LCIA could be the potentially *disappeared* fraction of species (PDF), rather than the more conservative potentially *affected* fraction of species (PAF), which has been applied in this study.

While there remain large uncertainties and gaps in the data underlying this effect factor model, better data is expected to become available in the coming years as marine plastic debris models are improved and standardized species entanglement data collection is more widely adopted (Claro et al. 2018). The recent INDICIT ("*Implementation of the indicator of marine litter on sea turtles and biota in Regional Sea Conventions and Marine Strategy Framework Directive Areas*") project was funded by the European Commission in order to develop and standardize litter impact monitoring in European and international sea regions, including a consortium of scientific experts in marine litter (Miaud et al. 2018). The resulting reports cover both ingestion and entanglement impacts, including standardized forms and guidelines for recording stranding observations that will be used to implement harmonized reporting of debris impacts on marine biota throughout Europe. It is hoped that more uniform and comprehensive data reporting will also become the norm in other regions, especially in areas where data is particularly lacking such as on African coasts and throughout the Indian ocean. More consistent global and harmonized reporting of debris impacts is key to uncertainty reduction, data validation and comprehensiveness of species represented in the entanglement effects model.

5.5 The methodology in context

The immediate purpose of the methodology presented here is to further the development of EFs for use as part of the characterization of mismanaged plastic waste in the LCIA phase of LCA. However, as plastic limits and bans are being debated in many

communities around the world, the causative link between plastic pollution and resulting environmental harms is a hot topic of discussion in the wider scientific and policy-making community, as well as society at large. Additionally, while the reduction of ecological harms related to plastic pollution is an important end in itself, all forms of pollution and waste are essentially resources which have been lost to society. The reduction of resource use/waste and associated climate and pollution impacts are central ambitions of realizing more 'circular economies' but also go a long way in rectifying the environmental pollution injustices borne disproportionately by the global poor.

As noted in Woods et al. (2016), LCA was originally developed to measure the impacts of land-based production and consumption on terrestrial and freshwater ecosystems, and adequate marine biodiversity loss characterization tools are currently lacking in the methodology. Without characterization of the full range of impacts due to mismanaged plastic waste, LCA studies risk ranking plastic products and processes as most environmentally desirable when this may not actually be the case (Schweitzer et al. 2018). The addition of plastic waste impact characterization can allow for more comprehensive measurement of the environmental impacts of products and industries producing or mishandling this waste.

Quantification of entanglement impacts resulting from exposure to marine macroplastic debris is the first step in addressing impacts from mismanaged plastic waste, a major omission in the current practice of LCA analysis for plastic products. However, as "marine biota entanglement in plastic debris" is only one impact pathway resulting from plastic pollution, it will be important to develop EFs for other significant impacts (e.g. ingestion, habitat transformation/ destruction, non-native species introduction via rafting), as well as "fate factors" to account for the occurrence of plastic waste in the environment, before considering the characterization to be complete.

6 Conclusion

This research has focused on the growing problem of mismanaged plastic waste and one effect it has on marine biota: entanglement. A global marine species sensitivity distribution model was developed, along with subsets of the sensitivity distribution focusing on eight marine regions and three taxon groups and their sensitivity to debris entanglement at existing densities of macroplastics in marine ecosystems. All models are spatially-specific and visualized through vectorized maps, each including a potentially affected fraction of species and average effect factor model. A median linear EF_{50}, corresponding with 50% PAF, was calculated for each model, as well as the density of macroplastic debris at which this is projected to occur. Despite various underlying uncertainties, the models produce feasible predictions. Based on the global model, it is estimated that 50% or more of modeled marine species are currently affected by entanglement at greater than a 50% rate in 0.8% of marine regions, amounting to nearly 4.1 million km^2 of world oceans with a high level of entanglement risk. As plastic debris impact hotspots occur in many regions where species also face the additional threats of climate change, ocean acidification, sea level rise, and overexploitation of marine resources, the accumulated repercussions on marine biodiversity are devastating (United Nations (Ed.) 2017).

The full extent to which marine biota entanglement is a vector of biodiversity loss remains unknown, but this thesis has attempted bring together existing information in a new way to formulate a quantification methodology for this impact. The method relates rates of entanglement to current and future levels of plastic debris in marine ecosystems and is expandable as new data becomes available. This research produced an effect factor formulation which can be directly connected to the production, transportation, use and disposal of plastic products. Gaps and variance in the underlying data may prevent the model from being immediately exploitable, but it is expected that with recent standardization of data collection more uniform documentation will soon be available to supplement the model and reduce uncertainties. While a fate factor and corresponding effect factors for other influential impact pathways need to be further investigated in order to complete this characterization, the research presented here is a significant advancement towards a quantification of mismanaged plastic waste impacts in LCIA.

References

Adimey, N. M., Hudak, C. A., Powell, J. R., Bassos-Hull, K., Foley, A., Farmer, N. A., White, L., & Minch, K. (2014). Fishery gear interactions from stranded bottlenose dolphins, Florida manatees and sea turtles in Florida, U.S.A. *Marine Pollution Bulletin, 81*(1), 103-115. doi:10.1016/j.marpolbul.2014.02.008

Allen, K., Cohen, D., Culver, A., Cummins, A., Curtis, S., Eriksen, M., Gordon, M., Howe, A., Lapis, N., Prindiville, M., Thorpe, B., & Wilson, S. (2017). *Better Alternatives Now: B.A.N. LIST 2.0*. Retrieved from: https://www.5gyres.org/s/5Gyres_BANlist2.pdf

Basel Convention. (2018). UN convention on wastes makes breakthrough recommendations to address global marine litter and other types of wastes [Press release]. Retrieved from http://www.basel.int/?tabid=7655&utm_source=newsletter201809&utm_medium=email&utm_campaign=brsNewsletter

Başkale, E., Sözbilen, D., Katılmış, Y., Azmaz, M., & Kaska, Y. (2018). An evaluation of sea turtle strandings in the Fethiye-Göcek Specially Protected Area: An important foraging ground with an increasing mortality rate. *Ocean & Coastal Management, 154*, 26-33. doi:https://doi.org/10.1016/j.ocecoaman.2018.01.003

BirdLife International. (2018a). BirdLife Data Zone: http://datazone.birdlife.org/species/requestdis.

BirdLife International. (2018b). Fulmarus glacialis. The IUCN Red List of Threatened Species 2018: e.T22697866A132609419. Retrieved from http://dx.doi.org/10.2305/IUCN.UK.2018-2.RLTS.T22697866A132609419.en

BirdLife International. (2018c). Morus bassanus. The IUCN Red List of Threatened Species 2018: e.T22696657A132587285. Retrieved from http://dx.doi.org/10.2305/IUCN.UK.2018-2.RLTS.T22696657A132587285.en

BirdLife International. (2018d). Pelecanus occidentalis. The IUCN Red List of Threatened Species 2018: e.T22733989A132663224. Retrieved from http://dx.doi.org/10.2305/IUCN.UK.2018-2.RLTS.T22733989A132663224.en

BirdLife International. (2018e). Uria aalge. The IUCN Red List of Threatened Species 2018: e.T22694841A132577296. Retrieved from http://dx.doi.org/10.2305/IUCN.UK.2018-2.RLTS.T22694841A132577296.en

Bonin, C. A. (2012). *Population genetics and mating system of Antarctic fur seals, Arctocephalus gazella, at Livingston Island, Antarctica.* UC San Diego. ProQuest ID: Bonin_ucsd_0033D_12952. Merritt ID: ark:/20775/bb0342594t., Retrieved from https://escholarship.org/uc/item/1c26c5sh

Bowen, D. (2016). Halichoerus grypus. The IUCN Red List of Threatened Species 2016: e.T9660A45226042. Retrieved from http://dx.doi.org/10.2305/IUCN.UK.2016-1.RLTS.T9660A45226042.en

Brooks, A. L., Wang, S., & Jambeck, J. R. (2018). The Chinese import ban and its impact on global plastic waste trade. *Science Advances, 4*.

Browne, M. A., Underwood, A. J., Chapman, M. G., Williams, R., Thompson, R. C., & van Franeker, J. A. (2015). Linking effects of anthropogenic debris to ecological impacts. *Proceedings of the Royal Society B: Biological Sciences, 282*(1807), 20142929. doi:10.1098/rspb.2014.2929

Claro, F., Fossi, M. C., Ioakeimidis, C., Baini, M., Lusher, A. L., Mc Fee, W., McIntosh, R. R., Pelamatti, T., Sorce, M., Galgani, F., & Hardesty, B. D. (2019). Tools and constraints in monitoring interactions between marine litter and megafauna: Insights from case studies around the world. *Marine Pollution Bulletin, 141*, 147-160. doi:https://doi.org/10.1016/j.marpolbul.2019.01.018

Claro, F., Pham C.K., Liria Loza A., Bradai M.N., Camedda A., Chaieb O., Darmon G., de Lucia G.A., Attia El Hili H., Kaberi H., Kaska Y., Matiddi M., Monzon-Arguelo C., Moussier J., Ostiategui P., Paramio L., Revuelta O., Silvestri C., Sozbilen D., Tòmas J., Tsangaris C., Vale M., Vandeperre F., & C., M. (2018). *State of the art and feasibility study for the implementation of indicator "Entanglement of Biota with Marine Debris" in the areas of the marine strategy framework directive and the regional sea conventions OSPAR, HELCOM AND Barcelona*. Retrieved from: indicit-europa.eu

Committee on Taxonomy. (2018). List of marine mammal species and subspecies. Retrieved from www.marinemammalscience.org

Cooke, J. G. (2018a). Balaenoptera acutorostrata. The IUCN Red List of Threatened Species 2018: e.T2474A50348265. Retrieved from http://dx.doi.org/10.2305/IUCN.UK.2018-2.RLTS.T2474A50348265.en

Cooke, J. G. (2018b). Eubalaena glacialis. The IUCN Red List of Threatened Species 2018: e.T41712A50380891. Retrieved from http://dx.doi.org/10.2305/IUCN.UK.2018-1.RLTS.T41712A50380891.en

Curran, M. A. (2013). Life Cycle Assessment: a review of the methodology and its application to sustainability. *Current Opinion in Chemical Engineering, 2*(3), 273-277. doi:https://doi.org/10.1016/j.coche.2013.02.002

Curran, M. A., de Baan, L., De Schryver, A. M., Van Zelm, R., Hellweg, S., Koellner, T., Sonnemann, G., & Huijbregts, M. A. (2011). Toward meaningful end points of biodiversity in life cycle assessment. *Environ Sci Technol, 45*(1), 70-79. doi:10.1021/es101444k

Dau, B. K., Gilardi, K. V., Gulland, F. M., Higgins, A., Holcomb, J. B., Leger, J. S., & Ziccardi, M. H. (2009). Fishing gear-related injury in California marine wildlife. *J Wildl Dis, 45*(2), 355-362. doi:10.7589/0090-3558-45.2.355

Deutsch, C. J., Reid, J. P., Bonde, R. K., Easton, D. E., Kochman, H. I., & O'Shea, T. J. (2003). Seasonal Movements, Migratory Behavior, and Site Fidelity of West Indian Manatees along the Atlantic Coast of the United States. *Wildlife Monographs*(151), 1-77.

Deutsch, C. J., Self-Sullivan, C., & Mignucci-Giannoni, A. (2008). Trichechus manatus. The IUCN Red List of Threatened Species 2008: e.T22103A9356917. Retrieved from http://dx.doi.org/10.2305/IUCN.UK.2008.RLTS.T22103A9356917.en

Dewey, T. (2009). "Morus bassanus" (On-line), Animal Diversity Web. Retrieved from https://animaldiversity.org/accounts/Morus_bassanus/

Dierschke, J., Dierschke, V., Hüppop, K., Hüppop, O., & Jachmann, K. F. (2011). Trottellumme: Uria aalge (Guillemot). In OAG Helgoland (Ed.), *Die Vogelwelt der Insel Helgoland*. Helgoland, Germany.

Duncan, E. M., Botterell, Z. L. R., Broderick, A. C., Galloway, T. S., Lindeque, P. K., Nuno, A., & Godley, B. J. (2017). A global review of marine turtle entanglement in anthropogenic debris: A baseline for further action. *Endangered Species Research, 34*, 431-448. doi:10.3354/esr00865

Edwards, E. W. J., Quinn, L. R., Wakefield, E. D., Miller, P. I., & Thompson, P. M. (2013). Tracking a northern fulmar from a Scottish nesting site to the Charlie-Gibbs Fracture Zone: Evidence of linkage between coastal breeding seabirds and Mid-Atlantic Ridge feeding sites. *Deep Sea Research Part II: Topical Studies in Oceanography, 98*, 438-444. doi:https://doi.org/10.1016/j.dsr2.2013.04.011

Elliott, A., Christie, D.A., Jutglar, F., de Juana, E. & Kirwan, G.M. (2018). Brown Pelican (Pelecanus occidentalis). In: del Hoyo, J., Elliott, A., Sargatal, J., Christie, D.A. & de Juana, E. (eds.). *Handbook of the Birds of the World Alive.* Retrieved from https://www.hbw.com/node/52616

Eriksen, M., Lebreton, L. C. M., Carson, H. S., Thiel, M., Moore, C. J., Borerro, J. C., Galgani, F., Ryan, P. G., & Reisser, J. (2014). Plastic Pollution in the World's Oceans: More than 5 Trillion Plastic Pieces Weighing over 250,000 Tons Afloat at Sea. *PLOS ONE, 9*(12), e111913. doi:10.1371/journal.pone.0111913

ESRI. (2017). ArcGIS Desktop 10.6. *Zonal Statistics.* Retrieved from http://desktop.arcgis.com/en/arcmap/10.3/tools/spatial-analyst-toolbox/zonal-statistics.htm

European Commission. (2018). *Impact Assessment: Reducing Marine Litter- action on single use plastics and fishing gear*. Luxembourg: Office for Official Publications of the European Communities Retrieved from https://eur-lex.europa.eu/resource.html?uri=cellar:4d0542a2-6256-11e8-ab9c-01aa75ed71a1.0001.02/DOC_1&format=PDF#page=12

FAO. (2016). Abandoned, lost or otherwise discarded gillnets and trammel nets: methods to estimate ghost fishing mortality, and the status of regional monitoring and management. Gilman, E., Chopin, F., Suuronen, P., & Kuemlangan, B., *FAO Fisheries and Aquaculture Technical Paper No. 600*. Rome, Italy.

Flanders Marine Institute. (2018). IHO Sea Areas, version 3. Available online at http://www.marineregions.org/. doi:10.14284/323

Fort, J., Pettex, E., Tremblay, Y., Lorentsen, S.-H., Garthe, S., Votier, S., Pons, J. B., Siorat, F., Furness, R. W., Grecian, W. J., Bearhop, S., Montevecchi, W. A., & Grémillet, D. (2012). Meta-population evidence of oriented chain migration in northern gannets (Morus bassanus). *Frontiers in Ecology and the Environment, 10*(5), 237-242. doi:10.1890/110194

Gall, S. C., & Thompson, R. C. (2015). The impact of debris on marine life. *Marine Pollution Bulletin, 92*(1), 170-179. doi:https://doi.org/10.1016/j.marpolbul.2014.12.041

Gelatt, T., & Sweeney, K. (2016a). Eumetopias jubatus ssp. monteriensis. The IUCN Red List of Threatened Species 2016: e.T17345844A66991740. http://dx.doi.org/10.2305/IUCN.UK.2016-1.RLTS.T17345844A66991740.en. Downloaded on 08 May 2019.

Gelatt, T., & Sweeney, K. (2016b). Eumetopias jubatus. The IUCN Red List of Threatened Species 2016: e.T8239A45225749. http://dx.doi.org/10.2305/IUCN.UK.2016-1.RLTS.T8239A45225749.en. Downloaded on 03 May 2019.

Geyer, R., Jambeck, J. R., & Law, K. L. (2017). Production, use, and fate of all plastics ever made. *Science Advances, 3*(7). doi:10.1126/sciadv.1700782

Gill & Donsker (Eds). (2018). IOC World Bird List (v8.2) (Publication no. 10.14344/IOC.ML.8.2). Retrieved 2018-11-01 https://www.worldbirdnames.org

Gregory, M. R. (2009). Environmental implications of plastic debris in marine settings—entanglement, ingestion, smothering, hangers-on, hitch-hiking and alien invasions. *Philosophical Transactions of the Royal Society B: Biological Sciences, 364*(1526), 2013-2025. doi:10.1098/rstb.2008.0265

Hauschild, M. Z. (2018). Introduction to LCA Methodology. In Hauschild, M. Z., Rosenbaum, R. K., & Olsen, S. I. (Eds.), *Life Cycle Assessment: Theory and Practice* (pp. 59-66). Cham: Springer International Publishing.

Hauschild, M. Z., & Huijbregts, M. A. J. (2015a). Introducing Life Cycle Impact Assessment. In Hauschild, M. Z. & Huijbregts, M. A. J. (Eds.), *Life Cycle Impact Assessment* (pp. 1-16). Dordrecht: Springer Netherlands.

Hauschild, M. Z., & Huijbregts, M. A. J. (2015b). *Life Cycle Impact Assessment*. Dordrecht: Springer Netherlands.

Haward, M. (2018). Plastic pollution of the world's seas and oceans as a contemporary challenge in ocean governance. *Nature Communications, 9*(1), 667. doi:10.1038/s41467-018-03104-3

Henderson, A. D., Hauschild, M. Z., van de Meent, D., Huijbregts, M. A. J., Larsen, H. F., Margni, M., McKone, T. E., Payet, J., Rosenbaum, R. K., & Jolliet, O. (2011). USEtox fate and ecotoxicity factors for comparative assessment of toxic emissions in life cycle analysis: sensitivity to key chemical properties. *The International Journal of Life Cycle Assessment, 16*(8), 701. doi:10.1007/s11367-011-0294-6

Hofmeyr, G. J. G. (2015). Arctocephalus pusillus. The IUCN Red List of Threatened Species 2015: e.T2060A45224212. Retrieved from http://dx.doi.org/10.2305/IUCN.UK.2015-4.RLTS.T2060A45224212.en

Hofmeyr, G. J. G. (2016). Arctocephalus gazella. The IUCN Red List of Threatened Species 2016: e.T2058A66993062. Retrieved from http://dx.doi.org/10.2305/IUCN.UK.2016-1.RLTS.T2058A66993062.en

Huijbregts, M. A. J., Hellweg, S., & Hertwich, E. (2011). Do We Need a Paradigm Shift in Life Cycle Impact Assessment? *Environmental Science & Technology, 45*(9), 3833-3834. doi:10.1021/es200918b

ISO14044. (2006). Environmental management—Life cycle assessment—Requirements and guidelines. Geneva, Switzerland: International Organization for Standardization.

IUCN. (2018). The IUCN Red List of Threatened Species. Version 2018-1. http://www.iucnredlist.org

IUCN. (2019). The IUCN Red List of Threatened Species. Version 2019-1. Retrieved 15 May 2019 http://www.iucnredlist.org

Kameda, K., Asari, Y., Sugitani, K., & Wakatsuki, M. (2013). Stranding status of sea turtles at Iriomote Island, Okinawa Prefecture, Japan. [In Japanese]. *Umigame Newsletter of Japan, 96*, 2-8.

Kirkwood, R., Pemberton, D., Gales, R., Hoskins, A. J., Mitchell, T., Shaughnessy, P. D., & Arnould, J. P. Y. (2010). Continued population recovery by Australian fur seals. *Marine and Freshwater Research, 61*(6), 695-701. doi:https://doi.org/10.1071/MF09213

Knowlton, A., K. Hamilton, P., Marx, M., Pettis, H., & Kraus, S. (2012). Monitoring North Atlantic right whale Eubalaena glacialis entanglement rates: A 30 yr retrospective. *Marine Ecology Progress Series, 466*, 293-302. doi:10.3354/meps09923

Koch, V., Peckham, H., Mancini, A., & Eguchi, T. (2013). Estimating At-Sea Mortality of Marine Turtles from Stranding Frequencies and Drifter Experiments. *PLOS ONE, 8*(2), e56776. doi:10.1371/journal.pone.0056776

Kot, C., Fujioka, E., DiMatteo, A., Wallace, B., Hutchinson, B., Cleary, J., Halpin, P., & Mast, R. (2015). The State of the World's Sea Turtles Online Database: Data provided by the SWOT Team and hosted on OBIS-SEAMAP. Oceanic Society, Conservation International, IUCN Marine Turtle Specialist Group (MTSG), and Marine Geospatial Ecology Lab, Duke University. http://seamap.env.duke.edu/swot

Kramer, V. J., Etterson, M. A., Hecker, M., Murphy, C. A., Roesijadi, G., Spade, D. J., Spromberg, J. A., Wang, M., & Ankley, G. T. (2011). Adverse outcome pathways and ecological risk assessment: Bridging to population-level effects. *Environmental Toxicology and Chemistry, 30*(1), 64-76. doi:doi:10.1002/etc.375

Kühn, S., Bravo Rebolledo, E. L., & van Franeker, J. A. (2015). Deleterious Effects of Litter on Marine Life. In Bergmann, M., Gutow, L., & Klages, M. (Eds.), *Marine Anthropogenic Litter* (pp. 75-116). Cham: Springer International Publishing.

Lawson, T. J., Wilcox, C., Johns, K., Dann, P., & Hardesty, B. D. (2015). Characteristics of marine debris that entangle Australian fur seals (Arctocephalus pusillus doriferus) in southern Australia. *Marine Pollution Bulletin, 98*(1-2), 354-357. doi:10.1016/j.marpolbul.2015.05.053

Lebreton, L., & Andrady, A. (2019). Future scenarios of global plastic waste generation and disposal. *Palgrave Communications, 5*(1), 6. doi:10.1057/s41599-018-0212-7

Li, W. C., Tse, H. F., & Fok, L. (2016). Plastic waste in the marine environment: A review of sources, occurrence and effects. *Science of The Total Environment, 566-567*, 333-349. doi:https://doi.org/10.1016/j.scitotenv.2016.05.084

Macfadyen, G., Huntington, T., & Cappell, R. (2009). Abandoned, lost or otherwise discarded fishing gear. *UNEP Regional Seas Reports and Studies No.185;*

FAO Fisheries and Aquaculture Technical Paper, No. 523. (pp. 115p.). Rome: UNEP/FAO

Mackarous, K., & Griffiths, A. D. (2016). Northern Territory Marine Megafauna Strandings: July 2014-December 2015. Report by Department of Land Resource Management, Darwin.

Mcconnell, B. J., Fedak, M. A., Lovell, P., & Hammond, P. S. (1999). Movements and foraging areas of grey seals in the North Sea. *Journal of Applied Ecology, 36*(4), 573-590. doi:10.1046/j.1365-2664.1999.00429.x

McHardy, C. (2018). Investigating options for developing an effect factor for impacts of macro-plastic debris in terrestrial, freshwater and marine ecosystems within the framework of Life Cycle Impact Assessment. Trondheim, Norway: Norwegian University of Science and Technology.

McKone, T., Kyle, A., Jolliet, O., Olsen, S., & Hauschild, M. (2006). *Dose-Response Modeling for Life Cycle Impact Assessment - Findings of the Portland Review Workshop* (Vol. 11).

Miaud, C., Darmon G., Bradai M.N., Claro F., Camedda A., Chaieb O., de Lucia G.A., Attia El Hili H., Kaberi H., Kaska Y., Liria Loza A., Matiddi M., Monzon-Arguelo C., Moussier J., Ostiategui P., Paramio L., Pham C.K., Revuelta O., Silvestri C., Sozbilen D., Tòmas J., Tsangaris C., Vale M., & F., V. (2018). *Pilot and feasibility studies for the implementation of litter impacts indicators in the MSFD and RSCs OSPAR-Macaronesia, HELCOM and Barcelona*. Retrieved from: indicit-europa.eu

Monteiro, D. S., Estima, S., Gandra, T., P. Silva, A., Bugoni, L., Swimmer, Y., Seminoff, J., & Secchi, E. (2016). *Long-term spatial and temporal patterns of sea turtle strandings in southern Brazil*.

Mowbray, T. (2002). Northern Gannet (Morus bassanus). In Poole, A. (Ed.), The Birds of North America Online (Vol. 693, pp. 1-10). Ithaca: Cornell Lab of Ornithology. Retrieved from http://bna.birds.cornell.edu/bna/species/693.

NOAA STSSN. (2014). Sea Turtle Stranding and Salvage Network Reports. U.S. National Oceanic and Atmospheric Administration Southeast Fisheries Science Center: https://www.sefsc.noaa.gov/species/turtles/strandings.htm.

OBIS. (2018). Ocean Biogeographic Information System. Intergovernmental Oceanographic Commission of UNESCO www.iobis.org.

Orós, J., Montesdeoca, N., Camacho, M., Arencibia, A., & Calabuig, P. (2016). Causes of Stranding and Mortality, and Final Disposition of Loggerhead Sea Turtles (Caretta caretta) Admitted to a Wildlife Rehabilitation Center in Gran Canaria Island, Spain (1998-2014): A Long-Term Retrospective Study. *PLOS ONE, 11*(2), e0149398. doi:10.1371/journal.pone.0149398

Peltier, H., Dabin, W., Daniel, P., Van Canneyt, O., Dorémus, G., Huon, M., & Ridoux, V. (2012). The significance of stranding data as indicators of cetacean populations at sea: Modelling the drift of cetacean carcasses. *Ecological Indicators, 18*, 278-290. doi:https://doi.org/10.1016/j.ecolind.2011.11.014

Peltier, H., & Ridoux, V. (2015). Marine megavertebrates adrift: A framework for the interpretation of stranding data in perspective of the European Marine Strategy Framework Directive and other regional agreements. *Environmental Science & Policy, 54*, 240-247. doi:https://doi.org/10.1016/j.envsci.2015.07.013

Pettis, H. M., Pace, R. M., Schick, R. S., & Hamilton, P. K. (2018). North Atlantic Right Whale Consortium annual report card. Amended Report to the North Atlantic Right Whale Consortium, October 2017.

Posthuma, L., (Ed.), Suter II, G. W., (Ed.), & Traas, T. P., (Ed.). (2002). *Species Sensitivity Distributions in Ecotoxicology*. Boca Raton

: CRC press.

Quintela, M., Skaug, H. J., Øien, N., Haug, T., Seliussen, B. B., Solvang, H. K., Pampoulie, C., Kanda, N., Pastene, L. A., & Glover, K. A. (2014). Investigating Population Genetic Structure in a Highly Mobile Marine Organism: The Minke Whale Balaenoptera acutorostrata acutorostrata in the North East Atlantic. *PLOS ONE, 9*(9), e108640. doi:10.1371/journal.pone.0108640

Rasmussen, A. R., Murphy, J. C., Ompi, M., Gibbons, J. W., & Uetz, P. (2011). Marine Reptiles. *PLOS ONE, 6*(11), e27373. doi:10.1371/journal.pone.0027373

Raum-Suryan, K. L., Jemison, L. A., & Pitcher, K. W. (2009). Entanglement of Steller sea lions (Eumetopias jubatus) in marine debris: Identifying causes and finding solutions. *Marine Pollution Bulletin, 58*(10), 1487-1495. doi:https://doi.org/10.1016/j.marpolbul.2009.06.004

Reality Check team. (2019, 2 Jun). Why some countries are shipping back plastic waste. *BBC News*. Retrieved from https://www.bbc.com/news/world-48444874

Rochman, C. M., Browne, M. A., Underwood, A. J., Franeker, J. A., Thompson, Richard C., & Amaral-Zettler, L. A. (2016). The ecological impacts of marine debris: unraveling the demonstrated evidence from what is perceived. *Ecology, 97*(2), 302-312. doi:10.1890/14-2070.1

Rodríguez, B., Bécares, J., Rodríguez, A., & Arcos, J. M. (2013). Incidence of entanglements with marine debris by northern gannets (Morus bassanus) in the non-breeding grounds. *Marine Pollution Bulletin, 75*(1-2), 259-263. doi:10.1016/j.marpolbul.2013.07.003

Rosenbaum, R. K. (2015). Ecotoxicity. In Hauschild, M. Z., Rosenbaum, R. K., & Olsen, S. I. (Eds.), *Life*

Cycle Assessment: Theory and Practice (pp. 139-162). Cham: Springer International Publishing.

Rosenbaum, R. K., Hauschild, M. Z., Boulay, A. M., Fantke, P., Laurent, A., Núñez, M., & Vieira, M. (2017). Life cycle impact assessment. In *Life Cycle Assessment: Theory and Practice* (pp. 167-270).

Ryan, P. G. (2018). Entanglement of birds in plastics and other synthetic materials. *Marine Pollution Bulletin, 135*, 159-164. doi:https://doi.org/10.1016/j.marpolbul.2018.06.057

Santos, B. S., Kaplan, D. M., Friedrichs, M. A. M., Barco, S. G., Mansfield, K. L., & Manning, J. P. (2018). Consequences of drift and carcass decomposition for estimating sea turtle mortality hotspots. *Ecological Indicators, 84*, 319-336. doi:https://doi.org/10.1016/j.ecolind.2017.08.064

Schulz, M., Dürselen, C.-D., Fleet, D., Dau, K., Schulze-Dieckhoff, M., Schernewski, G., Klesse, K., Haseler, M., Weder, C., Ohnesorge, V., Weiel, S., Guse, N., Garthe, S., Siebert, U., Unger, B., Krone, R., & Dederer, G. (- in publication). Final report of r&d- project: „Kohärentes Monitoring der Belastungen deutscher Meeres- und Küstengewässer mit menschlichen Abfällen und der ökologischen Konsequenzen mit weiterem Fokus auf eingehende Identifizierung der Quellen.".

Schweitzer, J.-P., Petsinaris, F., & Gionfra, C. (2018). *Justifying plastic pollution: how Life Cycle Assessments are misused in food packaging policy*. Retrieved from: http://www.foeeurope.org/unwrapped-throwaway-plastic-food-waste

Secretariat of the Convention on Biological Diversity. (2016). Marine Debris: Understanding, Preventing and Mitigating the Significant Adverse Impacts on Marine and Coastal Biodiversity. (Vol. Technical Series No.83, pp. 78 pages). Montreal.

Spalding, M. D., Fox, H. E., Allen, G. R., Davidson, N., Ferdaña, Z. A., Finlayson, M., Halpern, B. S., Jorge, M. A., Lombana, A., Lourie, S. A., Martin, K. D., McManus, E., Molnar, J., Recchia, C. A., & Robertson, J. (2007). Marine Ecoregions of the World: A Bioregionalization of Coastal and Shelf Areas. *BioScience, 57*(7), 573-583. doi:10.1641/b570707

Suganuma, H., Tanaka, S., Inoguchi, E., & Narushima, K. (2010). What can be understood from sea turtle strandings *Aquabiology, 32*(5), 407-412.

Thorley, J. a. S. C. (2018). ssdtools: An R package to fit Species Sensitivity Distributions. *Journal of Open Source Software, 3*(1082). doi:10.21105/joss.01082

Traas, T. P., & van Leeuwen, C. J. (2007). Ecotoxicological Effects. In Leeuwen, C. J. v. & Vermeire, T. G. (Eds.), *Risk Assessment of Chemicals: An Introduction* (pp. 281-356). Dordrecht: Springer Netherlands.

UN Environment. (2018). Mapping of global plastics value chain and plastics losses to the environment (with a particular focus on marine environment). Ryberg, M., Laurent, A., & Hauschild, M. Z. Nairobi, Kenya: United Nations Environment Programme.

UNEP/SETAC Life Cycle Initiative. (2016). *Global guidance for environmental life cycle impact assessment indicators, Volume 1*. Retrieved from: https://www.lifecycleinitiative.org/life-cycle-impact-assessment-indicators-and-characterization-factors/

United Nations (Ed.). (2017). *The First Global Integrated Marine Assessment: World Ocean Assessment I*. Cambridge: Cambridge University Press.

van Leeuwen, C. J. (2007). General Introduction. In Leeuwen, C. J. v. & Vermeire, T. G. (Eds.), *Risk Assessment of Chemicals: An Introduction* (pp. 1-36). Dordrecht: Springer Netherlands.

van Sebille, E., England, M. H., & Froyland, G. (2012). Origin, dynamics and evolution of ocean garbage patches from observed surface drifters. *Environmental Research Letters, 7*(4), 044040. doi:10.1088/1748-9326/7/4/044040

Vélez-Rubio, G. M., Estrades, A., Fallabrino, A., & Tomás, J. J. M. B. (2013). Marine turtle threats in Uruguayan waters: insights from 12 years of stranding data. *160*(11), 2797-2811. doi:10.1007/s00227-013-2272-y

Wallace, B. P., DiMatteo, A. D., Hurley, B. J., Finkbeiner, E. M., Bolten, A. B., Chaloupka, M. Y., Hutchinson, B. J., Abreu-Grobois, F. A., Amorocho, D., Bjorndal, K. A., Bourjea, J., Bowen, B. W., Dueñas, R. B., Casale, P., Choudhury, B. C., Costa, A., Dutton, P. H., Fallabrino, A., Girard, A., Girondot, M., Godfrey, M. H., Hamann, M., López-Mendilaharsu, M., Marcovaldi, M. A., Mortimer, J. A., Musick, J. A., Nel, R., Pilcher, N. J., Seminoff, J. A., Troëng, S., Witherington, B., & Mast, R. B. (2010). Regional Management Units for Marine Turtles: A Novel Framework for Prioritizing Conservation and Research across Multiple Scales. *PLOS ONE, 5*(12), e15465. doi:10.1371/journal.pone.0015465

Waluda, C. M., & Staniland, I. J. (2013). Entanglement of Antarctic fur seals at Bird Island, South Georgia. *Marine Pollution Bulletin, 74*(1), 244-252. doi:https://doi.org/10.1016/j.marpolbul.2013.06.050

Waste Management Review. (2018). Malaysia, Thailand and Vietnam waste imports crackdown. http://wastemanagementreview.com.au/battling-sovereign-risk/

Wells, R. S., Natoli, A., & Braulik, G. (2019). Tursiops truncatus. The IUCN Red List of Threatened Species 2019: e.T22563A50377908. Retrieved from www.iucnredlist.org/species/22563/50377908

Wells, R. S., & Scott, M. D. (1999). Bottlenose dolphin tursiops truncatus (montagu, 1821).

Handbook of marine mammals: the second book of dolphins and porpoises, 6, 137-182.

Werner, S., Budziak, A., van Franeker, J., Galgani, F., Hanke, G., Maes, T., Matiddi, M., Nilsson, P., Oosterbaan, L., Priestland, E., Thompson, R., Veiga, J., & Vlachogianni, T. (2016). Harm caused by Marine Litter. MSFD GES TG Marine Litter - Thematic Report; JRC Technical report; EUR 28317 EN; doi:10.2788/690366.

Wilcox, C., Mallos, N. J., Leonard, G. H., Rodriguez, A., & Hardesty, B. D. (2016). Using expert elicitation to estimate the impacts of plastic pollution on marine wildlife. *Marine Policy, 65*, 107-114. doi:https://doi.org/10.1016/j.marpol.2015.10.014

Woods, J. S., Damiani, M., Fantke, P., Henderson, A. D., Johnston, J. M., Bare, J., Sala, S., de Souza, D. M., Pfister, S., Posthuma, L., Rosenbaum, R. K., & Verones, F. (2018). Ecosystem quality in LCIA: status quo, harmonization, and suggestions for the way forward. *The International Journal of Life Cycle Assessment, 23*(10), 1995-2006. doi:10.1007/s11367-017-1422-8

Woods, J. S., Rødder, G., & Verones, F. (2019). An effect factor approach for quantifying the entanglement impact on marine species of macroplastic debris within life cycle impact assessment. *Ecological Indicators, 99*, 61-66.

Woods, J. S., Veltman, K., Huijbregts, M. A. J., Verones, F., & Hertwich, E. G. (2016). Towards a meaningful assessment of marine ecological impacts in life cycle assessment (LCA). *Environment International, 89-90*, 48-61. doi:10.1016/j.envint.2015.12.033

Worm, B., Lotze, H. K., Jubinville, I., Wilcox, C., & Jambeck, J. (2017). Plastic as a Persistent Marine Pollutant. *Annual Review of Environment and Resources, 42*(1), 1-26. doi:10.1146/annurev-environ-102016-060700

Young, C., Eguchi, T., Ames, J. A., Staedler, M., Hatfield, B. B., Harris, M., & Golson-Fisch, E. A. (2019). Drift and beaching patterns of sea otter carcasses and car tire dummies. *Marine Mammal Science*. doi:10.1111/mms.12609

Zampori, L., Saouter E., Castellani V., Schau E., Cristobal J., & Sala S. (2016). Guide for interpreting life cycle assessment result; EUR 28266 EN.

Appendices

Appendix 1: Sources of entanglement data and calculation of regional entanglement rates.

Appendix 2: Species' ranges and sub-ranges used to calculate average macroplastic density (g/km2) coinciding with regional population entanglement rates.

Appendix 3: Species-specific dose-response models

Appendix 1: Sources of entanglement data, calculation of regional entanglement rates

Bold: sums of sample size and nr. affected, overall percent affected and average plastic density in delineated (sub)range.

Common name	**Scientific name**	**Collection Year(s)** *(if reported)*	**Size of sample**	**total nr. affected**	**% affected**	**Avg. plastic conc. in range** (g/km^2)	**collection location:** *(grouped by region)*	**range delineation for plastic density statistics**	**Reference to primary data**	**Report source**
Northern gannet	*Morus bassanus*	2014 (breeding)	656	17	2.60%	915.84	North Sea, Helgoland, Germany (entangled in nest)	Helgoland Isl. breeding range: 450km radius	(Schulz et al. - in publication)	(Werner et al. 2016)
		2015 (breeding)	684	24	3.50%				(Schulz et al. - in publication)	
			1340	**41**	**3.06%**	**915.84**		**Helgoland Isl. breeding range: 450km radius**		
Northern gannet	*Morus bassanus*	2010 (winter)	2245	8	0.36%	580.39	Atlantic, North Spanish coast (Cantabrian Sea)	NE Atlantic/Medit. wintering areas (non-breeding grounds)	(Rodríguez et al. 2013)	(Li et al. 2016)
		2007 (winter)	266	0	0.00%		Mediterranean, Spain			
		2007 (summer, non-breeding)	97	0	0.00%		Mediterranean, Spain			
		2010 (winter)	926	1	0.11%		Atlantic, South Spanish coast (Gulf of Cadiz)			
		2010 (spring)	14	0	0.00%		Atlantic, Canary Islands, Spain			
		2008 (summer, non-breeding)	124	25	20.16%		Atlantic, N Africa, Mauritania			
			3672	**34**	**0.93%**	**580.39**		**E Atlantic/Medit. wintering areas (non-breeding grounds)**		
Common Guillemot/ Common Murre	*Uria aalge*	2014	2880	32	1.10%	343.61	North Sea, Helgoland, Germany	IUCN sub-range Atlantic split with IHO quadrant E. Atlantic	(Schulz et al. - in publication)	(Werner et al. 2016)
		2015	3381	34	1.00%				(Schulz et al. - in publication)	
			6261	**65.49**	**1.05%**	**343.61**		**IUCN sub-range Atlantic split with IHO quadrant E. Atlantic**		

Common name	Scientific name	Collection Year(s) *(if reported)*	Size of sample	total nr. affected	% affected	Avg. plastic conc. in range (g/km^2)	collection location: *(grouped by region)*	range delineation for plastic density statistics	Reference to primary data	Report source
Northern Fulmar	*Fulmarus glacialis*	-	**67**	**1**	**1.80%**	**186.71**	North Sea, Helgoland, Germany	**IUCN sub-range Atlantic**	(Schulz et al. - in publication)	(Werner et al. 2016)
Brown Pelican	*Pelecanus occidentalis*	-	**557**	**351**	**63.00%**	**390.93**	California, USA	**IUCN sub-range N. Pacific**	(Dau et al. 2009)	(Werner et al. 2016)
Antarctic fur seal	*Arctocephalus gazella*	1995–2013	No data	No data	0.0002	0.32	Bird Island, South Georgia & the South Sandwich Islands	IUCN range subsection: intersection with IHO Atlantic + Southern Ocean (Atlantic quadrant) sea regions	(Waluda & Staniland 2013)	(Li et al. 2016)
		1995–2013			0.0002		Signy Island, S. Orkney Isl			
		1995–2013			0.0009		Maiviken, Cumberland Bay, South Georgia & the South Sandwich Islands			
					0.04%	**0.32**		**IUCN range subsection: intersection with IHO Atlantic + Southern Ocean (Atlantic quadrant) sea regions**		
Afro-Australian Fur Seal	*Arctocephalus pusillus*	1997–2012	**60000**	**79**	**0.13%**	**2859.99**	Southern coast: Seal Rocks & Lady Julia Percy Islands, Australia	**Sub-range Australia**	(Lawson et al. 2015)	(Li et al. 2016)
Common bottlenose dolphin	*Tursiops truncatus*	1997-2009	**2413**	**132**	**5.50%**	**1264.42**	Florida, USA	**Intersection: IHO North Atlantic & IUCN range**	(Adimey et al. 2014)	
Common minke whale	*Balaenoptera acutorostrata*	-	**11**	**1**	**9.10%**	**1048.78**	UK	**IUCN range**	Deaville et al., 2010	(Werner et al. 2016)

Common name	Scientific name	Collection Year(s) *(if reported)*	Size of sample	total nr. affected	% affected	Avg. plastic conc. in range (g/km^2)	collection location: *(grouped by region)*	range delineation for plastic density statistics	Reference to primary data	Report source
Florida manatee	*Trichechus manatus*	1997-2009	**4962**	**380**	**7.70%**	**3931.27**	Florida, USA	**IUCN range in Florida**	(Adimey et al. 2014)	
Grey seal	*Halichoerus grypus*	-	**58**	**3**	**4.30%**	**1398.01**	Cornwall, UK	**IUCN range intersection with IHO subregions around Cornwall: Celtic Sea & English Channel**	Allen et al., 2012	(Werner et al. 2016)
North Atlantic right whale	*Eubalaena glacialis*	2004-2017	**61**	**51**	**83.60%**	**668.20**	Atlantic northwest, USA & Canada	**IUCN range**	(Pettis et al. 2018)	
Steller sea lion	*Eumetopias jubatus*	2000–2007	**73077**	**190**	**0.26%**	**98.30**	Southeast Alaska and northern British Columbia (USA & Canada)	**IUCN sub-range: E Pacific subspecies**	(Raum-Suryan et al. 2009)	(Li et al. 2016)
Green Sea Turtle	*Chelonia mydas*	Jul 2014-Dec 2015	**28**	**13**	**46.43%**	**312.28**	Timor and Arafura Seas, Northern Territory Australia	**Average of rmu39 & 40 (undefined populations)**	(Mackarous & Griffiths 2016)	
		2012-2017	**14**	**3**	**21.43%**	**6385.61**	Mediterranean Sea, Greece	**rmu48**	Corsini-Foka pers. comm 2017	(Claro et al. 2018)
		2014	**2328**	**113**	**4.85%**	**2584.55**	USA coast	**rmu50**	(NOAA STSSN 2014)	
Hawksbill Sea Turtle	*Eretmochelys imbricata*	Jul 2014-Dec 2015	**23**	**15**	**65.22%**	**811.62**	Timor and Arafura Seas, Northern Territory Australia	**rmu14+12 (non-overlapping)**	(Mackarous & Griffiths 2016)	
Hawksbill Sea Turtle	*Eretmochelys imbricata*	1997-2009	362	30	8.30%	2372.16	Florida, USA	rmu10	(Adimey et al. 2014)	(Werner et al. 2016)
		2014	23	3	13.04%		USA coast		(NOAA STSSN 2014)	
			385	**33**	**8.58%**	**2372.16**		**rmu10**		

Common name	Scientific name	Collection Year(s) *(if reported)*	Size of sample	total nr. affected	% affected	Avg. plastic conc. in range (g/km^2)	collection location: *(grouped by region)*	range delineation for plastic density statistics	Reference to primary data	Report source
Leatherback Sea Turtle	*Dermochelys coriacea*	1994-2017	10	1	10.00%	1426.54	Mediterranean Sea, Spain	rmu51	UVEG	(Claro et al. 2018)
		1988-2016	13	2	15.38%		Atlantic, Canary Islands, Spain		Liria-Loza A. pers. Comm	
		1978-2013	275	49	17.82%		Atlantic, Portugal		Nicolau et al 2016	
		2014	9	2	22.22%		Atlantic, UK		Deaville et al., 2014	
		1988-2016	405	27	6.67%		Atlantic, France		RTMAE CESTM, pers. Comm 2017	
		1988-2016	1265	33	2.61%		Atlantic, France		RTMAE CESTM, pers. Comm 2017	
		1997-2009	304	43	14.14%		Florida, USA		(Adimey et al. 2014)	(Werner et al. 2016)
		2014	75	5	6.67%		USA coast		(NOAA STSSN 2014)	
			2281	**162**	**7.10%**	**1426.54**		**rmu51**		
Olive Ridley Sea Turtle	*Lepidochelys olivacea*	Jul 2014-Dec 2015	**31**	**26**	**83.87%**	**712.66**	Timor and Arafura Seas, Northern Territory Australia	**rmu03**	(Mackarous & Griffiths 2016)	
Flatback Sea Turtle	*Natator depressus*	Jul 2014-Dec 2015	**10**	**4**	**40.00%**	**165.70**	Timor and Arafura Seas, Northern Territory Australia	**rmu59 & 60 (pop. weighted)**	(Mackarous & Griffiths 2016)	
Kemp's Ridley Sea Turtle	*Lepidochelys kempii*	1997-2009	1346	69	5.10%	2289.24	Florida, USA	rmu58	(Adimey et al. 2014)	(Werner et al. 2016)
		2014	1151	27	2.35%		USA coast		(NOAA STSSN 2014)	
			2497	**96**	**3.83%**	**2289.24**		**rmu58**		

Common name	Scientific name	Collection Year(s) *(if reported)*	Size of sample	total nr. affected	% affected	Avg. plastic conc. in range (g/km^2)	collection location: *(grouped by region)*	range delineation for plastic density statistics	Reference to primary data	Report source
Loggerhead Sea Turtle	*Caretta caretta*	2014	**1411**	**43**	**3.05%**	**1902.88**	USA Coast	**rmu25**	(NOAA STSSN 2014)	
			47	**18**	**38.30%**	**1781.85**	Atlantic, Gran Canaria, Canary Islands, Spain	**rmu25 & rmu23**	(Orós et al. 2016)	(Claro et al. 2018)
Loggerhead Sea Turtle	*Caretta caretta*	1978-2013	386	96	27.87%	2052.11	Atlantic, Portugal	rmu25 & rmu26	Nicolau et al 2016	(Claro et al. 2018)
		2010-2016	103	9	8.74%		Mediterranean Sea, France		RTMMF 2017	
		1994-2017	1415	38	2.69%		Mediterranean Sea, Spain		UVEG	
		2008-2017	176	27	15.34%		Mediterranean Sea, Sardinia, Italy		Camedda 2018	
			2080	**170**	**8.17%**	**2052.11**		**rmu25 & rmu26**		
Loggerhead Sea Turtle	*Caretta caretta*	-	38	12	31.58%	4248.78	Mediterranean Sea, Turkey	rmu26	Kaska et al. 2017	(Claro et al. 2018)
		2014	10	7	70.00%		Mediterranean Sea, Turkey, Fethiye-Gocek SPA		E. Başkale pers. comm. 2019	
		2012-2017	86	8	9.30%		Mediterranean Sea, Greece		Corsini-Foka pers. comm 2017	(Claro et al. 2018)
			134	**27**	**20.15%**	**4248.78**		**rmu26**		
Loggerhead Sea Turtle	*Caretta caretta*	Jul 2014-Dec 2015	**3**	**1**	**33.33%**	**755.32**	Timor and Arafura Seas, Northern Territory Australia	**rmu29**	(Mackarous & Griffiths 2016)	
		1995-2012	**535**	**1**	**0.19%**	**1689.67**	Iriomote Island – Okinawa and Kantō region - Honshu, Japan	**rmu31**	(Kameda et al. 2013; Suganuma et al. 2010) K. Kameda pers. comm. 2019	

Appendix 2: Species' sub-ranges used to calculate average macroplastic density (g/km^2), coinciding with regional population entanglement rates.

A 2.1: Summary of sub-ranges used in species sensitivity distribution calculations pink: marine mammals; blue: sea birds; green: marine turtles. IUCN Red List status: DD: data deficient; LC: least concern; NT: near threatened; VU: vulnerable; EN: endangered; CR: critically endangered (IUCN 2019).

Common name	Scientific name	Red List status	Entanglement data locations	Sub-range	Rationale for sub-range *(ssp. Red List status)*	Citations
Antarctic fur seal	*Arctocephalus gazella*	LC	South Atlantic: Bird Isl. & Cumberland Bay (South Georgia & the South Sandwich Isl.); Signy Isl. (S. Orkney Isl.)	Intersection: IHO South Atlantic/ Southern Ocean & IUCN sub-range South Atlantic	Limited range, subgroup stays in Atlantic around Scotia Arc	(Bonin 2012; Hofmeyr 2016)
Afro-Australian Fur Seal	*Arctocephalus pusillus*	LC	Great Australian Bight: Seal Rocks & Lady Julia Percy Isl. (Australia)	IUCN sub-range: Australia	Australian subspecies: *A. p. doriferus (LC)*	(Hofmeyr 2015; Kirkwood et al. 2010)
Common bottlenose dolphin	*Tursiops truncatus*	LC	Northwest Atlantic: Florida (USA)	Intersection: IHO North Atlantic & IUCN range	non-migratory	(Wells et al. 2019; Wells & Scott 1999)
Common minke whale	*Balaenoptera acutorostrata*	LC	Northeast Atlantic: (UK)	IUCN range cut by bottom margin of IHO N Atlantic region	North Atlantic subspecies: *B. a. acutorostrata (LC)*	(Cooke 2018a; Quintela et al. 2014)
American manatee	*Trichechus manatus*	VU	Northwest Atlantic: Florida (USA)	IUCN sub-range: Florida coast	Florida subspecies: *T. m. latirostris (EN)*	(Deutsch et al. 2003; Deutsch et al. 2008)
Grey seal	*Halichoerus grypus*	LC	Northeast Atlantic: Cornwall (UK)	Intersection: IHO Celtic Sea, English Channel & IUCN range	non-migratory	(Bowen 2016; Mcconnell et al. 1999)
North Atlantic right whale	*Eubalaena glacialis*	EN	Northwest Atlantic: (USA & Canada)	full IUCN range	full migratory species ranging throughout North Atlantic	(Cooke 2018b)
Steller sea lion	*Eumetopias jubatus*	NT	Northwest Pacific: (USA & Canada)	IUCN sub-range: E Pacific, east of 144°W, north of central California.	E Pacific subspecies: *E j. monteriensis (LC)*	(Gelatt & Sweeney 2016a, 2016b)
Brown Pelican	*Pelecanus occidentalis*	LC	Northeast Pacific: California (USA)	IUCN sub-range N Pacific British Columbia to El Salvador	Limited home range, subspecies: *P.o. californicus*	(BirdLife International 2018d; Elliott 2018)
Common Guillemot/ Common Murre	*Uria aalge*	LC	North Sea: Helgoland Isl. (Germany)	East Atlantic IUCN range split by IHO quadrant Northeast Atlantic	subgroup stays in Northeast Atlantic *(NT)*	(BirdLife International 2018e; Dierschke et al. 2011)
Northern Fulmar	*Fulmarus glacialis*	LC	North Sea: Helgoland Isl. (Germany)	Arctic Atlantic IUCN sub-range	subgroup stays in North Atlantic *(EN)*	(BirdLife International 2018b; Edwards et al. 2013)
Northern gannet	*Morus bassanus*	LC	Nonbreeding individuals: Atlantic (Spain, Canary Isl. & Mauritania); Mediterranean (Spain)	East Atlantic IUCN range split by IHO quadrant Northeast Atlantic	limited home range up to 7000km from breeding location; subgroup stays in Northeast Atlantic and Mediterranean	(BirdLife International 2018c; Fort et al. 2012)
			breeding individuals (entanglement in nest): North Sea - Helgoland Isl. (Germany)	NESTING: 540km buffer around Helgoland in IUCN range	Limited breeding range, subgroup stays within 540km of Helgoland, Germany	(BirdLife International 2018c);(Mowbray 2002) cited in (Dewey 2009)

Common name	Scientific name	Red List status	Entanglement data locations	Sub-range	Rationale for sub-range *(ssp. Red List status)*	Citations
Flatback Sea Turtle	*Natator depressus*	DD	Timor and Arafura Seas: Northern Territory (Australia)	RMU 59 & RMU 60 (population weighted average)	Flatback population in Northern, Western and Eastern Australia	(Kot et al. 2015; Wallace et al. 2010)
Green Sea Turtle	*Chelonia mydas*	EN	Timor and Arafura Seas: Northern Territory (Australia)	RMU 39-RMU 40: avg, for undefined populations	Average of Green Sea Turtle Regional Management Units 39 and 40: Southwest Pacific and Southeast Indian Oceans	(Kot et al. 2015; Wallace et al. 2010)
			Mediterranean Sea: (Greece)	RMU 48	Green Sea Turtle in Mediterranean Sea	
			Northwest Atlantic: (USA); Gulf of Mexico: (USA)	RMU 50	Green Sea Turtle in Central America, Gulf of Mexico, Caribbean (excluding Antilles), to Bermuda and Midwest Atlantic.	
Hawksbill Sea Turtle	*Eretmochelys imbricata*	CR	Timor and Arafura Seas: Northern Territory (Australia)	RMU 14 + RMU 12 (non-overlapping)	Hawksbill in Southwest Pacific and Southeast Indian Ocean	(Kot et al. 2015; Wallace et al. 2010)
			Northwest Atlantic: (USA); Gulf of Mexico: (USA)	RMU 10	Hawksbill in Caribbean, Midwest Atlantic to 35W to mid-Guyana	
Leatherback Sea Turtle	*Dermochelys coriacea*	VU	Northeast Atlantic: (Canary Isls. Spain, Portugal, UK, France, USA)	RMU 51	Leatherback in Northwest Atlantic	(Kot et al. 2015; Wallace et al. 2010)
Loggerhead Sea Turtle	*Caretta caretta*	VU	Northeast Atlantic: Gran Canaria, Canary Isls. (Spain)	RMU 23 & RMU 25 (population weighted average)	Loggerhead population in Northeast and Northwest Atlantic	(Kot et al. 2015; Wallace et al. 2010)
			Northwest Atlantic: (USA); Gulf of Mexico: (USA)	RMU 25	Loggerhead population in Northwest Atlantic	
			Northeast Atlantic: (Portugal); Mediterranean: (France, Spain), Sardinia (Italy)	RMU 25 & RMU 26 (population weighted average)	Loggerhead population in Northwest Atlantic and Mediterranean	
			Mediterranean: (Greece, Turkey), Fethiye-Gocek SPA (Turkey)	RMU 26	Loggerhead population in Mediterranean *(LC)*	
			Timor and Arafura Seas: Northern Territory (Australia)	RMU 29	Loggerhead population in Southeast Indian Ocean	
			Northwest Pacific: Iriomote Isl., Okinawa (Japan)	RMU 31	Loggerhead population in North Pacific	
Kemp's Ridley Sea Turtle	*Lepidochelys kempii*	CR	Northwest Atlantic: (USA); Gulf of Mexico: (USA)	RMU 58	Kemp's Ridley population in North Atlantic	(Kot et al. 2015; Wallace et al. 2010)
Olive Ridley Sea Turtle	*Lepidochelys olivacea*	VU	Timor and Arafura Seas: Northern Territory (Australia)	RMU 03	Olive Ridley population in West Pacific	(Kot et al. 2015; Wallace et al. 2010)

x

Marine Mammal Geographic Ranges: Full IUCN ranges (outlined) were subdivided into subranges (hatched) representing studied population segments (IUCN 2019). Global average SSD model PAFs shown in color scale.

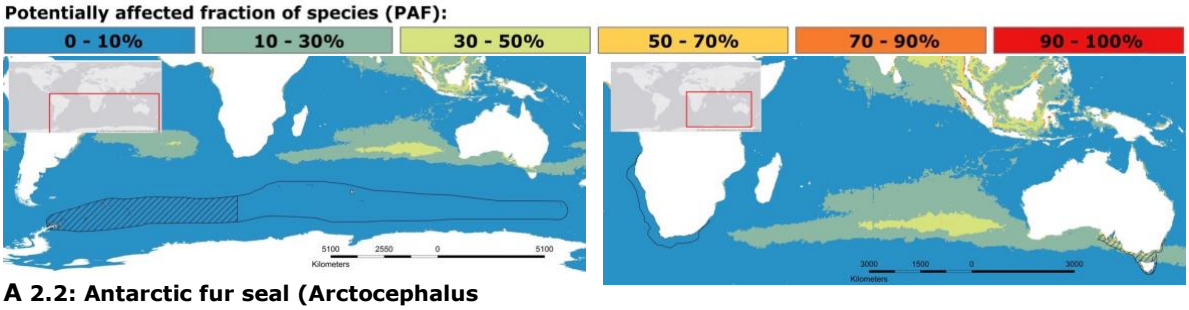

A 2.2: Antarctic fur seal (Arctocephalus gazella)– Outlined: IUCN range (Hofmeyr 2016). Sub-range used (hatched): Maximum range of South Atlantic Scotia Arc population (Bonin 2012), split by IHO South Atlantic and Southern Ocean quadrants (Flanders Marine Institute 2018).

A 2.3: Afro-Australian Fur Seal *(Arctocephalus pusillus)* – Outlined: IUCN range (Hofmeyr 2015). Sub-range used (hatched): Australian subspecies *'A. p. doriferus'* (Kirkwood et al. 2010).

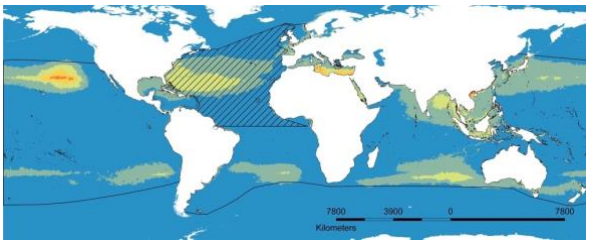

A 2.4: Common bottlenose dolphin (Tursiops truncatus) – Outlined: IUCN range (Wells et al. 2019). Sub-range used (hatched): Northwest Atlantic population (Wells & Scott 1999), split by intersection of IHO North Atlantic quadrant (Flanders Marine Institute 2018).

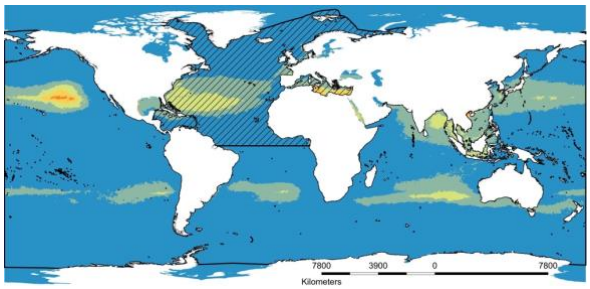

A 2.5: Common minke whale (Balaenoptera acutorostrata) – Outlined: IUCN range (Cooke 2018a). Sub-range used (hatched): North Atlantic subspecies 'B. a. acutorostrata' (Quintela et al. 2014), split by bottom margin of IHO North Atlantic quadrant (Flanders Marine Institute 2018).

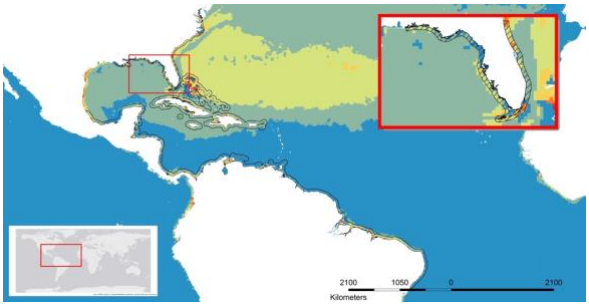

A 2.6: American manatee *(Trichechus manatus)* – Outlined: IUCN range (Deutsch et al. 2008). Sub-range used (hatched): Non-migratory. Florida coastal subpopulation of subspecies '*T.m. latirostris'* (Deutsch et al. 2003).

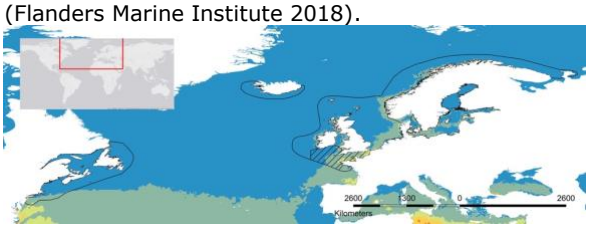

A 2.7: Grey seal *(Halichoerus grypus)* – Outline: IUCN range (Bowen 2016). Sub-range used (hatched): Cornwall, UK population of this non-migratory species (Mcconnell et al. 1999), split by IHO Celtic Sea and English Channel quadrants (Flanders Marine Institute 2018).

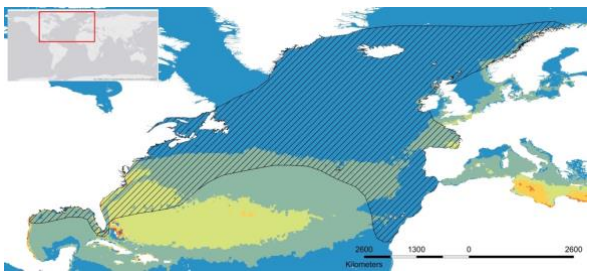

A 2.8: North Atlantic right whale *(Eubalaena glacialis)* – Range used (hatched): Full IUCN range of this migratory species (Cooke 2018b).

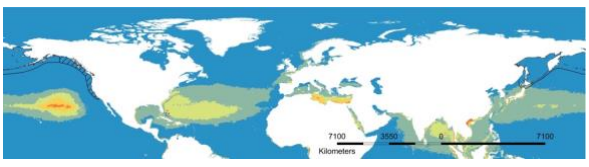

A 2.9: Steller Sea Lion *(Eumetopias jubatus)* – Outlined: IUCN range (Gelatt & Sweeney 2016b). Sub-range used (hatched): Eastern subspecies *'E. j. monteriensis'* (Gelatt & Sweeney 2016a).

Marine Bird Geographic Ranges: Full IUCN ranges (outlined) were subdivided into subranges (hatched) representative of studied population segments (IUCN 2019). Global average SSD model PAFs shown in color scale.

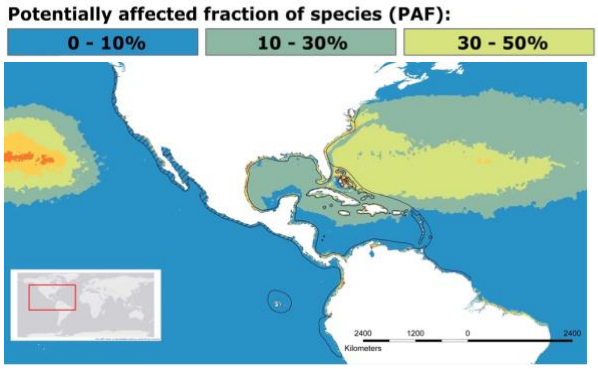

A 2.10: Brown Pelican (*Pelecanus occidentalis*) – Outlined: IUCN range P. occidentalis (BirdLife International 2018d). Sub-range used (hatched): Pacific subspecies '*P. o. californicus*' population - North Pacific, British Columbia to El Salvador (Elliott 2018).

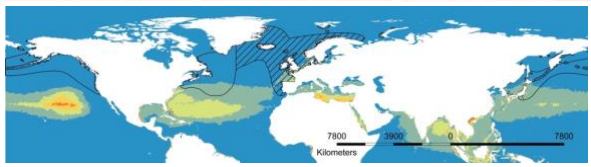

A 2.11: Common Guillemot/ Common Murre *(Uria aalge)* – Outlined: IUCN range (BirdLife International 2018e). Sub-range used (hatched): East Atlantic population (Dierschke et al. 2011)- IUCN range split by IHO Northeast Atlantic quadrant (Flanders Marine Institute 2018).

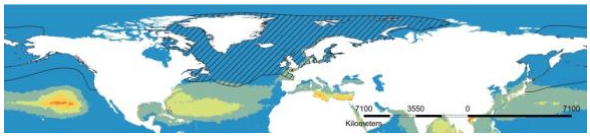

A 2.12: Northern fulmar *(Fulmarus glacialis)* – Outlined: IUCN range (BirdLife International 2018b). Sub-range used (hatched): Arctic Atlantic population (Edwards et al. 2013).

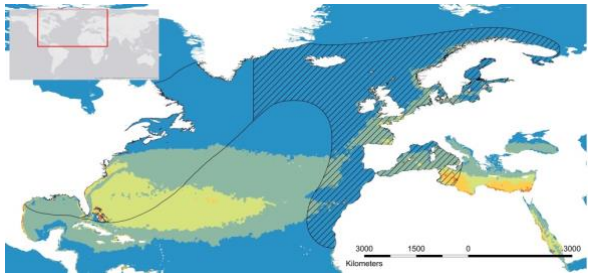

A 2.13: Northern gannet *(Morus bassanus)* – Outlined: IUCN range (BirdLife International 2018c). Sub-range used (hatched): East Atlantic population (Fort et al. 2012), split by IHO Northeast Atlantic quadrant (Flanders Marine Institute 2018).

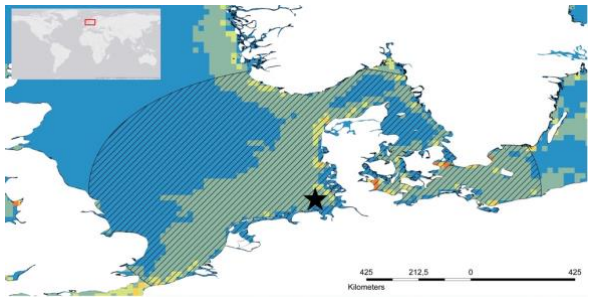

A 2.14: Northern gannet *(Morus bassanus)* – Sub-range used (hatched): foraging range during breeding season - 540km range around Helgoland Island, Germany (star) (Mowbray 2002) cited in (Dewey 2009).

Marine Turtle Geographic Ranges: Regional Management Units (RMUs) for Sea turtles (Wallace et al. 2010). RMUs downloaded from: "The State of the World's Sea Turtles Online Database:" (Kot et al. 2015). Global average SSD model PAFs shown in color scale.

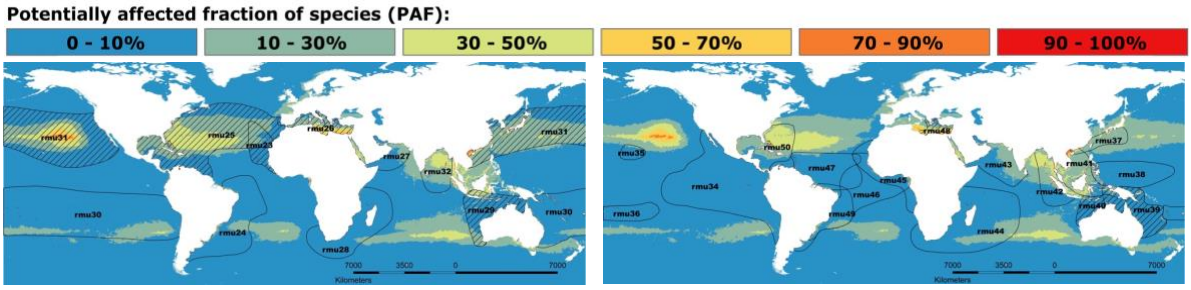

A 2.15: Loggerhead sea turtle *(Caretta caretta)* Outlined: Regional Management Units (RMUs); RMUs used (hatched): Population-weighted average of RMU 23 and RMU 25; RMU 25; Population-weighted average of RMU 25 and RMU 26; RMU 26; RMU 29; RMU 31.

A 2.16: Green sea turtle *(Chelonia mydas)* Outlined: Regional Management Units (RMUs); RMUs used (hatched): Average of RMU 39 and RMU 40; RMU 48.

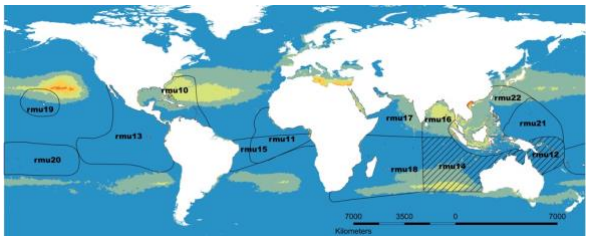

A 2.17: Hawksbill Sea Turtle *(Eretmochelys imbricata)* – Outlined: Regional Management Units (RMUs); RMUs used (hatched): RMU 14 and RMU 12 combined (non-overlapping).

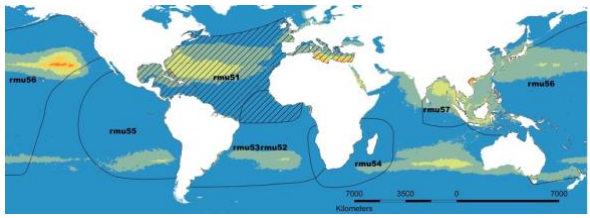

A 2.18: Leatherback Sea Turtle *(Dermochelys coriacea)* – Outlined: Regional Management Units (RMUs); RMU used (hatched): RMU 51.

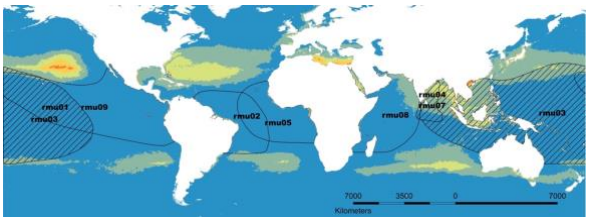

A 2.19: Olive Ridley Sea Turtle *(Lepidochelys olivacea)* – Outlined: Regional Management Units (RMUs); RMU used (hatched): RMU 03.

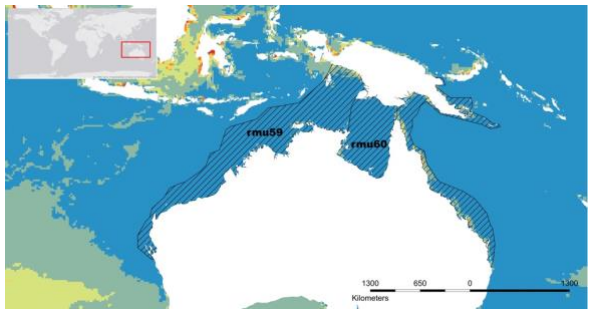

A 2.20: Flatback Sea Turtle *(Natator depressus)* Hatched: Regional Management Units (RMUs) used: population weighted average of RMU 59 and RMU 60.

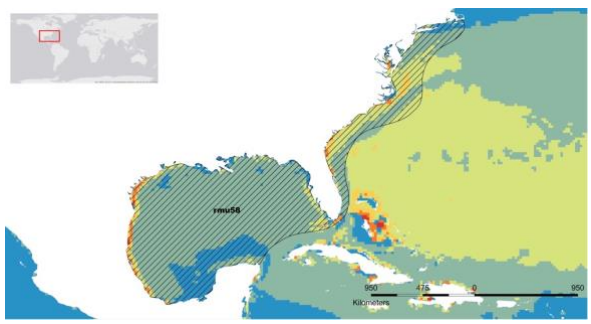

A 2.21: Kemp's Ridley Sea Turtle *(Lepidochelys kempii)* – Hatched: Regional Management Unit (RMU) used: RMU 58.

Appendix 3: Species-specific dose-response (DR) models: best-fitting linear regression models describing a causal relationship between marine plastic debris densities and known entanglement rates, projecting the debris densities at which a 50% entanglement rate (EC50) will be realized for each species-exposure group. Zero entanglement is expected at zero plastic density (models intersect the origin). Where multiple regional entanglement rates are known, models were weighted by total number of observations associated with each rate, and confidence intervals (grey bands) were calculated. All calculations were done in R Studio using linear regression-fitting analysis: `lm()`. For Caretta caretta, more available data points allowed for a more descriptive quasi-binomial logistic regression model: `glm(family = quasibinomial(link = 'logit'))`.

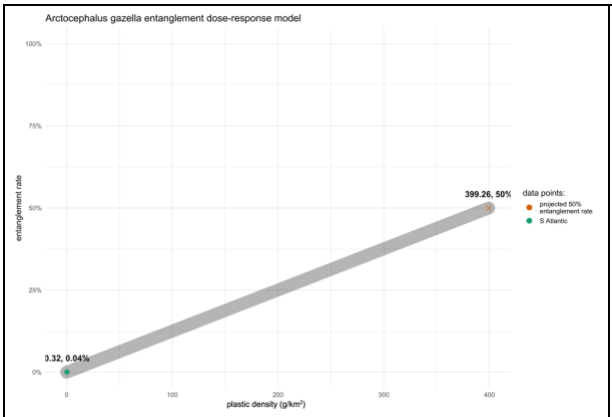

A 3.1: Arctocephalus gazella linear DR model

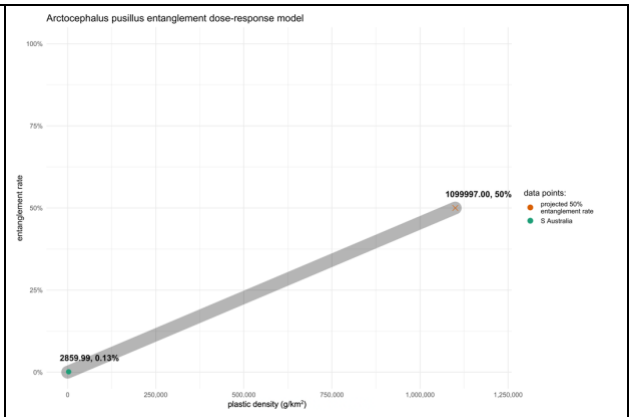

A 3.2: Arctocephalus pusillus linear DR model

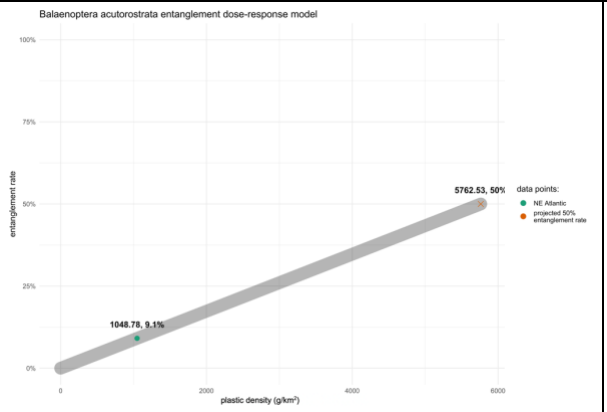

A 3.3: Balaenoptera acutorostrata linear DR model

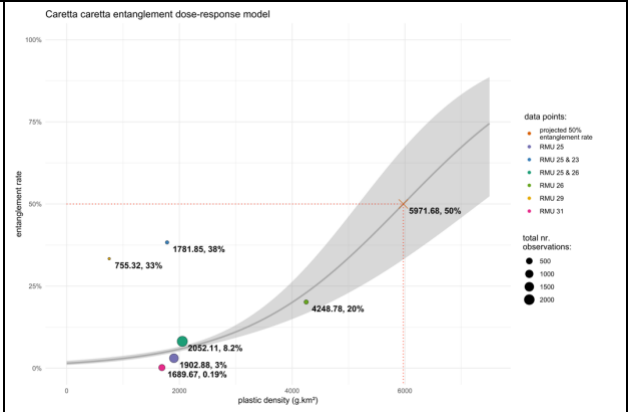

A 3.4: Caretta caretta weighted binomial generalized linear DR model with logistic link function (grey-shaded) confidence interval

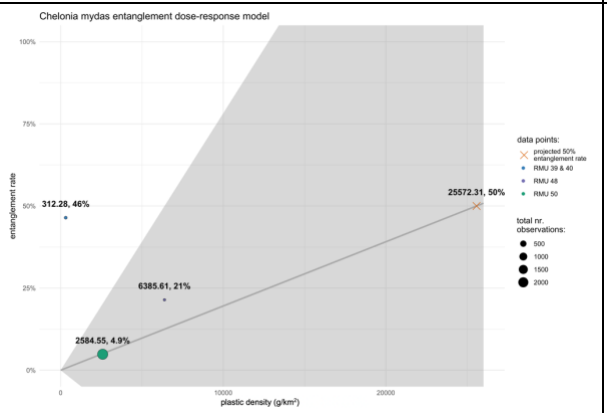

A 3.5: Chelonia mydas weighted linear DR model with (grey-shaded) confidence interval

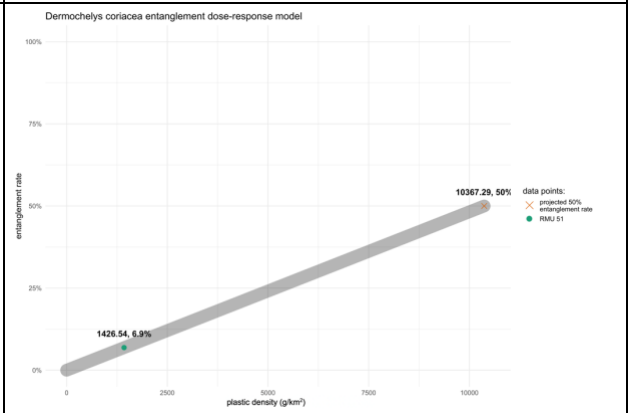

A 3.6: Dermochelys coriacea linear DR model

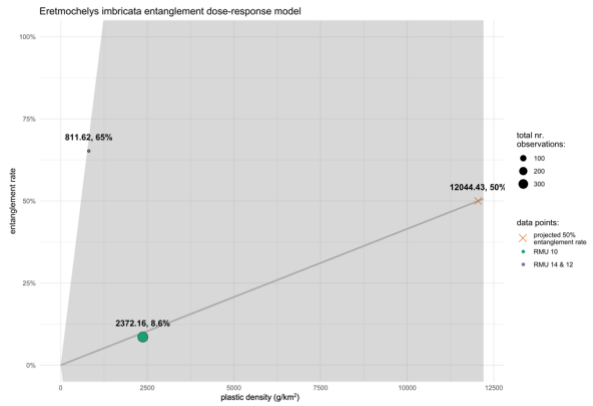

A 3.7: Eretmochelys imbricata weighted linear DR model with (grey-shaded) confidence interval

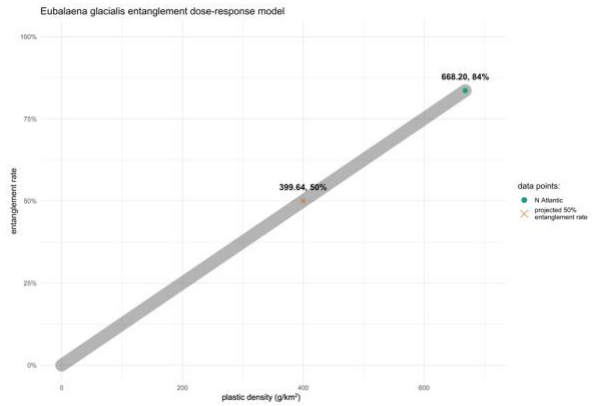

A 3.8: Eubalaena glacialis linear DR model

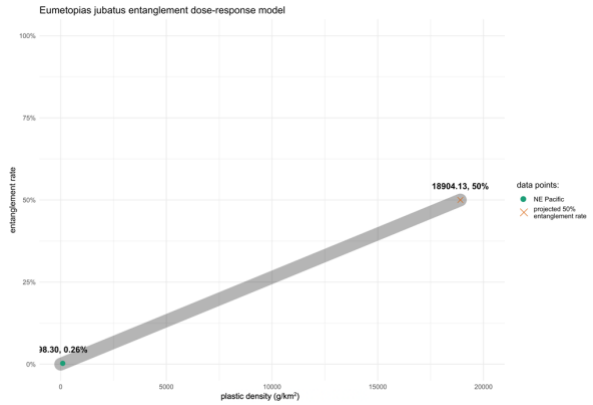

A 3.9: Eumetopias jubatus linear DR model

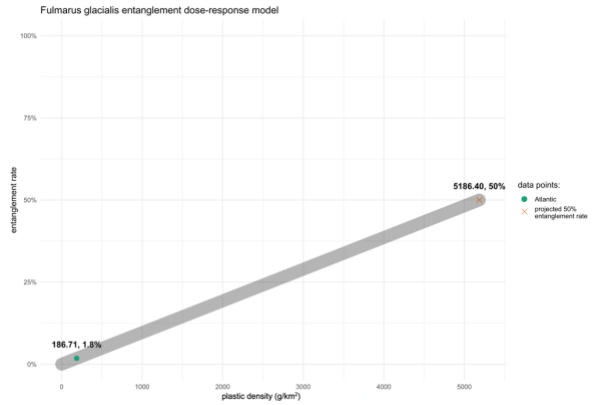

A 3.10: Fulmarus glacialis linear DR model

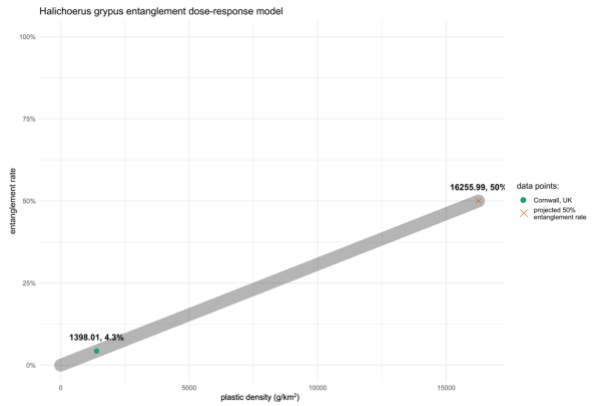

A 3.11: Halichoerus grypus linear DR model

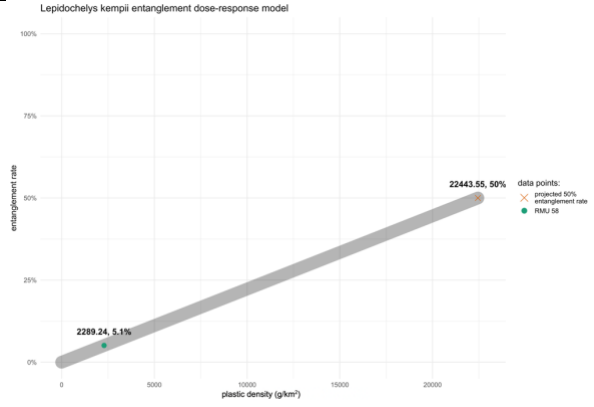

A 3.12: Lepidochelys kempii linear DR model

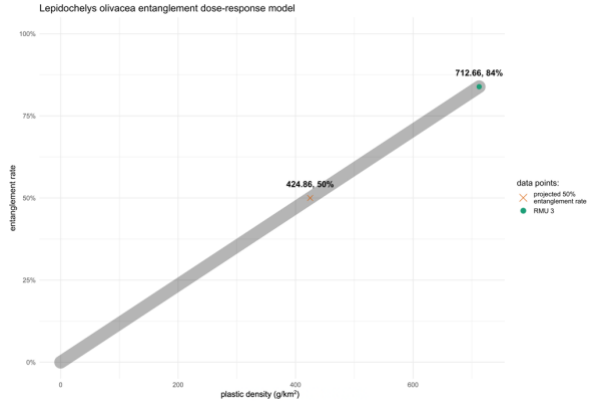

A 3.13: Lepidochelys olivacea linear DR model

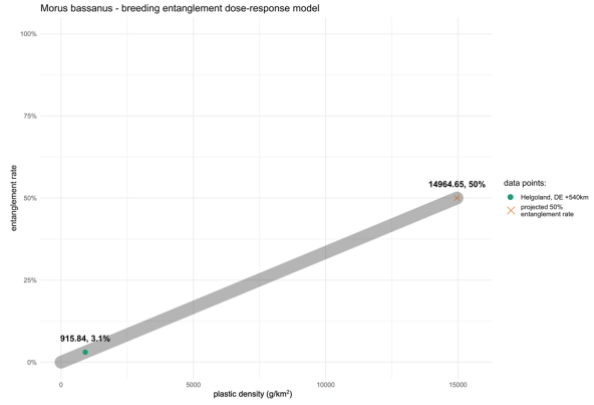

A 3.14: Morus bassanus, breeding linear DR model

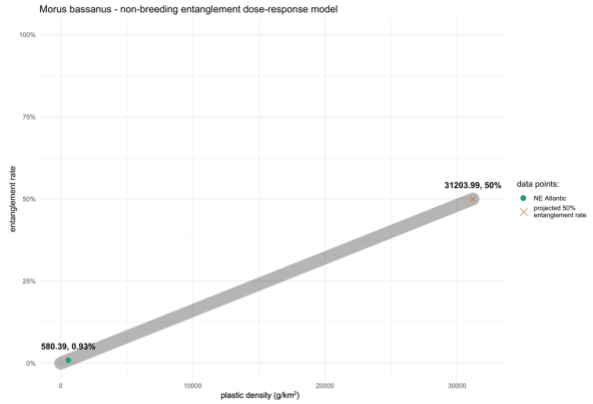

A 3.15: Morus bassanus, non-breeding linear DR model

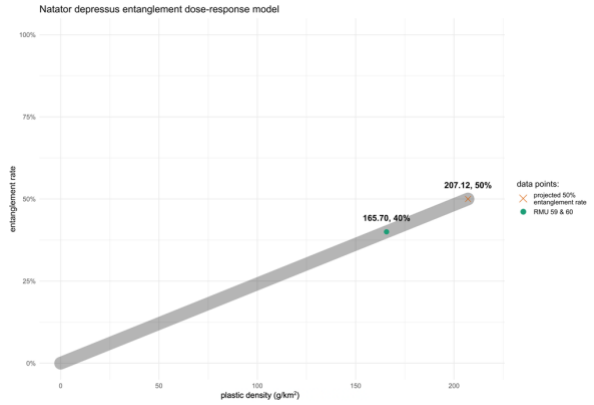

A 3.16: Natator depressus linear DR model

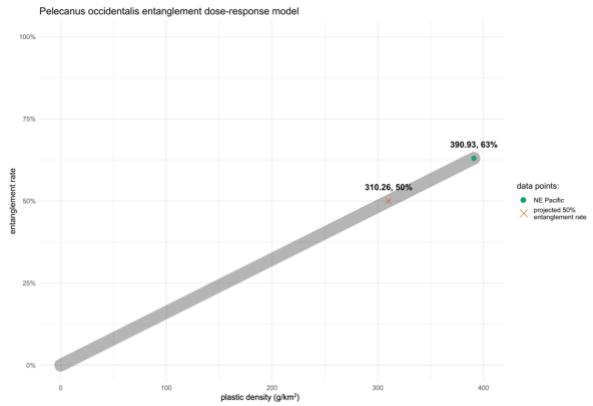

A 3.17: Pelecanus occidentalis linear DR model

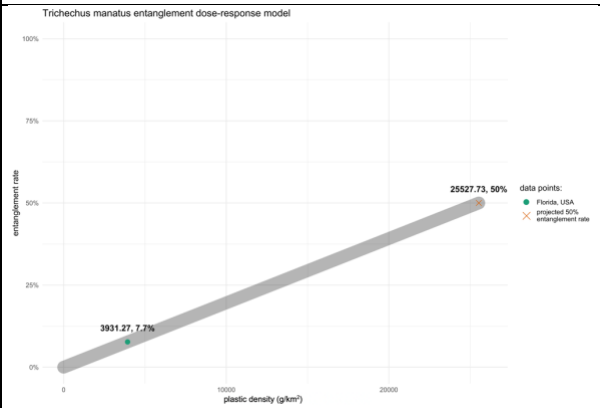

A 3.18: Trichechus manatus linear DR model

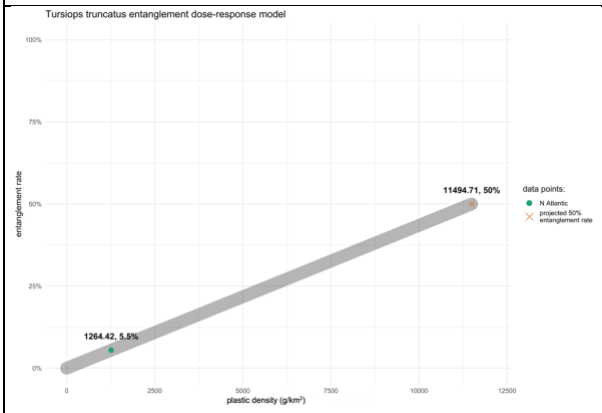

A 3.19: Tursiops truncatus linear DR model

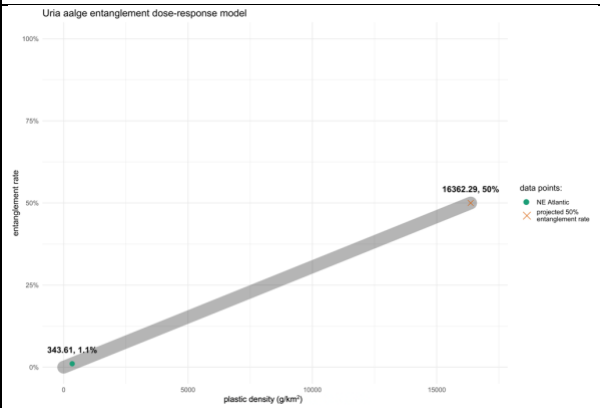

A 3.20: Uria aalge linear DR model

Appendix 4: Regional SSD and EF models: Cumulative species sensitivity distributions (SSD) used to calculate potentially affected fraction (PAF) of regional species; effect factor (EF) curves and associated maps. Each model (red line) is compared with average model (grey dashed line).

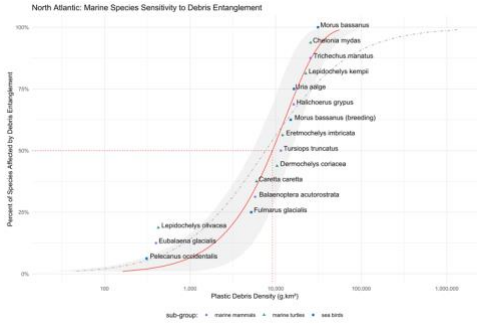

A 4.1: North Atlantic Ocean SSD model and PAF map

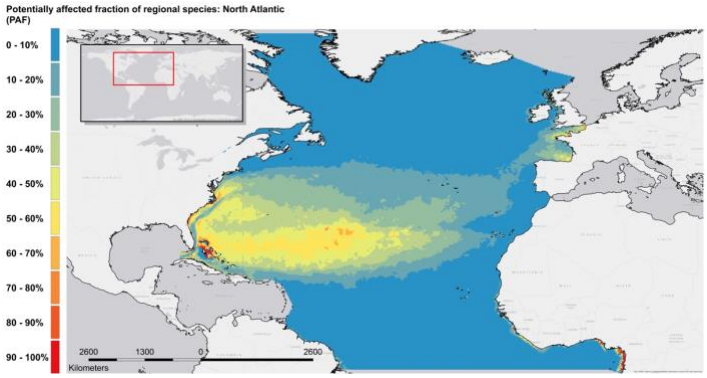

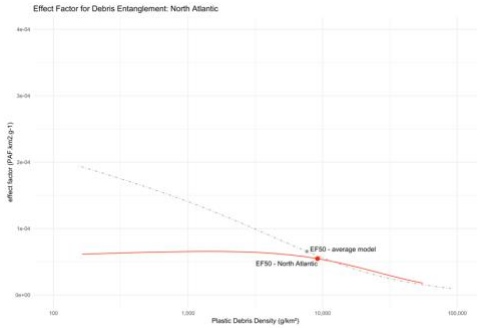

A 4.2: North Atlantic Ocean EF model and map

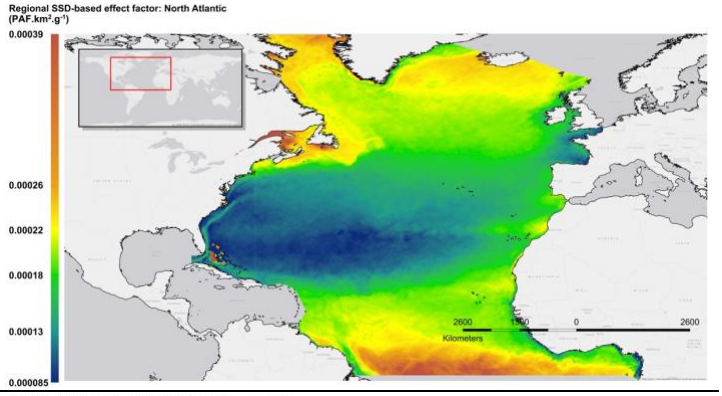

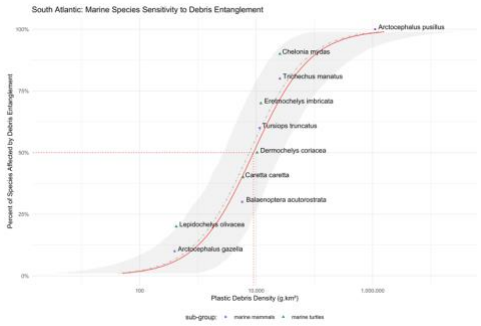

A 4.3: South Atlantic Ocean SSD model and PAF map

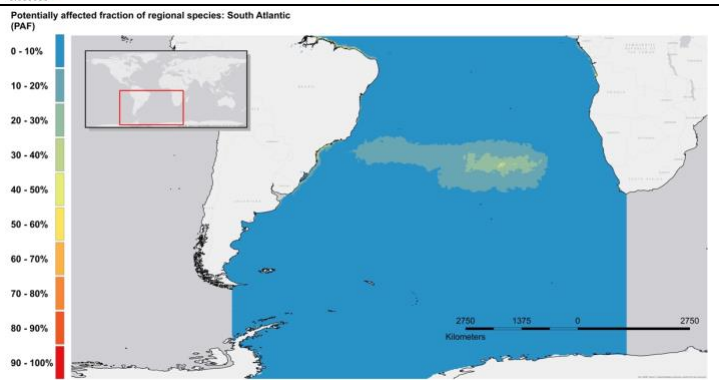

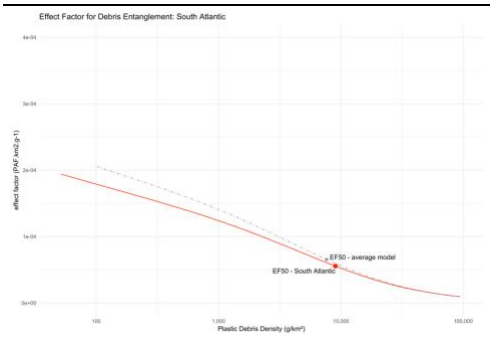

A 4.4: South Atlantic Ocean EF model and map

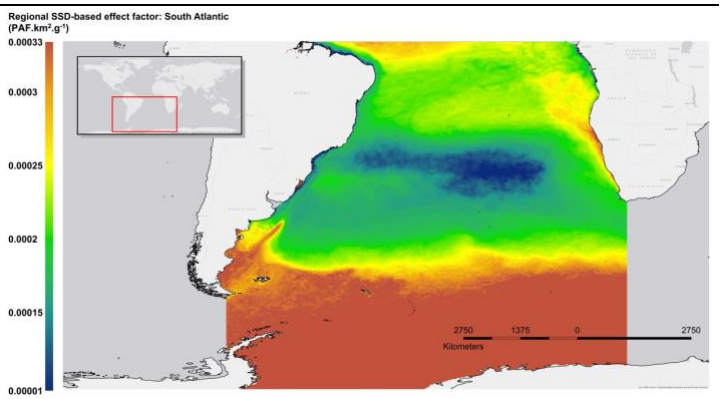

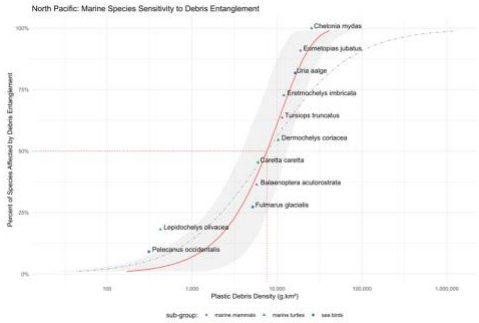

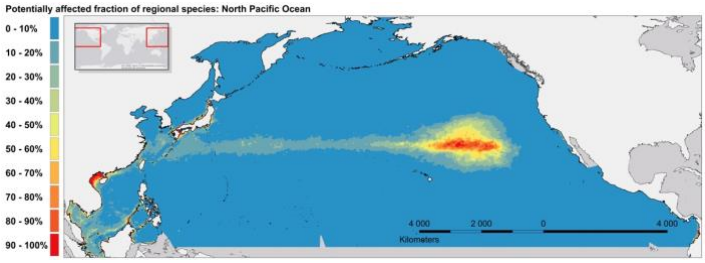

A 4.5: North Pacific Ocean SSD model and PAF map

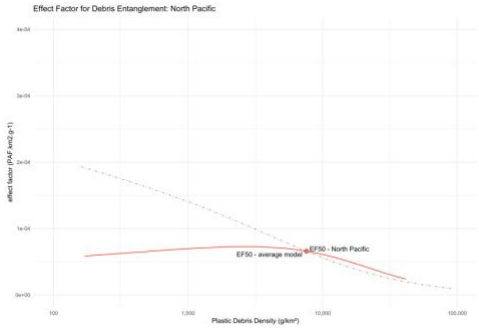

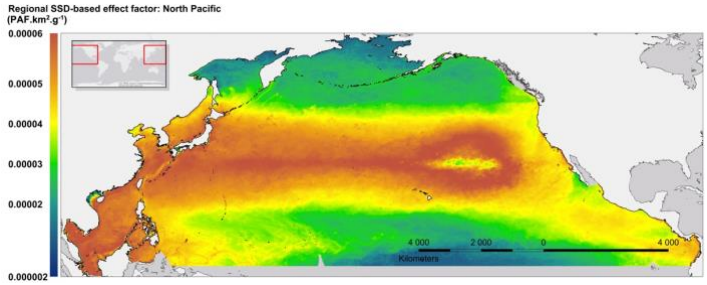

A 4.6: North Pacific Ocean EF model and map

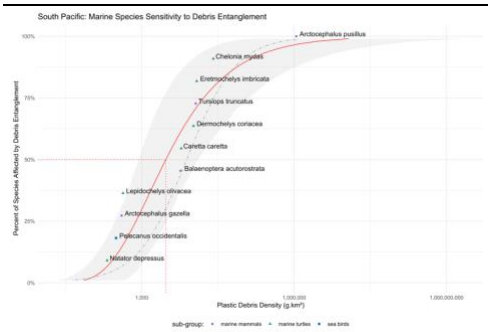

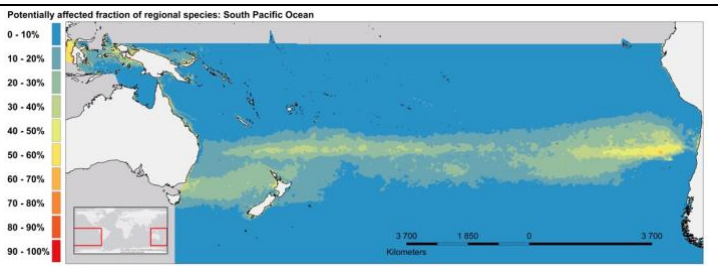

A 4.7: South Pacific Ocean SSD model and PAF map

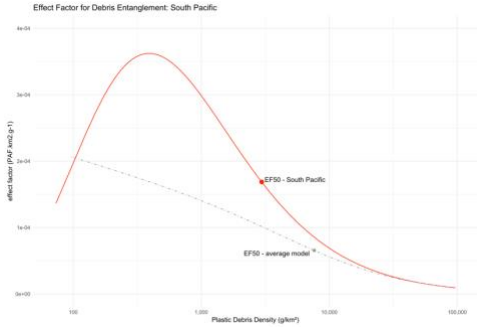

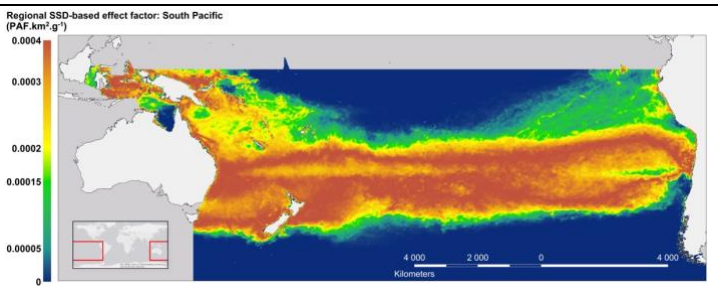

A 4.8: South Pacific Ocean EF model and map

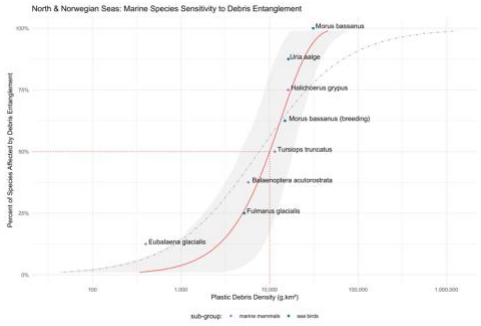

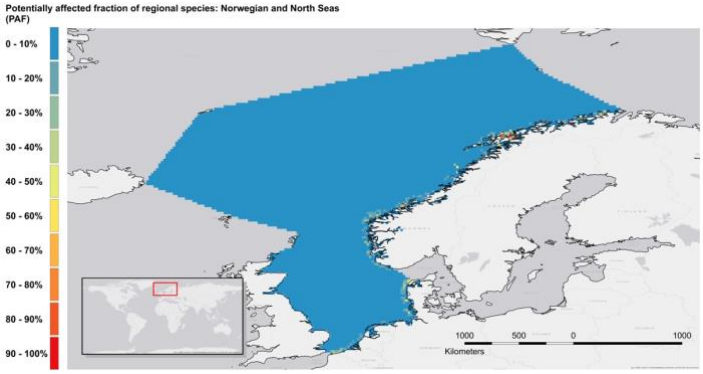

A 4.9: Norwegian & North Seas SSD model and PAF map

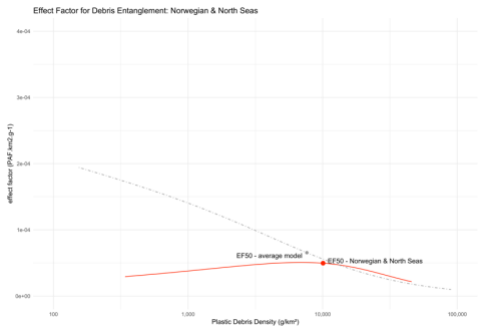

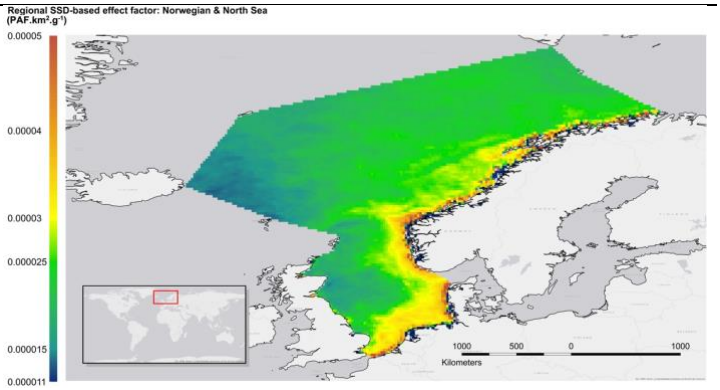

A 4.10: Norwegian & North Seas EF model and map

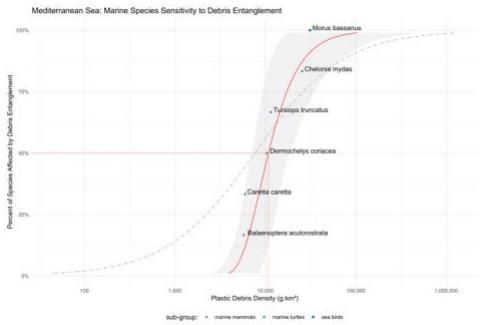

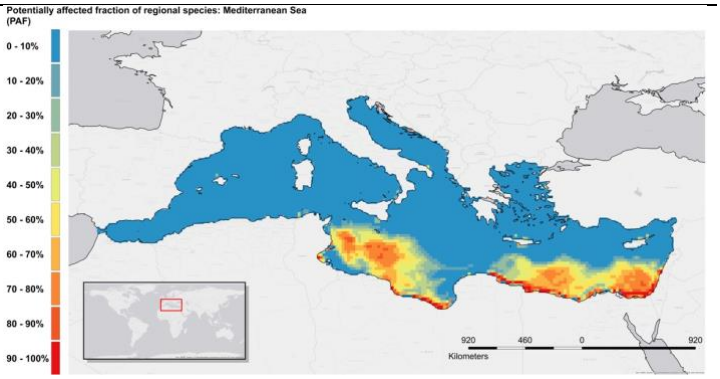

A 4.11: Mediterranean Sea SSD model and PAF map

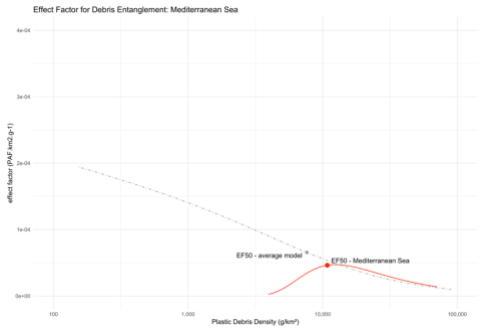

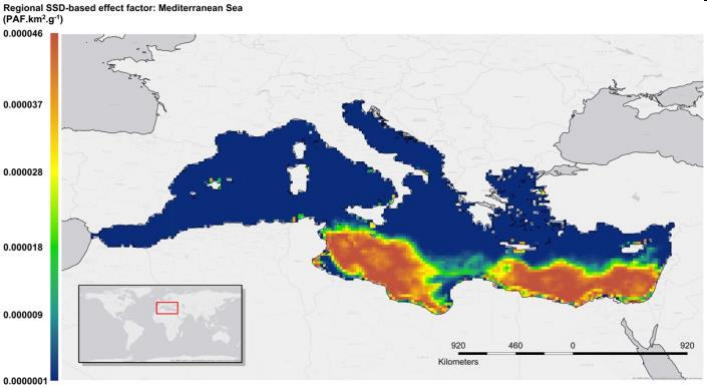

A 4.12: Mediterranean Sea EF model and map

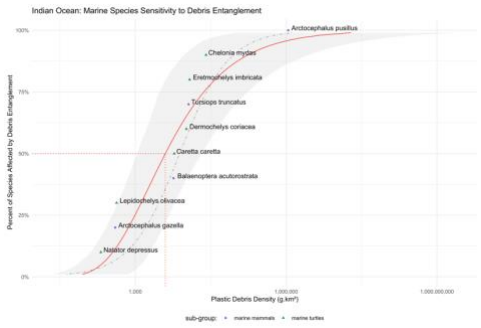

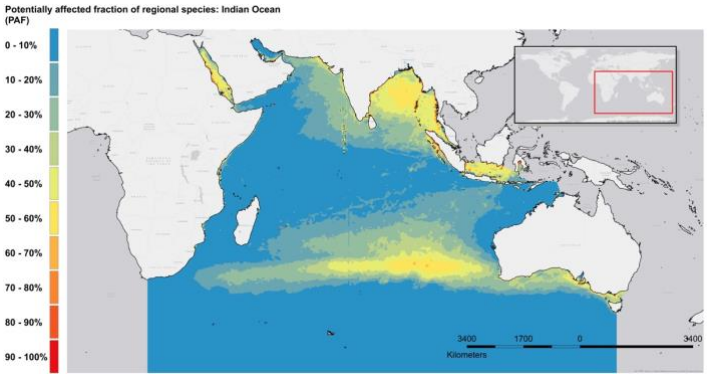

A 4.13: Indian Ocean SSD model and PAF map

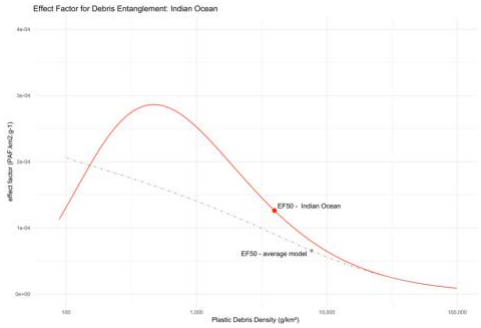

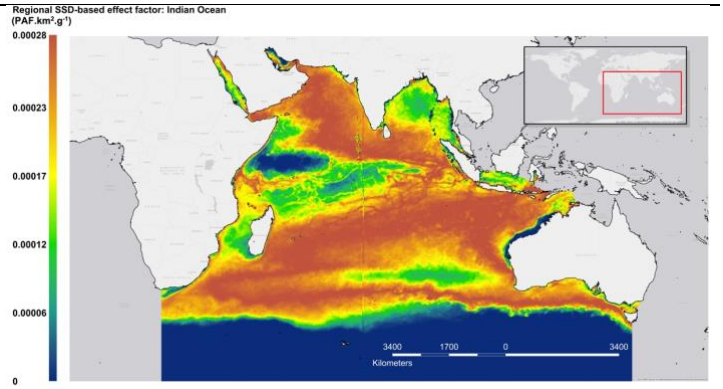

A 4.14: Indian Ocean EF model and map

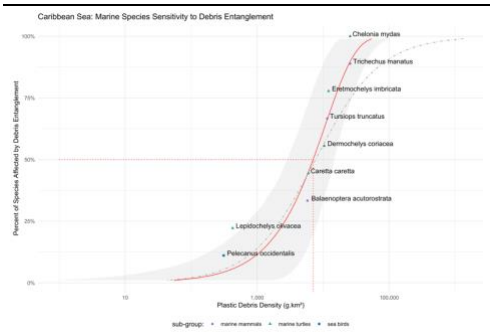

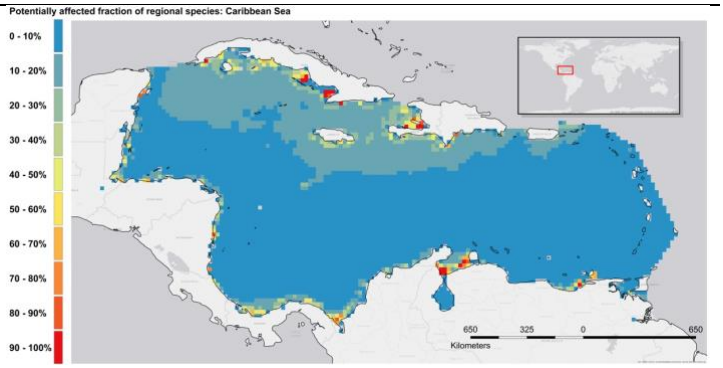

A 4.15: Caribbean Sea SSD model and PAF map

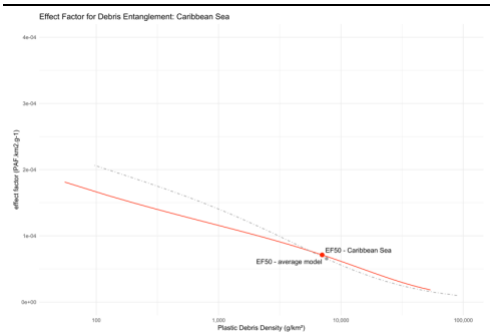

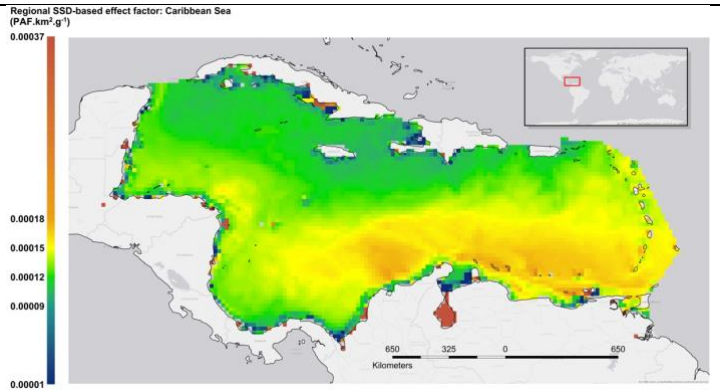

A 4.16: Caribbean Sea EF model and map

Appendix 5: Taxon-specific SSD and EF models - Cumulative species sensitivity distributions (SSD) used to calculate potentially affected fraction (PAF) of regional species; effect factor (EF) curves and associated maps. Each model (red line) is compared with average model (grey dashed line).

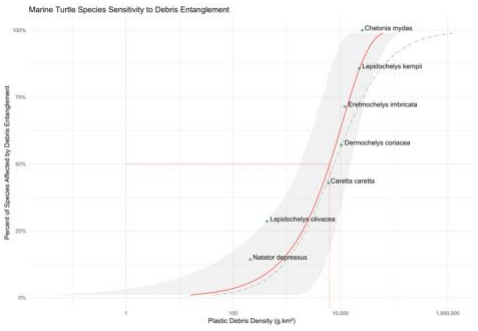

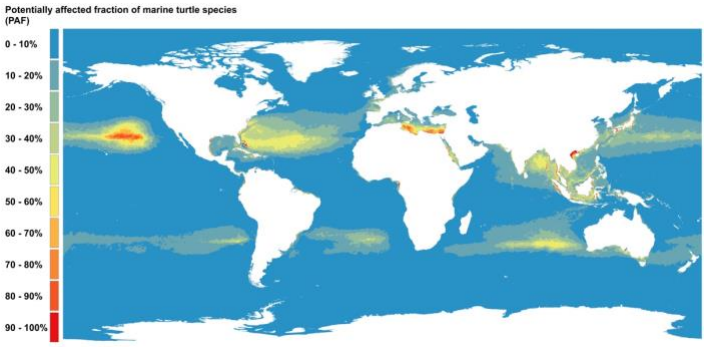

A 5.1: Marine turtles SSD model and PAF map

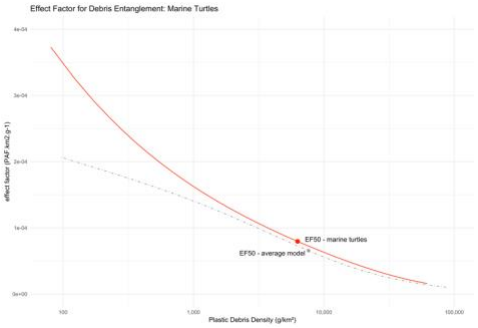

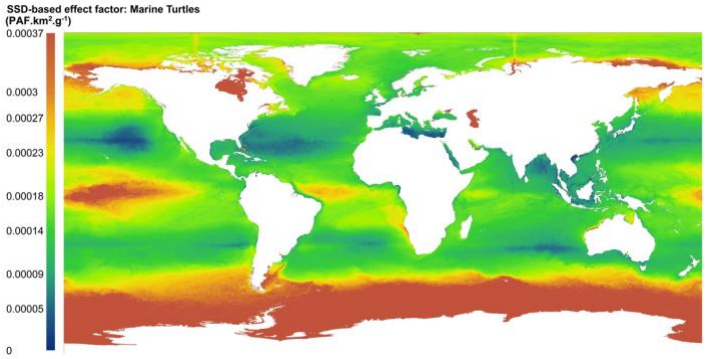

A 5.2: Marine turtles EF model and map

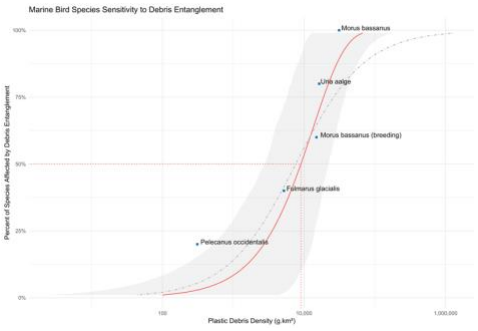

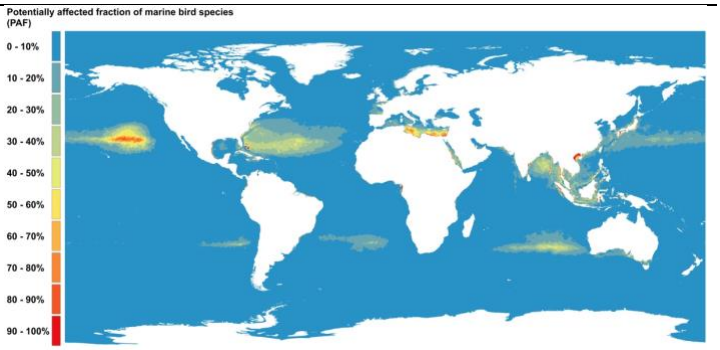

A 5.3: Marine birds SSD model and PAF map

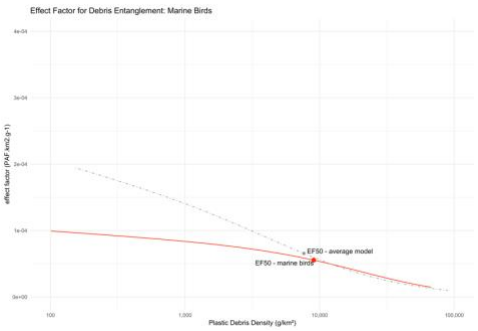

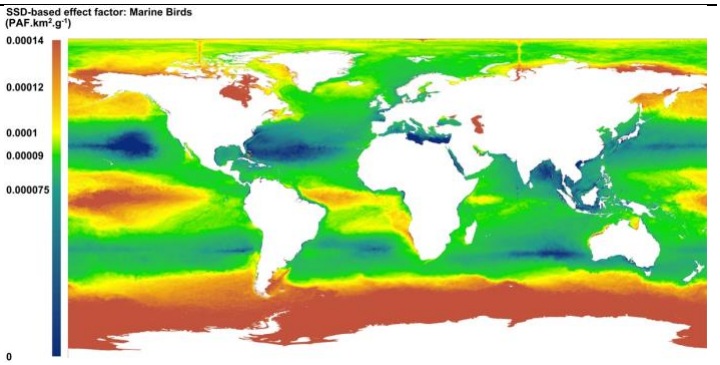

A 5.4: Marine birds EF model and map

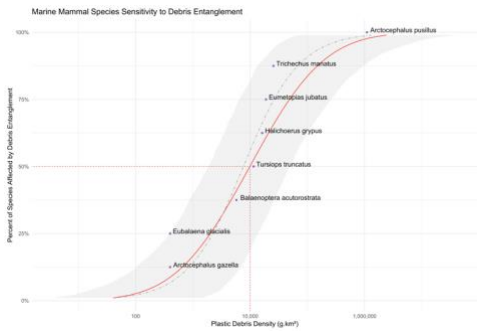

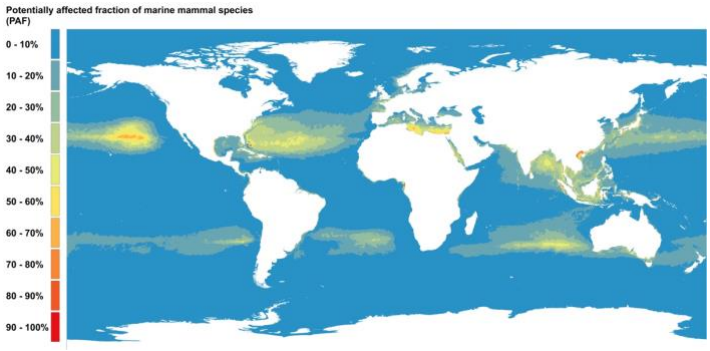

A 5.5: Marine mammals SSD model and PAF map

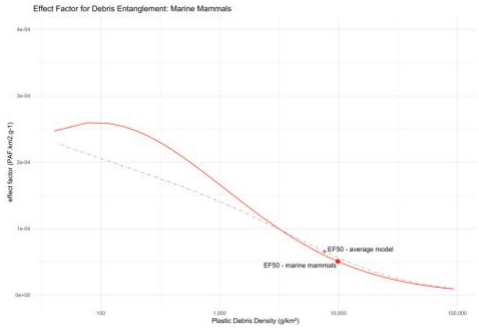

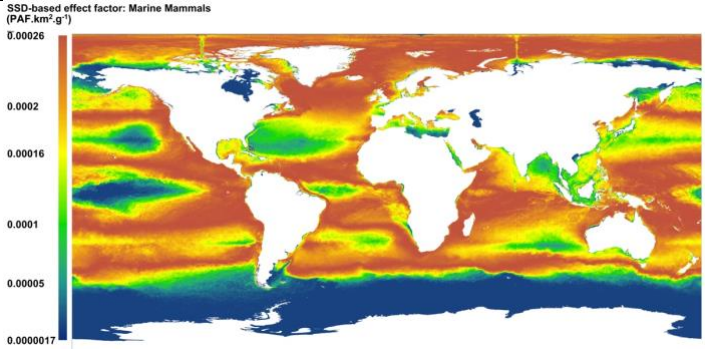

A 5.6: Marine mammals EF model and map

Appendix 6: Comparison of all models

All models sorted by lowest to highest HC_{50} marine macroplastic density (g/km^2), corresponding with highest to lowest linear median EF_{50} value. Better fitting model curves (lower AICC values) are associated with models including fewer species-exposure groups. Lower confidence limit (lcl) and upper confidence limits (ucl) for SSD model at 95% limits.

Region/taxa	**nr species**	**model function**	**parameters**	**AICC**	**Plastic density at HC_{50}** (g/km^2)	**std error** (g/km^2)	**LCL** (g/km^2)	**UCL** (g/km^2)	**EF_{50}** (PAF. km^2/g)
South Pacific	11	log-gumbel	scale 1.95 location 7.28	240	2.96E+03	3.63E+03	8.69E+02	1.30E+04	1.69E-04
Indian Ocean	10	log-gumbel	scale 2.01 location 7.55	224	3.96E+03	5.09E+03	1.10E+03	2.12E+04	1.26E-04
marine turtles	7	gamma	scale 16204.71 shape 0.68	150	6.29E+03	3.61E+03	1.77E+03	1.55E+04	7.95E-05
Caribbean	9	gamma	scale 12634.45 shape 0.86	191	7.02E+03	3.02E+03	2.86E+03	1.46E+04	7.12E-05
Global, minus *A. pusillus*	19	gamma	scale 16071.29 shape 0.732	398	7.03E+03	2.26E+03	3.63E+03	1.27E+04	7.11E-05
North Pacific	11	weibull	scale 10559.15 shape 1.12	230	7.60E+03	2.43E+03	3.85E+03	1.31E+04	6.58E-05
Global	20	log-logistic	scale 7627.66 shape 0.89	442	7.63E+03	3.64E+03	2.86E+03	1.71E+04	6.55E-05
South Atlantic	10	log-logistic	scale 9014.22 shape 0.89	232	9.01E+03	6.93E+03	2.73E+03	2.75E+04	5.55E-05
marine birds	5	weibull	scale 13314.56 shape 0.94	115	9.02E+03	5.14E+03	2.77E+03	2.20E+04	5.54E-05
North Atlantic	16	weibull	scale 12968.79 shape 1.05	339	9.15E+03	2.63E+03	5.31E+03	1.53E+04	5.46E-05
marine mammals	8	log-normal	meanlog 9.20 sdlog 2.36	190	9.89E+03	1.57E+04	1.86E+03	4.94E+04	5.06E-05
North Sea/ Norwegian Sea	8	weibull	scale 13498.32 shape 1.25	173	1.01E+04	3.44E+03	4.68E+03	1.85E+04	4.97E-05
Mediterranean	6	log-gumbel	scale 0.53 location 9.09	132	1.08E+04	3.15E+03	7.03E+03	1.87E+04	4.62E-05

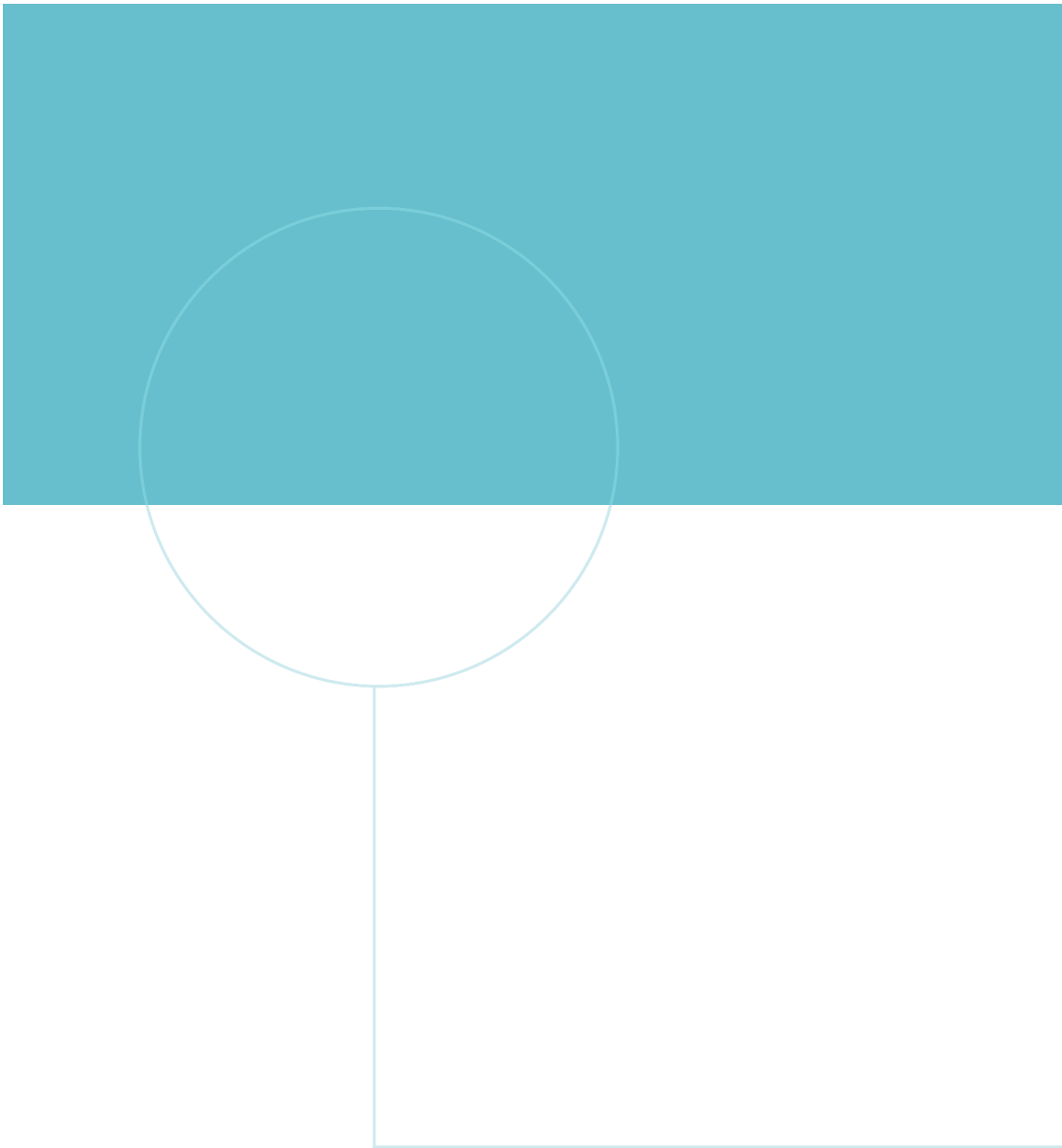

NTNU
Norwegian University of
Science and Technology

NTNU Industrial Ecology Programme
Universiteit Leiden